Cross-link variation in polyacrylic acid polymers for coating fertilizer pellets, promoting controlled release

RW Badenhorst

orcid.org 0000-0001-7276-9554

Dissertation submitted in partial fulfilment of the requirements for the degree *Master of Science in Chemistry* at the North-West University

Supervisor: Prof DA Young

Co-supervisor: Prof HCM Vosloo

Graduation May 2020

24133426

Abstract

Keywords: Polyacrylic acid, Polymer cross-linkers, Acrylate cross-linkers, Potassium Nitrate encapsulation, Monoammonium phosphate encapsulation & Controlled-Release

Polyacrylic acid (PAA) cross-linkers have been prepared by the esterification of acrylic acid (AA) with linear diols and glycerol using an acid exchange resin catalyst (Amberlyst B-23) and Dean-Stark water removal to promote di-ester formation. Fourier-transform infrared spectroscopy (FTIR), atmospheric pressure chemical ionised mass spectroscopy (APCI-MS) and nuclear magnetic resonance spectroscopy (NMR) served to verify the formation of ester products qualitatively. The esterification reaction optimization was carried out to determine the ideal conditions for di-ester product formation without needing to use pre-reaction reagent activation steps. Following the post-synthesis workup and purification, NMR was employed to quantify the mono-ester and di-ester components of the ester mixtures by using an internal biphenyl standard and ester-specific signal identification. Ester formation favoured the mono-ester, and the mono-ester-to-di-ester ratios exceeded 3:1. The ester mixtures were investigated as PAA cross-linkers for controlled-release fertilizer coatings. Potassium nitrate (KNO_3) and monoammonium phosphate (MAP) were obtained from Omnia and coated with single-layer and multiple-layer 5 weight-to-weight percentage (w/w%) coatings containing 5% cross-linker. Cross-linkers identified for multiple-layered coatings were determined by thermogravimetric analysis (TGA), and the application of 5% cross-linked PAA followed a 2 + 2 + 1 w/w% layered coating process. Cross-linking effect on PAA was determined by TGA of polymer samples formed under coating conditions. The coating efficiency and effect on controlled-release of the coating polymer on KNO_3 and MAP were determined by scanning electron microscopy (SEM) and moisture absorbance and solution rate analyses. The effect of the cross-linked PAA had a minor effect on the thermal degradation, characteristic of PAA, suggesting limited di-ester formation and thus the presence of cross-linking. From the moisture absorbance and solution rate testing decreased solution rates were observed, however, only minimal, with the 1,5-pentanediol esterification ester mixture resulting in the best controlled-release effects. SEM analysis of the coating efficiency and coating thickness showed ineffective coating with fertilizer surface areas remaining exposed, thus explaining the limited effect of imparted controlled-release characteristics.

Opsomming

Titel: Kruisbindingvariasie in poliakrielsuurpolimere vir bedekking van kunsmiskorrels om beheerde vrystelling te bewerkstellig

Sleutelwoorde: Poliakrielsuur, Polimeerkruisbinders, Akrilaatkruisbinders, Kaliumnitraatbedekking, Monoammoniumfosfaatbeddeking & Beheerde-vrystelling

Poliakrielsuurkruisbinders (PAA) is berei deur die verestering van akrielsuur (AA) met linêre diole en gliserol met behulp van ’n suuruitruilhars-katalisator (Amberlyst B-23) en Dean-Stark-waterverwydering om diëstervorming te bevorder. Fourier-transforminfrarooispektroskopie (FTIR), atomosferiese druk chemiese ionisasie massaspektroskopie (ADCI-MS) en kernmagnetiese resonansiespektroskopie (KMR) het gedien om die vorming van esterprodukte kwalitatief te verifieer. Optimalisering van die esterifikasiereaksie is uitgevoer om ideale omstandighede vir die vorming van di-esterprodukte te bepaal sonder om van reagensaktivering gebruik te maak. Na opstelling en suiwering is KMR gebruik om die mono- en di-esterkomponente van die estermengsels, met behulp van ’n interne bifenielstandaard en esterspesifieke seinidentifisering te kwantifiseer. Estervorming het die mono-ester bevoordeel en die mono-ester-tot-di-ester-verhoudings het 3:1 oorskry. Die estermengsels is as PAA-kruisbinders vir beheerde-vrystelling kunsmisbedekkings ondersoek. KNO_3 en monoammoniumfosfaat (MAP) is van Omnia verkry en bedek met meervoudige en enkellaag 5 gewig-tot-gewig persentasie (w/w%) bedekkings wat 5% kruisbinder bevat. Kruisbinders wat gebruik is vir meervoudige bedekkings was geidentifiseer met behulp van termogravimetriese-analise (TGA), en volg deur 2 + 2 + 1 w/w% lae toe te pas. Die kruisbindingseffek is bepaal deur TGA van polimeermonsters wat identies aan die bedekkingomstandighede gevorm is. Bedekkingdoeltreffendheid van die deklaagpolimeer en die effek daarvan op beheerdevrystelling van KNO_3 en MAP is bepaal deur skandeerelektronmikroskopie (SEM), vogabsorpsie en oplossingstempo-analises. Die effek van kruisgebinde-PAA het ’n geringe effek op die termiese ontbinding, kenmerkend van PAA, gehad wat beperkte diester-teenwoordigheid voorstel. Vanaf vogabsorpsie- en oplostoetse is verlaagde oplostempos waargeneem, alhoewel minimaal, met die 1,5-pentaandiolestermengsel wat die beste effekte met beheerde vrystellings tot gevolg gehad het. SEM-ontleding van die

doeltreffendheid en dikte van die deklaag het nie-doeltreffende bedekking getoon met kunsmisoppervlaktes wat ontbloot is, en sodoende word die beperkte effek van die toegepasde bedekkings verklaar.

Acknowledgements

Foremost I wish to thank my supervisors, Prof. DA Young and Prof. HCM Vosloo for their ceaseless patience and their guidance. I would also wish to thank all the following people for their help and contributions regarding this project:

Omnia for funding and supplying chemicals and analyses, without whom none of the research could have been done.

Dr. J Huyser and Dr. M Brand for the testing of samples, discussions and suggestions.

Dr. J Jordaan and Dr. D Otto for their help with the analyses and advice regarding the project.

Dr. F Marx and Dr. A Swarts for their support and insight.

Dr. A Jordaan and Dr. I Shuro for their help with SEM analysis.

To all my fellow students in the Catalysis and Synthesis Group for their support.

Last but not least, I wish to thank my loving family for their continued belief and support. They provide the basis of my self-belief and confidence to finish this project.

List of Abbreviations

AA	Acrylic Acid
APCI-MS	Atmospheric Pressure Chemical Ionization Mass Spectroscopy
DAA	Diacrylic Acid
EGDM	Ethylene Glycol Dimethacrylate
FTIR	Fourier Transform Infra-Red
GCMS	Gas Chromatography Mass Spectroscopy
MA	Methacrylic Acid
MAP	Monoammonium Phosphate
NMR	Nuclear Magnetic Resonance Spectroscopy
PAA	Polyacrylic Acid
PMA	Polymethacrylate
SEM	Scanning Electron Microscopy
TGA	Thermogravimetric Analysis
W/W%	Weight-to-Weight Percentage

Table of Contents

Chapter 4

Chapter 5

Chapter 1

Introduction and Objectives

1.1 Introduction

The population explosion predicted for the foreseeable future brings with it many problems that science will have to face, with one of the many challenges being the food shortages predicted and the increased food production required.[1] The required crop supplies can only be obtained by altering the current agricultural practices, while also employing greener alternatives. One such green practice proposed is using controlled-release fertilizers employing biodegradable and non-toxic polymer coatings.[2] The employment of such methods is motivated by green movements, as well as depleting natural materials and their inefficient use. Synthetic materials could thus provide an alternative by potentially solving problems associated with the current agricultural practices, while adhering to sustainable initiatives. The agricultural sector and its practices cannot be neglected due to their importance associated with the constant demand for food supplies and other crops utilized for common consumer goods. However, sustainability and green techniques are suffering, and are being ill-regarded due to cost and practical implications.[3] The need therefore exists to alter agricultural practices to the extent that cost effects can be minimized without major application changes.[4]

1.2 Controlled-Release fertilizer impacts and necessity

Fertilizer usage is an ineffective and wasteful process, however, due to the benefits and crop yield gains it is an irreplaceable method of nutrition for agricultural crops.[4-5] Fertilization is commonly applied by solution spraying of dissolved fertilizer pellets or by scattering of undissolved pellets, however, these methods are exposed to environmental effects. Due to the salt-like forms of fertilizers, the solution varies and

seeps through the soil at rates that are not ideal for crop utilization.[6] A variety of fertilizers predominantly composed of nitrogen, phosphorous and potassium derivatives are employed, which occurs in different ionic forms and with varied counter ions.[7] Thus, due to the different fertilizers used, the solubility and respective solution rates vary greatly. This is due to the ionic forms and additives in the fertilizer, the solution of which is uncontrollable once exposed to water and dissolved.[8] Uncontrolled fertilizer solution in soil causes leaching into subterranean water sources and eventually ends up in rivers and other ecosystems with disatrous results.[9] Coatings made of polymers can potentially slow the rate of solution, extend the total time of release and improve crop nutrition by acting as a physical barrier between the pellet and the soil.[10-11] Polymers that are biodegradable and non-toxic can be employed to serve as barriers and also improve the moisture retention of the soil after solution of the entrapped fertilizer.[12] These applications will reduce fertilizer usage and improve effectivity, thus reducing the cost, and making fertilization environmentally safe and more sustainable.[13]

1.3 PAA cross-linker synthesis

Polyacrylic acid (PAA) cross-linking has been used in varying studies to increased absorption, improved mechanical strength and copolymer incorporation optimize PAA polymers, depending on the polymer application.[14-15] The synthesis of most PAA cross-linker groups uses complex and expensive reaction routes to form the desired product and is not ideal for industrial application.[15] Effective industrial scale synthesis is often jeopardized due to a reliance on complex and multi-stepped reaction routes that are expensive and have toxic reagents that require special treatment.[16] However, due to the scale of industrial application and the variety of characteristics needing testing, different cross-linkers are required. Many studies have aimed to incorporate cross-linkers based on availability and green initiatives, however, few have focused solely on the effect of single factor cross-linker variation and its effect on controlled-release polymer coatings.[15] The wide variety of cross-linkers makes evaluation difficult due to the difference in their contributing factors, however, all cross-linkers are

employed in PAA synthesis to obtain improved mechanical, absorption or other properties.[17-18]

1.4 PAA cross-linking and Fertilizer coating

Due to the inherent solubility and weak mechanical strength of PAA, cross-linking is essential for greater adhesive ability to pellets and to ensure a controlled rate of release.[19] Cross-linked PAA should act as a mesh-like structure surrounding the pellet with an even layer of coating capable of adsorbing water to the polymer layer and absorbing water into and through the polymeric structure to the fertilizer. This absorption is due to the porous nature of the polymer, formed by inter-polymeric spaces.[20] This action of adsorption and penetration will form a barrier, the traversal of which will act to slow the penetration of water and the release of dissolved fertilizer ions to the surrounding environment.[3] Potentially, by varying the coating thickness and the number of applied layers, the controlled-release fertilizer can be 'programmed' for set times or release rates, depending on the requirement.

1.5 Aim and Objectives

This study aims to synthesize acrylic acid (AA)-based PAA cross-linkers without the need to use any preparatory activation reactions prior to esterification, whilst aiming to form the di-ester of the AA and multi-diol containing molecules. Following esterification, purification and characterisation, the product is used to cross-link polymer coatings, which are applied to fertilizer pellets to promote controlled-release fertilizer release in water solutions.

The objectives of the study are as follow:

1) Synthesis of di-ester cross-linker groups through the esterification of AA with diols, without reagent activation steps being employed. The linear diols, other alcohol baring molecules and alternative cross-linkers investigated for cross-linker synthesis and application are:

a) Linear straight chain diols.
b) Glycerol.
c) Ethylene glycol dimethacrylate.

2) Synthesis optimization by reaction condition variation for optimal product yield and purity.
3) Use of synthesized cross-linked products to form cross-linked PAA polymers and the evaluation thereof by physical characterisation for correlation with solution testing. Differing percentages of cross-linker presence will be employed to determine the effect on thermal characteristics.
    a) Differing percentage cross-linker presence effect on thermal characteristics.
4) Applying cross-linked PAA polymers to fertilizer pellets to investigate their effect on the solution rate of the fertilizer in an attempt to achieve controlled-release.
    a) KNO_3 and monoammonium phosphate (MAP) coated and analysed for controlled-release properties.

1.6 Layout of the Thesis

The research work is composed of five chapters. Chapter 3 describes the synthesis methodology, workup, characterisation and quantification of the cross-linker products from AA, and the linear diols and glycerol proposed. Chapter 4 describes the application of the cross-linkers synthesized in polymerization and testing thereof as coatings and polymer samples.

The layout is as follows:

Chapter 1: Introduction and objectives

Chapter 2: Problem statement and literature study

Chapter 3: Synthesis and characterisation of esterification products of linear diols and glycerol with AA

This chapter pertains to the esterification reaction of AA with the proposed linear diols and glycerol to form di-ester products for potential application as PAA cross-linkers. Synthesis optimization was done by varying reaction conditions to maximize the product yield and purity of the obtained sample prior to characterisation. The post-reaction workup of washing and separation of product mixtures were carried out for product isolation and characterisation. Characterisation of the formed products were performed to determine the product formation and quantification of products formed.

Chapter 4: Thermogravimetric testing cross-linked PAA and investigation of applied, uncross-linked and cross-linked polymers as coatings for controlled-release of fertilizers

Polymerization of AA with and without cross-linkers were carried out to form polymer samples for thermogravimetric analysis to determine the effect of the cross-linker on the physical characteristics of the polymer. The coating and testing methodologies of coated KNO_3 and MAP samples were carried out to determine the effect of uncross-linked and cross-linked PAA on the solution rates of coated fertilizer in order to determine the best performing controlled-release fertilizer sample conditions.

Chapter 5: Conclusions and recommendations for further work.

Chapter 2

Literature Study

2.1 Introduction

The benefit of applying modern, commercially produced fertilizer has been immense. Commercial fertilizers currently help produce crops in sufficient quantities to feed the current 7.6 billion global population.[1] However, prior to modern fertilizer practices, a population growth explosion throughout the 20th century caused commercial fertilizer production to undergo a similar explosive growth to reach modern levels of fertilizer usage.[3, 21] Similar to the population growth seen in decades passed, it will continue into the future and will require an increased food production to maintain it, as shown in Figure 2.1. A predicted global population of 9.7 billion people are expected by the year 2050, which places strain on the limited resources currently available, including limited terrestrial land, water resources and the potential for increased yields achieved by implementing genetic modification and breeding.[1] Therefore, effective fertilizer utilization is paramount to alleviate the growing concern of an impending global food shortage.[3]

Fortunately, the yield of crops, such as cereals, has increased steadily over the last fifty years, due to effective fertilizer usage and agricultural practice improvements.[1] The use of fertilizers has enabled increased production of staple foods due to the increased artificially supplied nitrogen and phosphorous.[3] However, ineffective nutrient-use plagues commercial fertilizer application, as yearly the returns of crops steadily decreases compared to the amount of fertilizer used.[1, 3, 21] Today, these efficiencies cause fertilizer utilization to decrease from first application, resulting in an estimated uptake of merely 30-50% for nitrogen fertilizers and approximately 45% for phosphorous fertilizers.[1, 3]

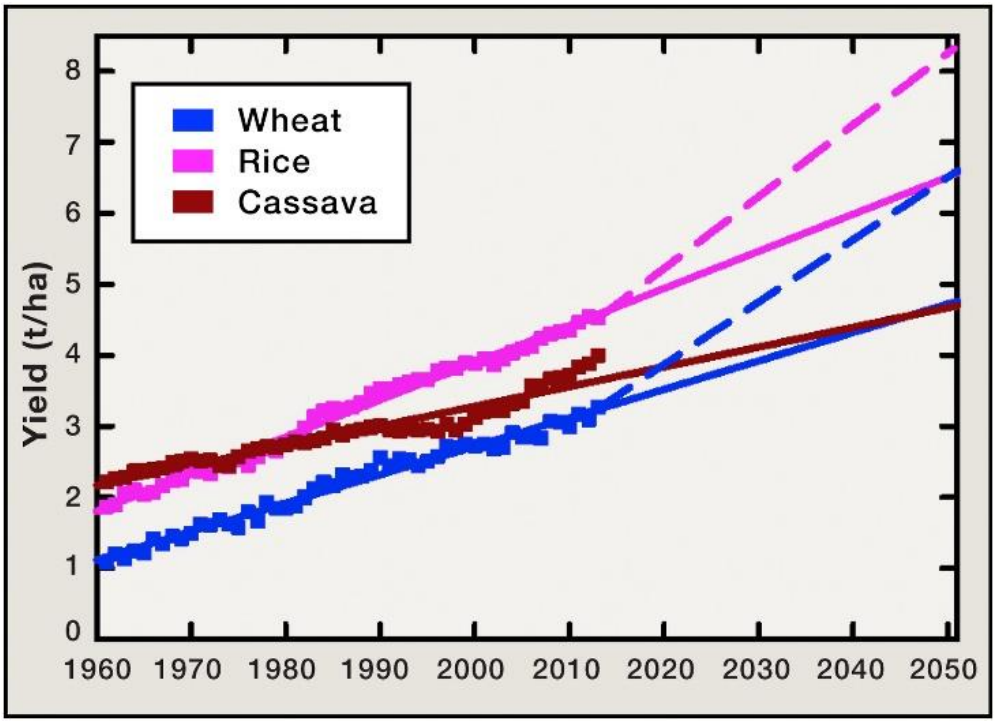

Figure 2.1 Food demand of wheat, rice and cassava from 1960 to the present and predicted future demand. (Copyright permission obtained from Elsevier).[22]

The ability of crops to efficiently utilize fertilizer may vary depending on the crop species, fertilizer application practices, soil and environmental conditions, and also on the fertilizer source used.[3] Many major grain and rice producing regions in east and southeast Asia are suffering from a slowing rate of yield increases, which is approaching a ceiling for maximal yield production.[23] These stagnating increases are attributable to the continuous production of crops, especially agricultural systems with two or three crops per year.[23] Implementation of such systems will inevitably lead to exhaustion of crop potentials and may become progressively vulnerable to diseases and pests.[1] Extensive and high nutrient demanding systems, producing multiple crops per year, frequently suffer from low fertilizer-usage efficiency and expensive labour requirements.[24] In addition, fertilizer retention is lowered further following application in farming areas with high rainfall and water supply, adding to the leaching of fertilizer from the soil prior to utilization.[23] As a result, these regions have had mostly stagnant yields between 1980 to 2000. However, with improved agricultural practices and modern fertilizers, increased yields could again be obtained.[1]

Agricultural practices in many parts of the world, especially in developing countries have lower crop yields than possible with modern commercial fertilizer and agricultural practices. Modern practices in developed countries use fertilizers such as industrially produced ammonium and nitrate applied at calculated points in time and often at an extreme scale. However, many areas are still suffering from malnutrition and could potentially increase their current crop yield through supplementation.[1, 21] The projected fertilizer needs and future use will be greatest in developing countries due to their urgent demand for increased food production, insuring its need and usage will continue to increase into the future. Modern fertilizer practices remain expensive due to the high costs and labour intensive measures required to implement them, which to date remain outside the capabilities of developing countries. Developed countries have, however, been implementing fertilizers for decades and are expected to undergo a far smaller yearly increase, until possibly reaching a maximum needed to ensure sustainable yields.[3]

2.2 Threats associated with fertilizer usage / over usage

Over application of fertilizer and insufficient retention in the soil causes leaching, which entails washing of the nutritional compounds from the soil into the underground and other water sources, such as rivers, lakes and the ocean, causing much of the fertilizer to be wasted. From Figure 2.2 it becomes apparent that if increased yields were to be obtained through the application of fertilizers, the efficiency of its use is decreasing with increased use. In Figure 2.3, the over application of phosphorus fertilizer is shown. Wasted fertilizer causes increased costs and affects the return of a crop per unit of fertilizer applied to achieve sustainable agriculture.[1, 3] These costs and the resulting effect of the wasted fertilizer are only some of the aspects that must be improved upon to enable sustainable agriculture.[3, 23] Sustainable agriculture is the ability to meet current and future societal needs of food and agricultural products, to promote ecosystem conservation, nutritional value, and to achieve these goals when all costs and consequences of their practices are taken into account.[1]

Figure 2.2 Nitrogen scenarios faced during 2010 and predicted for 2050. Fixed N, refers to nitrogen fertilizer fixed into soil, compared to the required nitrogen and the total loss of nitrogen. (Adapted from original figure).[25]

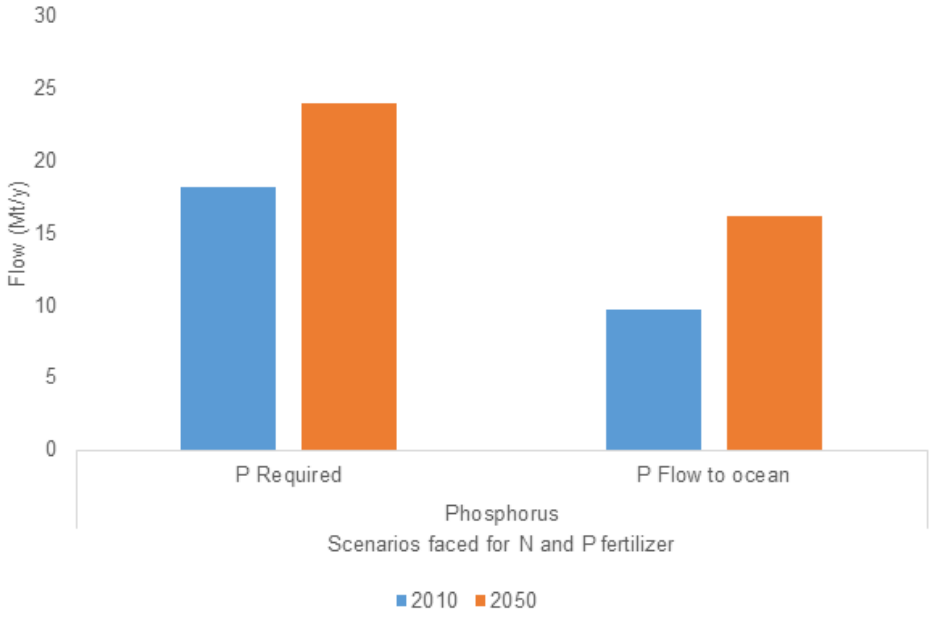

Figure 2.3 Phosphorus scenarios faced during 2010 and predicted for 2050. P required refers to the amount of Mt/y for adequate crop return and phosphorus flow to ocean shows contamination reaching the ocean. (Adapted from original figure)[25]

The protection of ecosystems is crucial for both environmental conservation and the natural benefits obtained from ecosystems. Also, the understanding of and smart implementation of modern agricultural practices such as the use of fertilizer will aid in the maintenance of the natural environment. Societal understanding of the benefits that natural ecosystems provide, and the protection thereof, may serve to increase awareness of alternative and less harmful methods employed in agriculture.[3, 21] Natural ecosystems are crucial as they provide food, fuel and building materials. In addition, they also help with flood prevention, climate regulation, removal of carbon dioxide from the atmosphere and the revitalization of the soil.[1] Soil farmed for long periods can become deprived of their nutritional value, resulting in lower yields while also increasing the risks of flooding and becoming barren when used without planned revitalization or resting periods.[24] Soil deprived of nutritional value becomes unprofitable with lowered returns, requiring increasing amounts of fertilization, irrigation and energy to maintain productivity at required yields.[1, 21] The revitalization of soil is frequently attempted by the application of fertilizers, often causing greater harm. The use of fertilizer, at the current rates, will cause an inevitable capitulation in the near future that will cause great damage to both land- and water quality, as well as the species of plants and animals native to the overexploited lands.[1, 21]

With another side effect of uncontrolled or heavy fertilizer application being the acidification and contamination of surface and groundwater with nitrates and also the evolution of nitrous oxide into the atmosphere.[23] Along with the over application of fertilizer, and the havoc it could potentially wreaks on the environment, the continually increasing demand for fertilizer exhausts its sources. Fertilizer sources are being exploited at an unmaintainable rate, and only a limited amount of quarries supply potassium and phosphorous fertilizers, causing an increased sufficiency of its use to become dominant.[21, 26] Fertilizers are also energy-consuming to produce, requiring conversion from mined phosphorous and potassium to its commercial form prior to application. Therefore, improved utilization of the limited fertilizer sources must be achieved to alleviate the need for fertiliser while sustainably employing natural resources.[23]

To achieve the required doubling of grain by 2050, the current employment of fertilization methods and practices will result in a three-fold increase in excess nitrogen and phosphorous in water resources.[1] The high food demand predicted for the near

future will require sustained high crop yields, due to limited agricultural soil, thus causing a further increased use of commercial fertilizer to agricultural soils.[27] Particularly nitrogen fertilizers, since they are relatively low-cost compared to the added value of increased crop production.[27] Nitrogen usage, however, has potential threats to the environmental quality, of which subterranean and surface waters are of major concern. Investigations done in Sweden by Bergström and Brink, have found that nitrogen leaching occurs mainly over periods of high rainfall in regions with no plant cover and when application of fertilizer was higher than optimal amounts.[27] Nitrogen fertilizer, when applied in greater than ideal quantities, would when in the form of nitrates, proceed to distribute down into the soil, leaching well below the effective uptake depth of plant roots and most specifically of crops.[27] These 'lost' nitrates remain dormant beneath the soil and remain unused until sufficient rainfall or other sources of water cause it to leach away. Leached fertilizers enter into water sources or rise to the surface during dryer periods due to increased evapotranspiration taking place at the surface.[27]

Bergström and Brink go on to conclude that leaching is caused by using excess amounts of fertilizer, and adds to fertilizer compounds found in subsurface and surface water sources.[27] A balanced application of fertilizer showed the likelihood to cause the least amount of contamination of surface and subsurface water sources, while maintaining adequate levels for crop cultivation and sufficient yields. Planning fertilizer application according to the crop showed a correlation, according to Bergström and Brink, and some crops were able to fully absorb even over-application amounts of fertilizer from the soil, avoiding leaching.[27]

The fertilizer used may also directly affect the soil's properties that determine runoff and erosion of the soil.[21, 28] However, avoiding high-runoff sources is not as simple as first appearances might suggest, due to the availability and price, to name a few. The loss of nutritional ions, such as phosphorous from the soil, can be ascribed to many factors including, but not limited to, soil phosphorous concentration, the rate, method and timing of phosphorous amendments.[21, 28] The potential of phosphorous sources to release phosphoric nutrients to runoff differ depending on the source used and therefore, also contributes to the addition of runoff phosphorous into water sources.[21, 28] An indication of the runoff that reaches the ocean is illustrated in Figure 2.3. Potential phosphorous nutrient losses occur, however, with peaks immediately

following the application of the fertilizer and then declines with time. This is due to the initially soluble phosphorous being converted to recalcitrant forms through interaction with the soil. The aforementioned factors can be limited, however, to reduce the leaching of phosphorous from the soil by altering the methods employed when applying phosphorous fertilizers or by altering the fertilizer itself to closer fit required expectations.[3, 21, 28]

Nutrients in fertilizer are essential to meet the needs of the population in the future, however, inadvertently fertilizer nutrients enter other ecosystems. Increased food production is therefore, required without an increase in the associated negative environmental impacts. Therefore, the need to optimize the application of fertilizers or the improvement of thereof in order to increase crop yields and limit the environmental effect of fertilizer is a possible solution to the problem faced.

2.3 Fertilizers used: KNO_3 and monoammonium phosphate (MAP)

Fertilizers come in various forms and are categorized according to their elemental makeup in its pure form or as a mixture, often given by an NPK value. Fertilizer offers nutrition to crops for improved qualities such as faster growth, increased immunity, seasonal protection and ground supplementation, among other benefits.[26] The essential nutrients, with nitrogen, phosphorous and potassium being most essential, thus given a NPK value, in the agricultural sector for healthy plant growth can be classified according to the elements that form the nutrient, these inorganic element groups are N, P, K, Ca, Mg, S, metal elements (Zn, Fe, Mn, Cu and Mo) and other minor groups (Cl and B).[29] Among the most common nitrogen-containing fertilizers used are ammonium nitrate, calcium ammonium nitrate and carbamide (urea), all made from ammonia with over 150 million tonnes are produced annually.[26]

Fertilizers rich in nitrogen compounds assist with leaf growth and protein production; phosphorous promotes root and early seedling growth, while potassium regulates the transport of nutrients and water within plants.[26] The nutritional compounds are, however ions that must be dissolved by soil water to be absorbed and used by plants. Phosphorous is mostly taken up by plant roots in the dihydrogenphosphate ion form.

This form is manufactured from phosphate rock to produce the most common water soluble calcium dihydrogenphosphate form.[26] Potassium is absorbed in its monoatomic positive potassium form (K^+) and is obtained from potash mining and used in the form of KCl.[26] Sulphur is increasingly added to fertilizer either in the form of sulphate salts or as elemental sulphur.[26] Fertilizer forms depend on the contents of the fertilizer because contents such as ammonium sulphate and KCl are crystals and are finely ground, whereas carbamides obtained from urea are spherically shaped due to their formation in prilling towers.[26] The nutrient content of a fertilizer is expressed in percentiles, showing the composition of the fertilizer according to the amount of nitrogen, phosphorous and potassium present, always in the same order and is called the fertilizer grade.[29]

KNO_3 and MAP obtained from Omnia was used in this study. KNO_3 is a commonly used fertilizer, especially for high-value crops, which is employed due to the absence of chloride.[30] Manufactured primarily by reacting KCl with a nitrate source, which may be sodium nitrate, nitric acid or ammonium nitrate, the formed products are identical and commonly referred to as nitrate of potash.[30] KNO_3 is a crystalline material that is primarily dissolved and applied with water or as a pellet direct-to-soil application, which is the method under investigation, seeing that solubilisation prior to application defeats the purpose of controlled-release.[30] KNO_3 is primarily used due to its unique composition and capability of providing specific benefits to growers, its ease of handling and dissolves easily.[30]KNO_3 is commonly used in agricultural applications that require highly soluble chloride-free nutrition, making immediate uptake and availability to the crops possible. Due to the soil salinity being a major factor in causing the soil to become unfit for agriculture, mostly due to sodium chloride, it is advantageous to use chloride-free fertilizers to not further increase soil salinity.[31] Due to the highly soluble nature of KNO_3, it is prone to leaching. Nitrate and potassium leaching are a growing concern, and, although not considered a serious threat, affects plant growth and quality.[32] The ratio of potassium relative to nitrogen in KNO_3 is 3:1 which is high, and favourable when potassium supplements are necessary. However, both nitrogen and potassium are necessary to support harvest quality, protein formation, disease resistance and water-use efficiency.[30]

MAP is a widely used fertilizer, a source of both phosphorous and nitrogen, and it constitutes two of the most important nutritional elements. Additionally, MAP has the highest phosphorous content of any common solid fertilizer.[33] MAP is manufactured by a one-to-one reaction of ammonium and phosphoric acid. The resulting slurry of MAP is solidified, and pelletized via a granulator.[33] The formation of MAP does not require the use of high purity phosphoric acid, which is advantageous economically. However, a result of using lower grade phosphoric acid is that the content of phosphorus pentoxide (P_2O_5), formed during the reaction, varies between 48-61%.[33] Widely employed, MAP is water-soluble and is readily dissolved in moisture sufficient soil. Once having dissolved, MAP dissociates into ammonium (NH_4^+) and dihydrogenphosphate ($H_2PO_4^-$). MAP is employed for healthy and sustained growth, and due to its slightly acidic nature, it is commonly employed in alkaline and neutral soils. Some of MAP's popularity can be ascribed to agronomic studies showing negligible differences between phosphorous nutrition, regardless of phosphorous type or the conditions of application, thus making MAP's high phosphorous content economically valuable.[33] Due to phosphate fertilizers being notoriously slow in leaching from the soil once applied, MAP is commonly applied in concentrated bands beneath the soil in close proximity to growing roots.[33] Phosphate exposure of seminal roots in high concentrations caused a promotion for new root formation and also the extension and elongation thereof.[34] Additionally, phosphate and ammonium containing inorganic fertilizer acts as a suppressor for many microbial populations that can be potentially harmful to the plant, one of which are nematode populations.[35]

Although problems associated with fertilizer ions easily leached into water sources are troubling, another difficulty includes that some ions inversely bind well with soil particles and are not easily leached and may remain in the soil for long periods after application.[26] Nitrates are highly mobile and prone to leaching, while phosphates tend to bind strongly to soil particles. Thus, their application and method of delivery must be determined accordingly.[9, 26] According to Arora and Juo,[9] by varying the application of nitrogen-containing fertilizers from one application to two or three segmental applications, leaching was decreased by 25%. Embracing this principle, fertilizer application can be planned and applied to maximize the amount of time the nutrients are available to the crop, while minimizing the amount of fertilizer leached from the

soil. Plants generally require nutrition at a much steadier rate than that maintained agriculturally, according to Wiedenhoeft,[36] which is inherently different from the nutritional supply achieved by instantaneous application, as is traditional in agricultural methods. Accordingly, fertilizer application methods can be altered by reducing the amount applied and increasing the number of applications. However, this is expensive to accomplish considering the logistics involved. Alternatively, crop nutrition can be improved by applying a coating to the fertilizer, slowing its solubilisation, while lengthening its availability and reducing potential leaching.

Nutrients are dissolved in soil water.[26] Fertilizer will dissolve and dissociate once in contact with soil water as positively or negatively charged ions. Slowing solubilisation depends on the time taken for the pellet to come into contact with water and for the dissolved fertilizer nutrients to be released into the soil.[5] Coatings made on the surfaces of fertilizer pellets, essentially cover and reduce the contact surface, to lengthen the time of ion release, which slows the rate of solution. A method of making such coatings is through the use of polymers, and it has proven effective in slowing release from coated fertilizer pellets.[11] The need for ion exchange from polymer-coated pellets to the soil is critical to the application of the pellets used as controlled-release fertilizer.[10]

2.4 Use of superabsorbent-polymer coated fertilizers

The encapsulation of fertilizers became an area of investigation due to the inefficient retention of fertilizers in the soil that instead leached away into the water, due to the high solubility of fertilizers as mentioned above.[10] Due to the traditional ‘naked’ application of solid fertilizer, solvation occurs uninhibited and can lead to leaching, with small divergences in degree and swiftness thereof whether applied on the soil surface or in the soil. According to Bergström and Brink, fertilizers applied in bulk, especially when uncovered and during high rainfall periods, caused the greatest increase in fertilizer nutrients to water sources by leaching.[27] Above maximum crop capacity application of fertilizers also led to the penetration of nitrate fertilizers far exceeding the effective depth of crop root penetration.[27]

Set increment fertilizer application opposed to continuous application is based on generally held conceptions of fertilizer application, however, it is also determined by the high costs involved when weighing continuous against incremental fertilization. It is more cost effective to apply fertilizers required by a crop in larger amounts spread out between fewer applications. However, due to the limiting amounts of fertilizer that plants are able to utilize in set time periods, the fertilizer not used remains in the soil and leaches away into water sources.[9] The benefit of continuous fertilizer release into the soil then becomes apparent.

The fertilizer could be applied and 'programmed' to release over a set period of time, with possible hydrophilic fertilizer coatings reducing nitrogen and potassium leaching.[10] Not only will the fertilizer be available to the plants for longer and at constant concentrations, but the amount of fertilizer wasted will substantially decrease and the fertilizer recovery and turnover will increase.[3, 10, 23, 38] Decreased fertilizer loss by leaching will also lead to a decrease in the amount of fertilizer needed for effective nutrition, resulting in lower application costs, which in turn makes systematic release economically viable. Lowered costs result in an increased use over greater areas, resulting in reduced fertilizer leaching to the ecosystem. The time it takes to release is determined by the time taken for the dissolved fertilizer ions to escape the encapsulated granule to be made available.

Shaviv and Mikkelsen [3] proposed that controlled-release fertilizers can be classified into four types: (1) inorganic materials of decreased or low solubility; (2) biologically or chemically degradable low solubility materials; (3) partially soluble materials with gradual decomposition in the soil; and (4) physical barriers used to coat fertilizers. Coated fertilizers, utilizing a physical barrier are the most promising categories of controlled-release fertilizer due to the coating not being removed or affected by degradation similar to that of the time of release. However, using coatings, such as polysulfone [11], polyvinyl chloride [39] and polystyrene [40] have decreased to the point of being abandoned due to the difficulty of degradation and potential environmental harm caused by the polymer itself or products formed by degradation.[41]

Coatings that have been made to date generally either degrade with time that allows its contents to exit once the coating has disappeared or by the systematic release of the fertilizer contents through the coating. The second mechanism is being

investigated in this study, and all methods of release are expected to occur by the fertilizer ions passing through the coating via an aqueous equilibrium forming. An aqueous equilibrium can be established by using highly absorbent coating materials to ensure sufficient water absorbance from the soil, allowing for the enclosed ions to dissolve and exit with water over time. Coatings considered for the encapsulation of fertilizer should generally be biodegradable and not form harmful products when in contact with the soil or after decomposition. Biodegradation occurs due to environmental factors such as sunlight exposure, temperature changes or the action of microbes causing chemical breakdown into simpler products.[42]

The design and use of polymers susceptible to biodegradation are of increasing importance and draws much research to be conducted towards expanding the field.[42] The reason being, polymers that degrade naturally and form nontoxic by-products, as a result, are considered greener than conventional polymers.[42] Biodegradation is a key component when considering that non-fertilizer compounds are being discarded into the environment. However, whereas recovery would prove too expensive, the removal of biodegradable polymers occurs naturally as a result of degradation by bacteria in the soil.[42] Polymer degradation is commonly associated with scission reactions occurring within the polymer chain to produce shortened fragments; a continuation thereof will eventually yield fragments small enough to wash away or be digested by microbes.[42]

Other contributing factors to degradation include; branched or linear chains, homo- or copolymer composition and the identity of the polymer itself. These polymeric characteristics must be taken into account when proposing a polymer for application as a fertilizer coating. Additionally, the physical properties mentioned previously, which control its rate of biodegradation, must be controlled to optimize degradation, to outlast its application while degrading quickly afterwards.

2.5 PAA as possible fertilizer encapsulation polymer

The highly absorbent polymer proposed for this investigation is polyacrylic acid (PAA), a polymer commonly used for its ability to absorb water far exceeding its mass.

Common examples of PAA's employment, include fibrous forms layered within diapers and healthcare products.[43] PAA is also used in water treatment for metal ion scavenging, ensnaring ions within its swollen state and preventing its penetration of the filtration membrane.[42] The aqueous interaction potential of PAA will allow for the interaction required to promote the systematic release of fertilizer ions from the coated pellet to the surrounding environment.[43] The absorbent polymer has a high water retention capacity, the ability to increase the solution potential of fertilizer ions into the membrane, a rapid water absorption rate and the ability to form a hydrogel that in turn allows increased soil interaction with the polymer and promotes the systematic release of the fertilizer ions from the gel into the soil.[43]

Biopolymers and other polymers incorporating biological compounds are growing in popularity and are gaining favour and are being implemented as possible agents to benefit many areas such as fertilizer optimization in agriculture.[2] PAA is not produced from biological compounds as in the case of biopolymers, however, the incorporation of biological compounds into PAA matrices as grafts or cross-links are well known and seen as potential biodegradable polymers.[2] PAA is soluble in its linear uncross-linked state, contributing to its potential biodegradability due to increased potential interaction and eventual breakdown by both plants and microbes.[42, 44] Complete solution of PAA in water can, however, prove to be a hindrance for fertilizer, since agricultural methods are commonly accompanied by the application of huge amounts of water.[44] The addition of water may therefore, cause immediate solution of the PAA and negate its purpose altogether if the polymer is not made to adhere to the fertilizer pellets sufficiently.

The need to use polymers with a high degree of water interaction or the capability to encourage the solution of the fertilizer will prove beneficial when designing a coating. By altering the water interaction, the absorption of water can be altered, and the release rate may be changeable. Additionally, superabsorbent PAA has been found to retain water well under strain and mechanical action, making it ideal for implementation in fertilizer coating.[45] It has been suggested by Witono et al., that a possible application of such polymers may be as moisture-retaining agents in the soil, especially in dry arid climates where water necessity and effective management thereof are dire.[45] The coated fertilizer pellet will be kept intact by the PAA layer applied. However, water will be absorbed by the PAA and penetrate to the fertilizer

ions held within. Once saturated with water, the polymer will form an equilibrium between the water in the pellet and the soil. This equilibrium forming membrane will allow for the transport of the fertilizer ions, dissolved in the exiting water, to release to the soil and to be made available to the crops as illustrated in Figure 2.3.

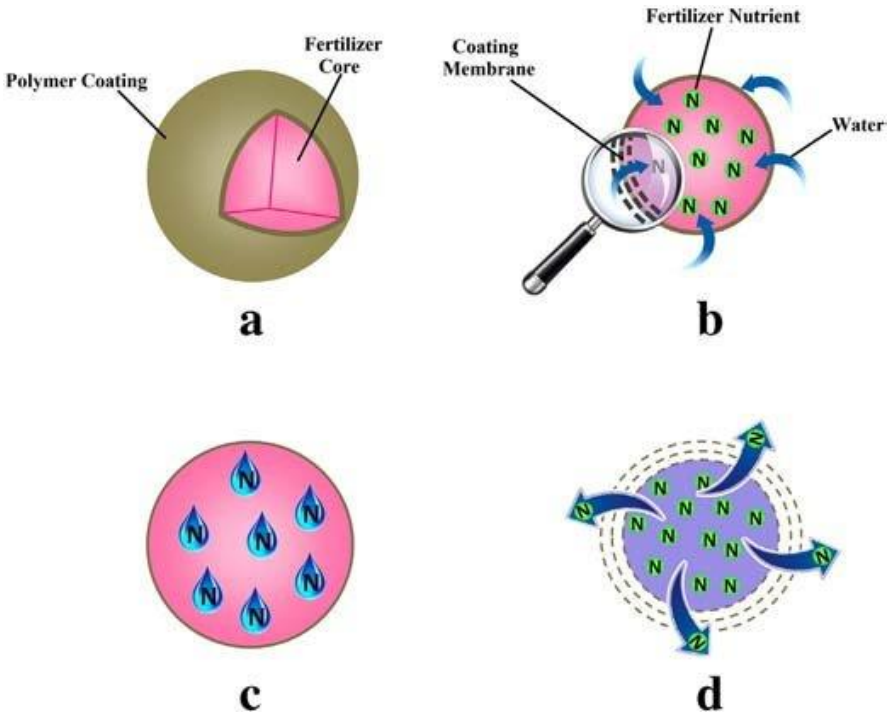

Figure 2.3 Example of diffusion mechanism of controlled-release fertilizer. (a) An encapsulated fertilizer core with surrounding polymer, (b) water penetration across the polymer coating to the fertilizer with, causing (c) fertilizer solution and osmotic pressure build-up and (d) release. (Copyright permission obtained from Elsevier).[46]

The rate of release could be programmed to replicate the nutritional requirements of different crops. Additionally, the effect of leaching will be minimized by the controlled-release, by limiting the amount of fertilizer present in the soil at any given time. Superabsorbent materials generally consist of cross-linked hydrophilic polymer chains, forming a three-dimensional network structure able to accommodate large amounts of water.[45] PAA has been cross-linked in past studies in an attempt to increase structural integrity, due to PAA's tendency to absorb large amounts of water and form a hydrogel.[43] The structure of a hydrogel is soft and without the rigid physical characteristics that dry PAA polymer possess, making it unsuitable for uses requiring

significant degrees of strength or structural integrity.[43] The employed PAA, for the coating of fertilizer pellets, will be cross-linked polymer structures, due to the coating being expected to grant structural support, abrasion protection, impact strength and tear resistance. However, the cross-linking will primarily prevent polymer solution and removal from the pellet.[44] The cross-linking of polymers is done prior to or following polymerization. However, due to the large amorphous and crystalline matrices formed , preventing penetration by chemicals, cross-linking occurs mostly in specific regions or on surfaces.[43]

According to a patent by Saotome, in an attempt to increase the water absorption capability of a PAA polymer, cross-linking was focussed primarily on the surface of the polymer and the central portion was left without cross-links.[43] Saotome's mention of surface cross-linking may attribute to the increased water absorbance, however, to maintain the membrane's structure on the pellet, cross-linking should be as uniform as possible. To regulate the release of fertilizer ions, uniform cross-link distribution will be improved by adding cross-linker to monomeric acrylic acid (AA) before polymerization. The more evenly distributed cross-links will help maintain the physical form of the coating when water is absorbed and prevent hydrogel formation and a loss of strength.[17]

Although water absorption is the main driving force for the use of PAA, cross-linking can limit the water absorption capacity by reducing it by half or more.[43] The degree of water absorption ability lost is dependent on cross-linking properties, such as the structure of the cross-linker used and its percentage presence. However, cross-linked PAA remains highly water absorbent despite the limited space for water accommodating of the cross-linked polymer.[43] Benefits found through the employment of cross-links include the retention of its shape and much of its structural characteristics, serving as runoff prevention, and thus many cross-linked polymers are classified as rigid gels.[43] Benefits of using cross-linked PAA rigid gels include that they will not absorb sufficient ambient water to cause runoff or deformation due to softening, which will remain on the applied surface for longer and under more stringent conditions when compared to uncross-linked soft gels.[44]

According to Witono et al, cross-linked polymers exhibit a specific maximum water absorption potential, reached by optimization of the available space to accompany

physical cavities between polymer chains to adsorb water into the structure, which increases with increased cross-links.[45] However, with increased percentages of cross-links, inverse effects will impact the hydrophobicity of the polymer due to more rigid polymer matrices being formed and the loss of hydrophobic groups.[45] An uncross-linked PAA polymer will, when introduced to water, instantly attract and move to accommodate water molecules. However, when water exceeds the polymer's capacity, solution of the polymer will occur, which follows when polymers move apart and enter the water.[45] Increased amounts of cross-links would form a more tightly packed matrix of polymers due to the higher frequency and closer proximity of cross-links, thus limiting available hydrophilic groups and decreasing inter-polymer spaces.[45] The highly cross-linked matrices lose the ability to swell and become rigid materials, as opposed to soft gels generally associated with superabsorbent PAA polymers.[45]

Examples of known superabsorbent polymers include PAA, often cross-linked with starch and other ester acrylates.[43] A similar cross-linked polymer will be implemented in this investigation for potential application as a fertilizer coating, with the goal to transport aqueous solutions of ions through its membrane and promote controlled-release. The ester cross-links employed will be derived from a collection of linear-hydrocarbon terminal-alcohol diols, to illustrate the effect of cross-link length on the release of ions from the pellet. Additionally, an ester cross-link formed from a biologically derived glycerol will be investigated to determine its use and effectiveness to promote controlled-release.

Cross-links similar to glycerol are used and described in literature, for example, starch derivative cross-links or esterification products of glycerol.[43] The 'green' aspect of using biologically derived compounds make their use an enticing prospect. The advantage being that glycerol is biologically occurring and a non-toxic compound, and will thus be consumed and degraded by bacteria.[43, 45] A combination of factors, aside from the ester cross-link structure will be investigated in this study to determine their effect on the controlled-release of ions from the fertilizer pellets. These factors include the thickness of the polymeric coating, the amount of coating layers used and the percentage of cross-linker present in relation to monomer.

Free radical polymerization will be employed to synthesize the polymers that will act as fertilizer coatings, using the polymerization method described by Mohammed.[15]

This method of polymerization is generally done via a free radical polymerization mechanism that employs some form of ferric catalyst to initiate the reaction. This method will be used for the coating of fertilizer pellets due to its simplistic nature and the ease of activation, being thermal.[47] Cross-linking and the effects on the resulting polymer network are strongly dependent on the concentration of cross-linker used. Properties of the produced polymer network can be altered and tailored for specific applications and characteristics by varying parameters such as the cross-linking density, achieved by an increased cross-linker implementation.[48]

Decreasing concentrations of cross-linker will favour cross-linker-free radical polymerization, resulting in a reduced cross-linking frequency and accordingly less dense cross-linked polymer networks.[47] Increased cross-linker concentrations will enable the availability of cross-linker polymeric active sites to partake more frequently, resulting in reduced segment lengths between cross-links and a denser polymer network. The density of the polymer structure will be changed through the use of cross-linkers, by varying the percentage or the type of cross-linker used. However, the density itself will not be determined. Instead, the effect on polymeric characteristics revealed by thermogravimetric investigation will be determined.

High degrees of cross-linking may increase the density of the polymer network to the extent that intermolecular spaces decrease and water retention is also decreased. The increased frequency of cross-linking and the close proximity of polymers will inevitably lead to crystallization of the polymer network or an increase thereof.[17] Crystallization and its effect on the polymeric network may lead to a reduction in the absorption of water due to denser polymer networks. However, the retention capability of the polymer network may be increased due to increased structural integrity. Other effects may be limited, such as penetration of water into the structure and slower permeation of water through the polymer network.[47]

Determining the effects and calculating the amount of cross-linkers required are essential towards determining the ideal cross-linker structure, cross-linker percentage presence and polymer coating amount to achieve specific controlled-release objectives.Highly cross-linked polymers are prone to solvent resistance, which will alter the ability of the polymer to retain water within a polymer network and is an essential factor to determine its effect on fertilizer coating and subsequent release.[49]

Solvation and solvent interaction of PAA is generally established in an aqueous medium by the interaction between the polymeric carboxylic acid groups and the water molecules.[50] Increased cross-linking will result in fewer carboxylic acid groups being available for interaction, thus resulting in reduced absorption, reduced retention and eventually becoming insoluble in aqueous solutions.[47, 49] Reduced interaction between the PAA polymer network and surrounding water is intended to promote slowed solvation of the fertilizer within the encapsulated pellet.

Slowed water penetration and permeation of the coating layer to enter, dissolve the contents, and exit the encapsulated fertilizer are the basis by which controlled-release is to be achieved. Reduced solvation times of the fertilizer will theoretically slow the release of fertilizer ions into the aqueous solution surrounding the coated fertilizer. The increased retention of water can be ascribed to the increased mechanical strength of the polymer network, as a result of additional bonds holding polymers together and crystallization.[47]

2.6 Linear diols, glycerol and EGDM as PAA cross-linkers

If increased crystallinity and the proximity of polymer chains in a polymer network affects its ability to absorb and retain water, then by varying the intermolecular spacing between polymers a change in physical properties will be observed. Intermolecular spacing between cross-linked polymers can be changed by varying the length of the cross-linker employed to form the cross-linked polymer network. By using different lengths of linear cross-linker molecules, the cross-linker changes in length similarly and increases the separation between polymer chains. This first factor of altering the cross-linking density of the polymer is possible due to specific spacing distances achieved between polymers.[47] The second factor determining the physical properties of polymer networks is the frequency of cross-linking. The frequency of cross-linking can be altered by changing the concentration of cross-linker used with regard to the monomer.[47]

Elliot et al. describes a cross-linker as a monomer or monomer derived compound containing two or more double bonds.[47] The cross-linkers act to connect the linear

polymers into a network, creating an interconnected structure and reducing free movement by individual polymers.[47] According to Kricheldorf, Nuyken and Swift,[51] linear diols are chemically well-known and commercially available, making their use ideal as a precursor for large scale PAA cross-linker synthesis. The position of hydroxyl groups relative to one another in linear diols makes it possible to synthesize PAA cross-linkers with controlled variations in the lengths of hydrocarbon chains separating the AA groups, located on the terminal positions.

The hydroxyl groups present enable the linear diols to undergo esterification with AA twice, enabling the formation of double, terminally located, polymeric active AA groups.[52] This control will enable investigation into the effect of cross-linker length on the morphology and physical properties of cross-linked PAA, according to Olsen and Sheares.[52] In a similar study to this study, using linear diol variation, the effect of the differing chain length of linear diols enabled variation in thermal and solubility properties.[52] The effect of these varying traits should impose variations on its ability to coat, and by altering conditions of the cross-linker employed and percentage presence, it should become possible to facilitate controlled-release of fertilizers coated with cross-linked PAA. Cross-linked polymers are generally used as superabsorbent materials, due to the cross-links allowing the individual polymer chains increased flexibility and capacity to retain water.[45, 47]

Additional to chemical similarity and single variable differences between the linear diols, linear diols are implemented due to their ease of esterification under mild conditions.[15] Ethylene glycol dimethacrylate (EGDM) is used as a PAA cross-linker, however, it is procured and not synthesized and used as a reference. Apart from being a methacrylic acid (MA) derivative, EGDM is used as a reference due to being structurally near-identical to all planned linear diol cross-linkers. The addition of EGDM as a reference to the list of cross-linkers will broaden the investigation by including a structural variation from the AA based cross-linkers, while also serving as an ideal synthesis product. The structural difference between the dimethacrylate and acrylic groups should bring about changes to the polymerization kinetics, polymer network structure, degree of cross-linking and physical properties of the polymer such as crystallinity.[53] An example of such an effect includes the slower polymerization rate of methacrylates relative to acrylates.[51]

However, the solubility of both methacrylates and acrylates are similar and will be usable in similar solutions when undergoing polymerization, which is important when comparing application.[51] To serve as a comparable cross-linker to that synthesised, EGDM must be similar in nature and be able to undergo identical reactions, which it is due to the nature of the ester group not affecting the copolymerization reaction itself, according to Kricheldorf, Nuyken and Swift.[51] The effects of EGDM on the resulting polymer network will serve as a benchmark for the synthesized cross-linkers, due to its commercial availability and past use as cross-linker.

Glycerol is chemically well-known and is used extensively. Glycerol is a multi-alcohol-containing molecule with three hydroxyl groups, two primary and one secondary, thus making it ideal for esterification reactions planned with AA. The presence of multiple esterification sites makes glycerol uncharacteristic in comparison to the linear diol cross-linkers also planned. The increased number of esterification sites will give insight into the effect of tri-ester containing groups on the cross-linking of PAA. Additionally, in support of its use similar to this study, glycerol has been used in carbonic forms as additives and cross-linkers in polymers.[15, 54]

Furthermore, adding to its low-cost and ease of procurement, glycerol occurs naturally.[55] Glycerol has a well consolidated presence in the world market and is widely applied in many fields, as fillers, in cosmetics, perfumery, food, pharmaceuticals, raw materials for chemical derivatives, automotive, tobacco and paints.[55-57] Such a wide area of application allows glycerol to have a continuous economic availability, resulting in low cost and ease of procurement. Glycerol's wide application can also be attributed to the rising concern of using fossil fuels, in terms of sustainability and environmental effects, and also its abundance.[58]

Chapter 3

Synthesis and characterisation of AA-based cross-linker ester compounds from linear diols and glycerol

3.1 Introduction and objectives

3.1.1 Esterification of linear diols and glycerol using AA

Esterification of linear diols and glycerol with acrylic acid (AA) is done via an acid-catalyzed dehydration reaction, with continuous water removal. The esterification reaction is optimized to increase yields and product purity, which is subsequently applied identically to all linear diol lengths and to glycerol. During esterification the removal of water, formed as a byproduct, is paramount to the success of the reaction, acting to drive the reaction to completion through Dean-Stark removal. The planned esterification reaction should occur to form the di-ester products from the linear diols and glycerol. However, if mono-ester or tri-ester products form, the quantification of the ester composition is done to give an estimated degree of esterification that occurred.

Di-ester formation from the linear diols is the only product usable as cross-linkers due to its ability to undergo polymerization reactions at both terminal acrylate sites. Polymerization of mono-ester compounds will only be able to undergo polymerization at one terminal location and will not be able to link two polymer chains together and act as a cross-linker, as shown in Figure 3.1. Also shown in Figure 3.1, is that the mono-ester is not favorable due to its inability to join two polymer chains together. Thus, reaction optimization will be attempted to favor the formation of the di-ester and achieve complete esterification.

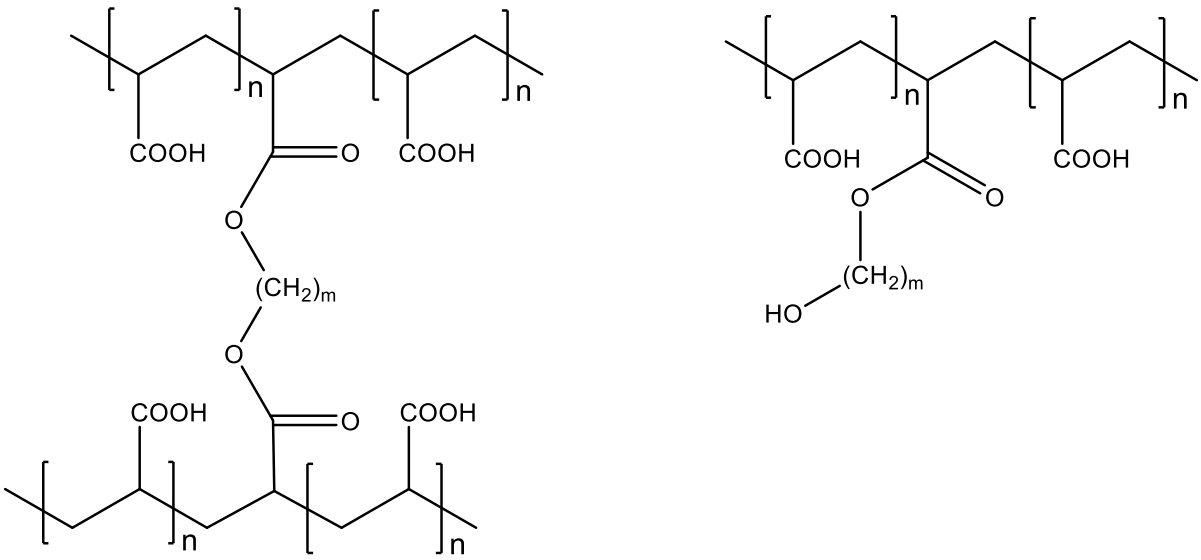

Figure 3.1 Polymeric insertion of the di-ester (left) and mono-ester (right). Illustrating the cross-linking potential of the di-ester of the linear diol compounds, with m = 2-6.

Similarly, glycerol has the ability to form multiple ester groups with its two primary and one secondary hydroxyl group. However, esterification of both primary and secondary hydroxyl groups could be difficult due the secondary hydroxyl being less reactive than the primary; consequently, glycerol derivatives formed are expected to be a mixtures.[59] A mixture of esters is still applicable and have cross-linking capabilities, however, the composition of the esters is crucial due to their varying effects on the polymer matrix structure. Glycerol, can thus undergo threefold esterification in comparison to twice for the linear diol di-ester products. The addition of a third ester group baring an acrylate capable of undergoing polymerization changes the cross-linking capability of the product.

The final tri-ester form of glycerol can undergo polymerization at each of its acrylate sites if reacted completely, and form a cross-linking structure, as shown in Figure 3.2. The effect of the structure shown in Figure 3.2 relative to structures formed by EGDM and theoretically by the linear diols should be major. Increased cross-linking, in particular the number of chains linked per cross-linker, will result in a greater potential to act as a cross-linker. Theoretically, glycerol tri-ester containing mixtures will form the most densely packed polymer matrix; the least hydrophilic structure and the strongest polymer network.[60] The change in thermogravimetric properties of the polymers, obtained by employing the synthesized cross-linkers, will be used as comparison of the eventual release rates that polymers enact on the coated fertilizer.

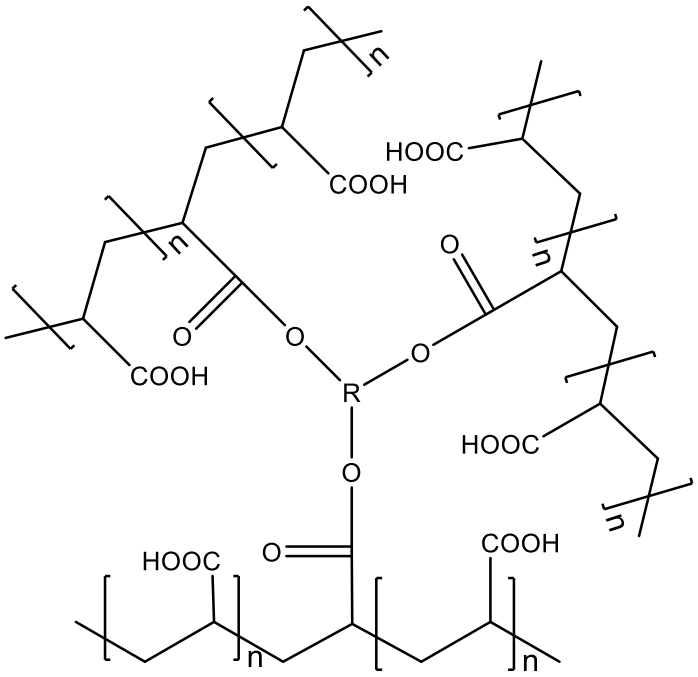

Figure 3.2 Glycerol tri-ester cross-linking potential at both primary and the secondary acrylate groups, with R = CH_2CHCH_2 from the starting glycerol.

To test the application of glycerol and its effect on the polyacrylic acid (PAA) network, a di-ester is planned by controlling initial reagent ratios, due to a homogeneous mixture of di-esters being preferred and yielding comparable cross-linking potential. Formally an acylation reaction between the linear diols and glycerol with AA, esterification of alcohols and carboxylic acids are commonplace organic chemistry reactions. Esterification is widely employed due to its simplicity and ability to increase chemical complexity by joining two molecules into one.

With water being the only expected by-product of the reaction, aside from solvents, the reaction is considered ‘green’ and will not be altered by employing more reactive forms of the reagents.[61] High reactivity reagents such as acryloyl chloride are employed by Mohammed [15], which, although prone to better conversion, form dangerous by-products that are expensive to process further. Thus, the simplest esterification route possible, with limited or no harmful products, is followed for possible industrial application and large scale synthesis. Acid-catalyzed esterification and continued water removal via azeotrope formation with the solvent are used to drive the reaction to completion. For this study, an acid resin catalyst is used, due to its

inability to dissolve into solution and recoverability post-reaction. Methods of optimization include the selection of an ideal solvent, variation of the molar equivalents of reagents relative to one another, variation of the method of water removal and also reaction time variation. Solvent variation inevitably causes temperature variation and is thus taken into consideration to determine its effect on the success of the esterification reaction.

3.1.2 Objectives

The objectives of Chapter 3:

- The synthesis of di-ester cross-linker products through the esterification of AA with linear diols and glycerol
- Optimization of esterification reaction conditions for optimum product formation and purification of linear diol and glycerol ester products
- Analysis and characterization of ester products using Fourier Transform Infra-Red (FTIR), Atmospheric Pressure Chemical Ionization Mass Spectroscopy (APCI-MS) and Nuclear Magnetic Resonance (NMR)
- Quantification of esterification products synthesised with NMR techniques

3.2 Experimental

3.2.1 Materials

1,2-ethanediol (Rochelle Chemicals), 1,3-propanediol (Aldrich), 1,4-butanediol (Sigma Aldrich), 1,5-pentanediol (Aldrich), 1,6-hexanediol (Aldrich), aluminium trifluoromethanesulfonate (WAKO), B-23 acid ion exchange resin catalyst (Sasol), benzene (Minema Chemicals), hydroquinone (Merck), sodium hydrogen carbonate (ProMark Chemicals), toluene (Rochelle Chemicals), ethyl acetate (Rochelle Chemicals) and sodium sulphate (anhydrous) were used as received from the respective suppliers without further purification unless stated otherwise. Freshly distilled AA (Sasol) was prepared prior to each reaction or application involving AA. AA distillation occurred under nitrogen and reduced pressure with the addition of hydroquinone prior to distillation.

3.2.2 Analytical techniques

Gas Chromatography Mass Spectrometry (GCMS) Analyses

An Agilent Technologies 6890N Network GC System was employed for the separation using an Agilent 19091S-413U 30 m x 320 µm x 0.25 µm column. The run was done from an initial starting temperature of 50 °C with a temperature programming of 10 °C/min for a run time of 22.0 min until a final 250 °C oven temperature. The GC system was coupled to an Electron Spray Ionization Mass spectrometer, serving as a detector. Sample injection volumes of 1.0 µL were used for final product analyses.

Atmospheric Pressure Chemical Ionization Mass Spectrometric (APCI-MS) Analyses

A Bruker mass spectrometer (Microtof-q II) was used with Atmospheric-Pressure Chemical Ionization (APCI) ionization methods. The sample was loaded directly via glass capillary and placed within the MS ionization source, without the use of solvent

Scanning was initiated at 50 m/z and ceased at 1500 m/z, using a positive ion polarity, the capillary was set at 4500 V and the endplate offset at -500 V. The nebulizer gas was set at 1.6 bar, the dry heater temperature set at 200 °C and the dry gas was pumped at 8 L/min.

Fourier Transform Infra-Red (FTIR) Analyses

A Bruker Alpha-p infrared spectrometer was set at 32 sample and background scans between 4000-400 cm^{-1}, a 7.5 KHz scanning velocity, 0-8000 wanted frequency limit and a 4 cm^{-1} resolution. The samples were mounted dry or as an oil, clamped down, and the measurements were made.

Nuclear Magnetic Resonance (NMR) Analyses

^{1}H, ^{13}C, DEPT135, DEPT90, COSY, HSQC, and HMBC analyses were performed on a 600 MHz Bruker Ultrashield Avance II NMR spectrometer. The spectrometer was equipped with a 5 mm diameter probe. A direct-observation, two-channel broadband observation probe was employed. ^{1}H spectra were recorded at approximately 600 MHz, and ^{13}C spectra were recorded at approximately 150 MHz. Sixteen scans were employed to record ^{1}H spectra and 256 scans to record the ^{13}C spectra. The Bruker proprietary software, Topspin 3.5 patch level 5, was employed during operation of the spectrometer as well as for processing data. Mass noted samples of approximately 35 mg were dissolved in 1.0 mL $CDCl_3$ or D_2O, the use of which is noted. DEPT135, DEPT90, COSY, HSQC, and HMBC analyses were performed as needed.

3.3 Synthesis of PAA cross-linkers by esterification of AA with linear diols and glycerol

3.3.1 AA distillation

AA was distilled using vacuum-assisted distillation, by connecting a 500 mL round bottom flask containing AA and hydroquinone to a nitrogen source and a condenser with a 100 mL round bottom collection flask placed in ice. Reduced pressure was maintained by using a vacuum pump, connected at the end of the condenser, and by sealing all connection points between the glassware. Distillation occurred under reduced pressure while stirring under nitrogen at 95 °C until sufficient AA was distilled for use.

AA distillation was necessary prior to any reaction due to the formation of diacrylic acid (DAA) from any AA latching onto another AA or any AA-derivative, which occurs spontaneously. [65] The reaction schematic describing the formation of these polyacrylic acid products is shown in Figure 3.4 in Chapter 3.

3.3.2 Linear diol and glycerol esterification

The distilled AA and linear diol (5:1 mole ratio), hydroquinone and B-23 acid resin catalyst were dissolved in 300 mL of benzene, and placed in a 500 mL two neck round bottom flask that was connected to a nitrogen source and a reflux collecting cylinder tap capable of removing water. Nitrogen was flushed throughout the reaction whilst stirring continuously and maintaining reflux at 85 °C for 3 hours. Azeotropic removal of water via utilization of the Dean-Stark extraction method and setup was employed to drive the reaction to conclusion as shown in Figure 3.3 with structures named and numbered. Following the allotted time, the reaction was stopped by ceasing the flow of nitrogen, stirring and heating of the reaction flask. The reaction flask contents were then filtered to remove any still solid hydroquinone and B-23 catalyst, after which the mixture was poured into a saturated mixture of sodium bicarbonate dissolved in water to neutralize the mixture and to separate the products from unreacted reagents.

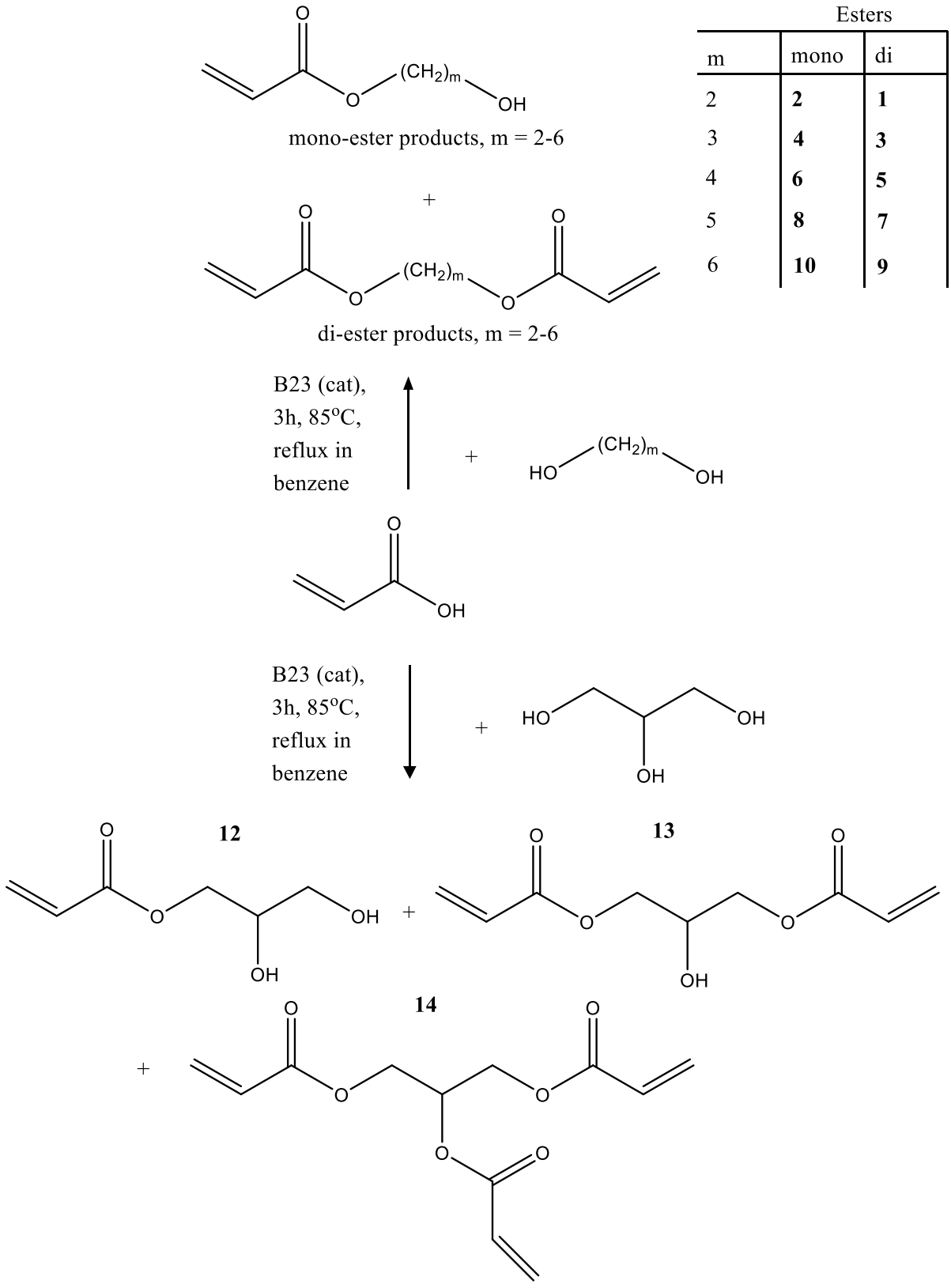

	Esters	
m	mono	di
2	**2**	**1**
3	**4**	**3**
4	**6**	**5**
5	**8**	**7**
6	**10**	**9**

Figure 3.3 Linear diol (upward arrow) and glycerol (downward arrow) esterification products formed with AA to obtain mono-ester, di-ester and tri-ester cross-linker products. For linear diols m = 2-6 in this study.

A 1 L separating funnel was used to separate organic and aqueous solutions; however, additional product separation from the residual aqueous mixture is possible by using diethyl ether following the removal of the benzene layer. The top organic layer was collected, dried with anhydrous Na_2SO_4 and concentrated by a vacuum-assisted rotary evaporator.

The esterification products from the linear diol and glycerol presented reactions percentage yields of 60.00 ± 22.93% (**1** & **2**), 35.50 ± 9.47% (**3** & **4**), 32.78 ± 11.24% (**5** & **6**), 29.86 ± 12.30% (**7** & **8**), 15.93 ± 9.84% (**9** & **10**) and 56.66 ± 12.19% (**12-14**). All the reactions lead to the formation of the di-ester product, due to similar cross-linking potential between cross-linkers. Ethylene glycol dimethacrylate (EGDM) (**11**) served as a reference for comparison to di-ester products, however, for optimal purity and assurance of function, **EGDM** was procured commercially. Multiple di-ester and mono-ester products can form based on the terminal or central location of acrylate groups; however, no specific distinction could be made between such isomers and will thus not be addressed. Analysis of the product by GC/MS did not indicate the expected product molar masses. However, the disappearance of the linear diol reagent could be observed. Due to the removal of AA, linear diols and glycerol by washing, no clear data could be gained from the GC/MS analysis. The inability to observe the product by GC/MS analysis is potentially due to high boiling point values of the desired product or thermally initiated polymerization in the injector port. MS and NMR analysis techniques was predominantly employed for qualitative and quantitative characterisation and analysis.

3.3.3 Optimization methods employed to improve purity and product formation

Acid-catalysed esterification to form acrylate esters via conventional chemical routes is, according to Nemec and Bauer[66] and Hajjar et al.,[67] inefficient for complete conversion. Nemec and Bauer,[66] goes on to state that multi-hydroxyl containing molecules reacted with acrylates or methacrylates will inevitably form a complex mixture of unreacted alcohols, as well as partially and fully substituted esters. A similar esterification reaction was carried out by Morita,[61] whom attempted the esterification of AA with glycerol, whilst using a similar acid-catalysed route and the addition of an

acid resin. This reaction, done under similar durations of time, temperature and molar ratios, yielded a mixture of mono-esters, di-esters and tri-esters of the substituted glycerol acrylate. The variation of conditions made, as shown in Table 3.1, showed little to no improvement on either product yield or purity, resulting in an unavoidable mixture of products and subsequently, the glycerol acrylate mixture was used as is for subsequent reactions.

Working from the notion that complete substitution of glycerol to its tri-ester or di-ester form will not occur, a series of optimization methods were proposed and were implemented as shown in Table 3.1. The alterations of reaction conditions were based on the avoidance of potential premature polymerization of the ester mixtures, the mass of product mixture that formed, the avoidance of by-product forming reagents and the purity of the products formed. If possible, multiple esterification reactions of substitution per linear diol or glycerol was the overall aim of the cross-linker synthesis of this study. However, optimization was implemented to increase the product yield and substitution to the highest degree possible, within reason and time constraints, and to purify the product mixture as effectively as possible. Optimizations were conducted on the esterification reaction of glycerol with AA and then applied identically to the esterification of all linear diols.

Table 3.1 List of reaction conditions used in the cross-linker syntheses.

Reaction Time (h)	3, 6, 12, 24
Catalyst	B-23 Amberlyst, $Al(OSO_2CF_3)_3$
Molar Ratio (Diol:AA)	1:1, 1:2, 1:3, 1:4, 1:5, 1:15, 1:20,1:25
Solvent / Temperature (°C)	$CHCl_3$ / 65, C_6H_6 / 95, $C_6H_5CH_3$ / 110

Variations in reaction time included longer reaction times than that prescribed in literature for similar reactions with AA, such examples include a patent by Kautter and Baumann,[68] who reported a yield of ester products within the first hour of synthesis. This is also supported by Morita,[61] that reports Amberlyst resin-catalysed esterification occurring in 1 hour and other esterification reactions occurring in 4-8 hours. The catalyst used for the acid catalysed esterification of AA with glycerol was B-23

Amberlyst acid resin catalysts, received from Sasol, similar to that employed by Morita,[61] while aluminium trifluoromethanesulfonate was also attempted. The B-23 catalyst was used following optimization investigation due to near-identical product formation relative to the aluminium trifluoromethanesulfonate, however, the purity of the product when analysed post-synthesis was better for that of the B-23. According to Almeida-Rivera and Grievink,[69] amberlyst acid ion-exchange resin catalysts are best for esterification of glycerol in biodiesel production.

Molar ratio variations were made to maximize the degree of substitution to form the di-ester glycerol product, and similarly the di-ester product for the linear diols. The molar ratio of AA relative to the alcohol-baring reagent was varied, as shown in Table 3.1, irrespective of the mole amount of hydroxyl groups present on the hydroxyl baring reagent. However, true to the statement made by Hajjar,[67] a mixture of ester products was always obtained despite maximizing reagent ratios to promote complete substitution products, and due to molar ratios exceeding 1:5 being wasteful, the molar ratio was maintained at 1:5 for glycerol and all other esterification reactions.

Reaction temperatures were maintained throughout the reaction at the temperature specific to the boiling point of the azeotrope that formed from the reaction of the solvent with the water by-product. The removal of water occurred for all of the aforementioned solvents, however, benzene was used for all subsequent esterification reactions due to its ease of removal post-esterification and being less prone to cause product polymerization. Following the optimization investigation, the use of toluene and chloroform resulted in product formation equivalent in yield, purity and composition (major and by-products) when compared to benzene. However, due to the high temperature (110 °C) needed for the removal of toluene, polymerization occurred and rendered the product unusable, which is also reported in literature.[55] Similarly, the removal of chloroform also caused polymerization, and its use was also discontinued.

3.3.4 Purification and separation methods

Additional to the methods of optimization, post-reaction attempts at purification and separation were made to remove unreacted reagents and by-products formed, and attempt to separate desired products. Separation was attempted to analyse mono-

ester, di-ester and tri-esters. Purification of the products was achieved by washing the reaction mixture post-esterification; first with sodium hydrogen carbonate in distilled water followed by washing twice with distilled water. The less water soluble products being esters, move to the organic diethyl ether layer, added to achieve product isolation. Washing proved effective at removing most by-products and yielded only mono-ester, di-ester and tri-ester products and derivatives thereof. Washing was employed following each reaction.

Phase separation of the product mixture post-washing with varying polarity organic solvents in an attempt to separate the individual ester products was done. However, no successful phase separation could be achieved. Thus the technique was disregarded. Product separation was done firstly by thin-layer chromatography (TLC), and then a similar mobile phase solution was used to separate and isolate the products via a packed-column chromatographic (PCC) separation. TLC separation was attempted with varying mobile phases and mixtures thereof, the best of which was a 4:1 mixture of diethyl ether to hexane. The separation yielded three bands. A recovery of these bands by PCC showed a less pure mixture with the products no longer being observed following analysis. Redistillation of the recovered ester product mixture was attempted, following the procedure of Morita,[61] with a similar vacuum distillation of AA from the mixture.

Deviating from the procedure of Morita [61] due to instrument limitations the temperature was not kept to the 66 °C as stated. Instead, vacuum was applied, and the temperature increased until distillation occurred. The attempt at distillation was two-fold. Firstly, the method was followed as prescribed by Morita[61] in an attempt to implement a simplified procedure as opposed to washing, to remove excess AA, however, washing was found to remove the excess AA in addition to its purification with improved results. Secondly, the AA dimer formation was observed in the NMR analysis of the products, similar to that of AA pre-distillation. Thus, an additional distillation could potentially break dimers apart similar to AA distillation. Additional distillation proved not to remove AA dimers and resulted in muddied spectra and increased by-products.

3.4 Results and discussion

3.4.1 Cross-linker synthesis

Cross-linker formation by reflux esterification using the acid resin Amberlyst B-23 catalyst caused a water and benzene azeotrope to form, which was removed periodically until the completion of the reaction time. The reagents of all reactions mixed successfully apart from 1,5-pentanediol and 1,6-hexanediol in which the diol and benzene remained separate. The acid resin catalyst floated freely in solution, whilst the hydroquinone, acting as a polymerization inhibitor, dissolved. Products of the linear diol and glycerol esterification reactions formed a mixture of faint yellow to dark yellow and orange viscous oils that were analysed by MS, IR and NMR techniques to determine structures and yields.

3.4.2 Infrared Analysis

FTIR was done on products following esterification and post-reaction workup to determine whether the reaction was completed and the purity of the product. The FTIR spectra of compounds **1**-**14** are available in the supporting information in the appendices. Key bands of absorption investigated were those of alcohol bands, reminiscent of unreacted diol or mono-esters, , carbonyl stretches shifting or multiple stretches appearing due to ester group formation, and lower ether group stretches also due to ester formation. FTIR analyses of the synthesized products **1**-**14** all showed similar absorption bands when compared to **11**, which was used as a reference due to being acquired and not synthesized.

Expected bands for di-ester structures: **1**, **3**, **5**, **7**, **9** and **12**, determined include; 3200-3000 cm^{-1} from weak alkene C=C-H alkene-hydrogen groups contributed by the AA addition to the structure, 3000-2850 cm^{-1} resulting from alkyl C-C-H stretches found within the original diol reagent, strong 1750-1720 cm^{-1} ester carbonyl stretches, 1480-1440 cm^{-1} alkyl-hydrogen CH_2 stretches, and several medium to strong ether C-O-C stretches in the 1250-1050 cm^{-1} range. Additional to the expected aforementioned absorption bands, C-OH alcohol bands are observed, caused by mono-ester products

(**2**, **4**, **6**, **8**, **10**, **13** and **14**) or alcohol baring molecules such as those in structures. The positioning and range of the carbonyl ester stretch were similar to that of **11**, which aids in confirming the formation of esters; however, multiple carbonyl stretches were observed in addition to the stretch expected, which was a result of dimerization.

Furthermore, no wide range carboxylic acid OH or COOH stretches were observed for the linear diol products, which supported the removal of AA from the reaction mixture by the workup method employed. However, a carboxylic acid COOH band was observed for the glycerol product mixture. Alkyl C-H stretches increase in intensity as the chain length of the diol increases from 1,2-ethanediol to 1,6-hexanediol, however, the alkene C=C-H peaks remained present throughout the spectra, which was essential to ensure terminal alkene groups for future polymerization.

3.4.4 APCI-MS analysis of linear diol and glycerol ester products

APCI-MS analysis was done in an attempt to minimize fragmentation and observe the original product ion. Using APCI-MS analysis, the formed products were compared to predicted masses, resulting fragments formed during analysis were determined from the investigation. MS analysis of **11**, the only acquired di-ester cross-linker, showed that fragment formation occurred. The resulting fragments formed by cleaving the ether bonds (C-O) adjacent to the ester group for all linear diol products are shown in Figure 3.4. The fragments shown in Figure 3.4 occurred for each of the synthesized di-ester cross-linkers and was used to determine the formation of the intended product.

The only linear diol ester products that did not follow the fragmentation pattern shown in Figure 3.4, was that of 1,5-pentanediol ester products, **7** & **8**, and 1,6-hexanediol ester products, **9** & **10**, which broke the C-O bond between the carbonyl and ether group, thus, essentially forming the fragment of the protonated mono-ester. This alluded to the possibility that mostly mono-ester formed from these diol species. Apart from the fragmented masses observed, the complete molecular mass of the product was observed and served to further prove successful product formation. However, larger molecular masses were also observed, which was due to dimerization or oligomerization as shown in the supporting information. Products: **1**-**10** showed fragmentation patterns similar to that seen in **11**.

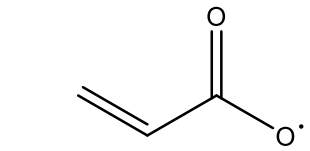

Chemical Formula: $C_3H_3O_2^{\bullet}$
Exact Mass: 71,01

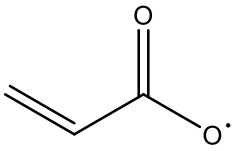

Chemical Formula: $C_3H_3O_2^{\bullet}$
Exact Mass: 71,01

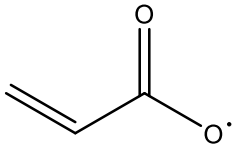

Chemical Formula: $C_3H_3O_2^{\bullet}$
Exact Mass: 71,01

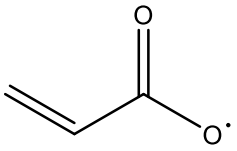

Chemical Formula: $C_3H_3O_2^{\bullet}$
Exact Mass: 71,01

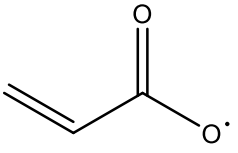

Chemical Formula: $C_3H_3O_2^{\bullet}$
Exact Mass: 71,01

Chemical Formula: $C_5H_7O_2^{\bullet}$
Exact Mass: 99,04

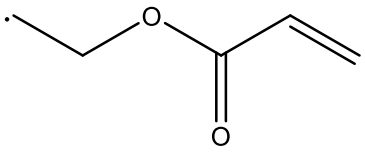

Chemical Formula: $C_6H_9O_2^{\bullet}$
Exact Mass: 113,06

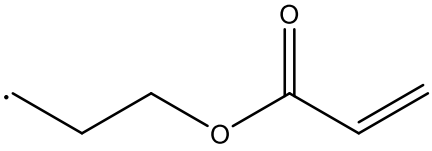

Chemical Formula: $C_7H_{11}O_2^{\bullet}$
Exact Mass: 127,08

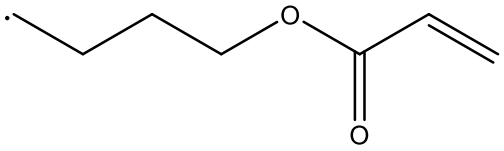

Chemical Formula: $C_8H_{13}O_2^{\bullet}$
Exact Mass: 141,09

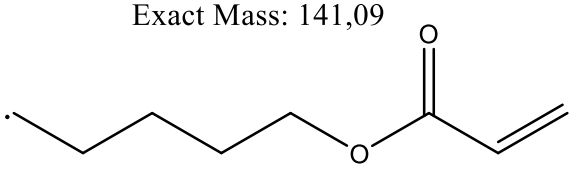

Chemical Formula: $C_9H_{15}O_2^{\bullet}$
Exact Mass: 155,11

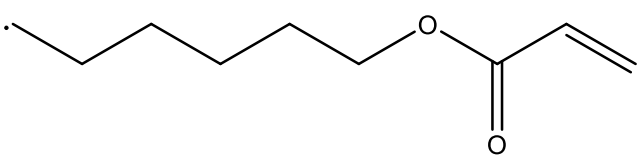

Figure 3.4 APCI-MS fragments from **1**-**2**, **3**-**4**, **5**-**6**, **7**-**8** and **9**-**10** respectively according to the fragmentation pattern of **11**, and represent the masses used to determine whether product formation occurred.

The dimeric form is an addition of AA groups to the product molecules, in a nucleophilic dimer addition of one AA to the unsaturated β-C alkene carbon, forming an elongated ester structure, while maintaining the alkene group of the added AA as shown in Figure 3.5. Possible molecular masses of the dimeric, trimeric or other oligomeric forms are given in Table 3.2, however, not all these masses appear. The occurrence of such acrylic acid derivative forms are later shown and was proven to form with NMR.

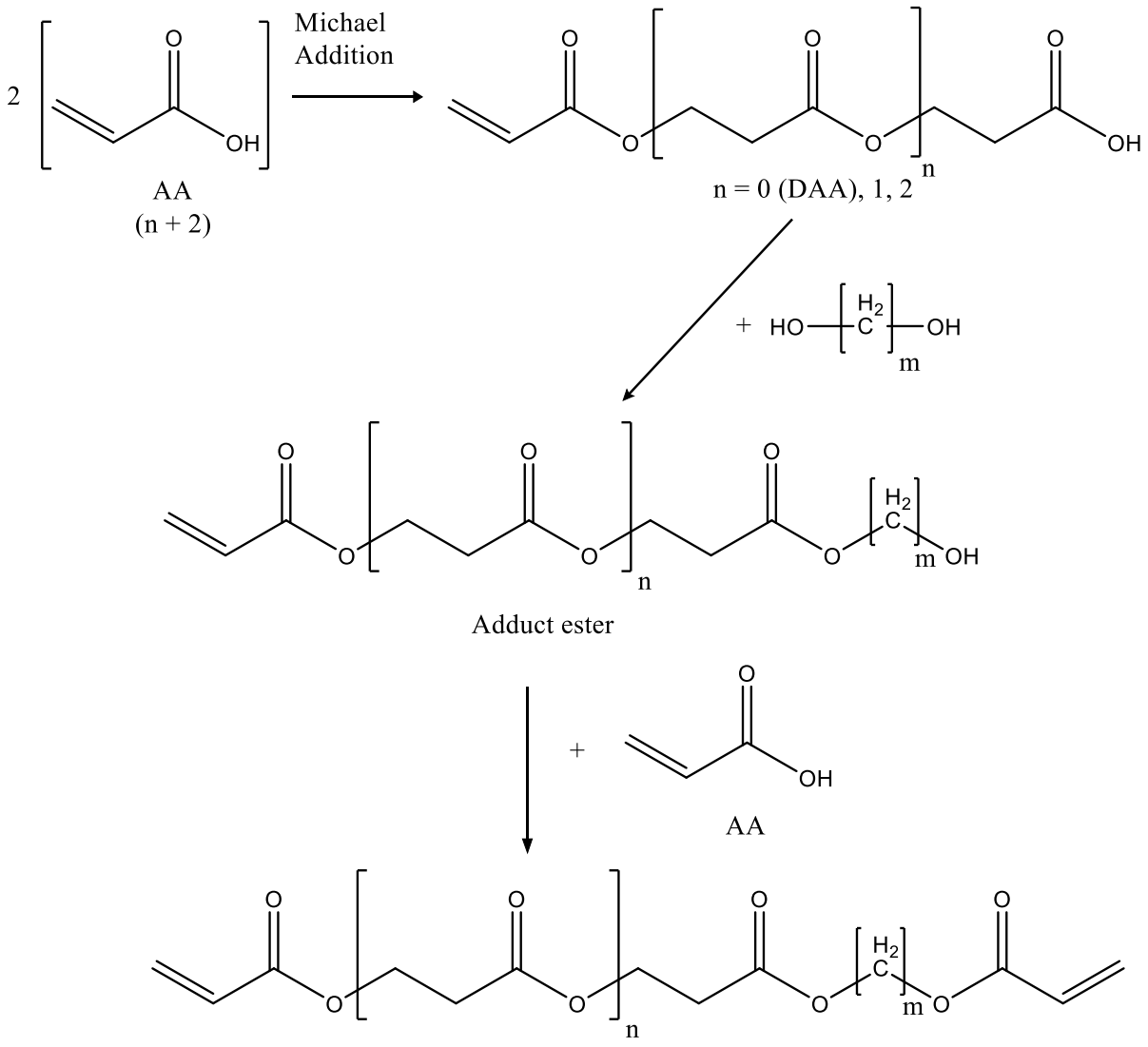

Figure 3.5 Michael addition products from AA or ester substrates.

However, the larger, possible oligomeric masses are seen in conjunction with the predicted product masses, revealing that larger product-related by-products formed. It is possible, in cases such as the 171 g/mol, 208 g/mol, 280 g/mol, 241 g/mol and 314

g/mol fragments observed in the **1** & **2** analysis, that correlates to dimeric or oligomeric forms of the planned mono-ester and di-ester.

Table 3.2 APCI-MS Michael addition products possible to form from the linear diol products **1**-**10**.

		Molar mass values of Michael addition fragments of m				
	n	2	3	4	5	6
Adduct ester	0	188	202	216	230	244
	1	260	274	288	302	316
	2	332	346	360	374	388
Adduct di-ester	0	242	256	270	284	298
	1	314	328	342	356	370
	2	386	400	414	428	442

Additional dimer formation is similar for 271 g/mol, the trimeric form 343 g/mol and the possible tetrameric form 415 g/mol in the **5** & **6** analysis. In the analysis of **7** & **8** many 72 g/mol (AA) associated fragment mass differences appear, however, the fragmentation pattern is not identical, with some fragments appearing with 18 g/mol (H_2O) increase or decrease in mass, most likely caused by water addition or elimination. The fragments formed predominantly follow the fragments as shown in Figure 3.4 and Table 3.2, however, taking the new fragmentation into account and adding 72 g/mol (AA) mass increments, the dimeric 245 g/mol fragment becomes apparent. During the formation of **12**, **13** & **14** the glycerol cross-linker, three distinct fragment masses were observed; 129 g/mol, 183 g/mol and 255 g/mol which are the predicted molar masses of the mono-ester, di-ester and tri-ester, as shown in Figure 3.3, **12**, **13** & **14**.

Dehydration was evident in the masses of **13** & **14** and is possible due to hydroxyl groups that remained unreacted, however, this was not the case for **12**. Similar occurrences of dimeric and oligomeric products to that observed in the linear diol ester products also occurred for glycerol products, with masses of 329 g/mol and 401 g/mol respectively showing a 72 g/mol addition. The occurrence of dimeric, trimeric and

oligomeric forms does not alter the application of the products formed, thus these oligomeric forms are not noted specially nor ascribed unique product numbers.

3.4.5 NMR Elucidation

NMR analysis of reference compound

11 was used as a reference for the positioning of the NMR signals expected, due to the similarity of **11** to linear diol mono-ester (**2**, **4**, **6**, **8** & **10**) and di-ester (**1**, **3**, **5**, **7** & **9**) structures. The primary difference being a methacrylate group replacing an acrylate and the linear chain connecting the terminal groups changing in a number of methylene groups. The greatest asset of the reference was its purity, thus negating any potential by-product signal interference as predicted by the MS data. The structure of **11** is labelled for analysis, as shown in Figure 3.6. Positions are numbered according to their position from the outer, terminal positions, to the inner 'linear diol' centre.

^{1}H-NMR analysis of **11**, as seen in Figure 3.6, showed the protons at position 1 as non-equivalent on the spectrum at 6.14 and 5.60 ppm, being the cis and trans position proton relative to the carbonyl, respectively. Splitting patterns for the protons on position 1 were not observed as expected, however, similar signals for **1**-**10** showed geminal coupling between the protons on position 1 and also with the vicinal position 2 located proton. The central protons on position 4 appeared further upfield, at 4.41 ppm, and the methylene protons at position 5 appeared the furthest upfield, at 1.96 ppm. ^{13}C-NMR analysis of **11** showed a simplistic signal distribution, as seen in Figure 3.7. The signals observed were identified as 167.2 ppm being the carbonyl carbon 3, 136.1 ppm being the alkene carbon 2, 126.1 ppm being the alkene carbon 1, 62.3 ppm is carbon 4, 18.2 ppm is carbon 5 and 77.1 ppm being the signal of chloroform.

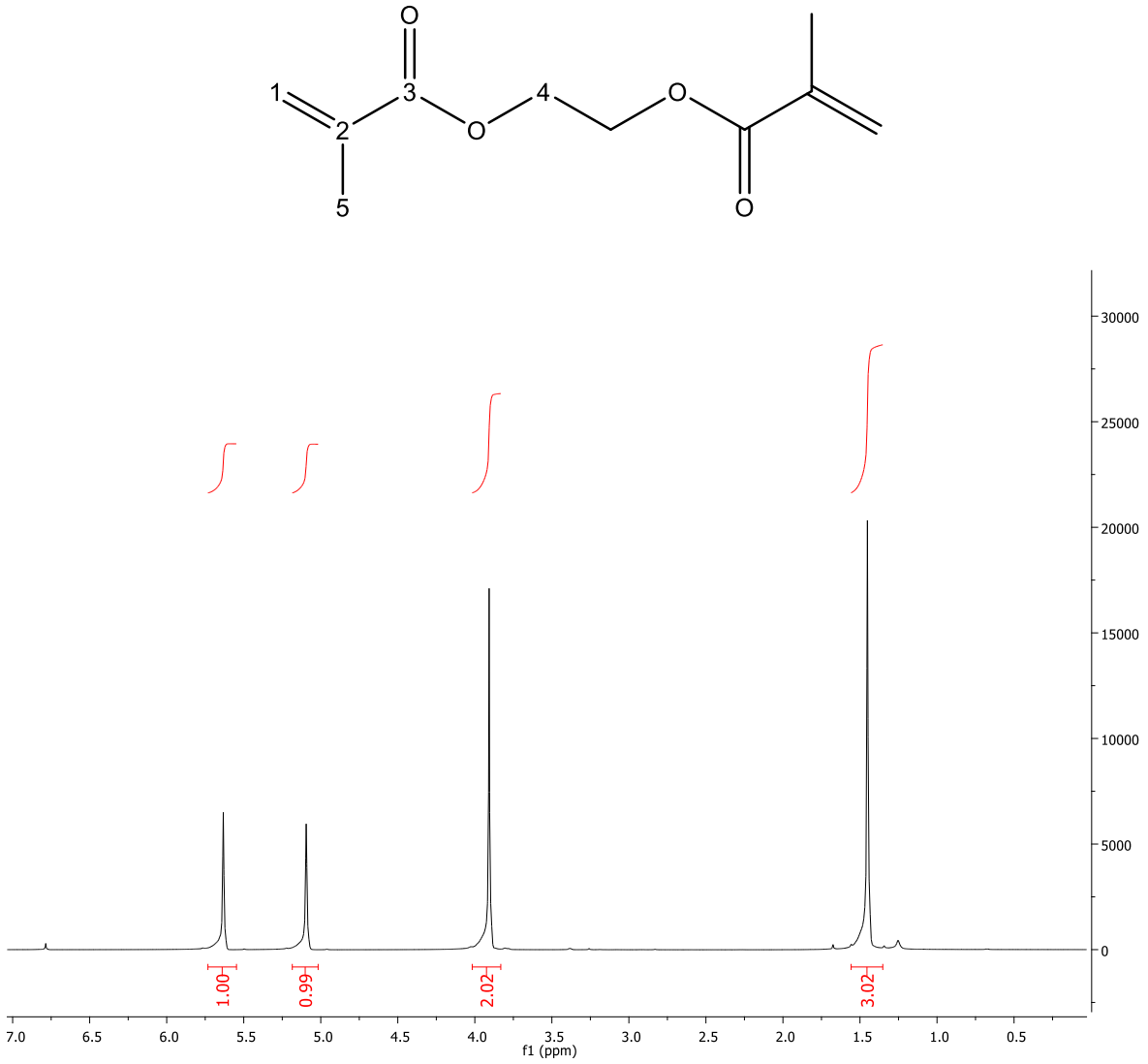

Figure 3.6 ^{1}H-NMR spectrum of **11** in $CDCl_3$.

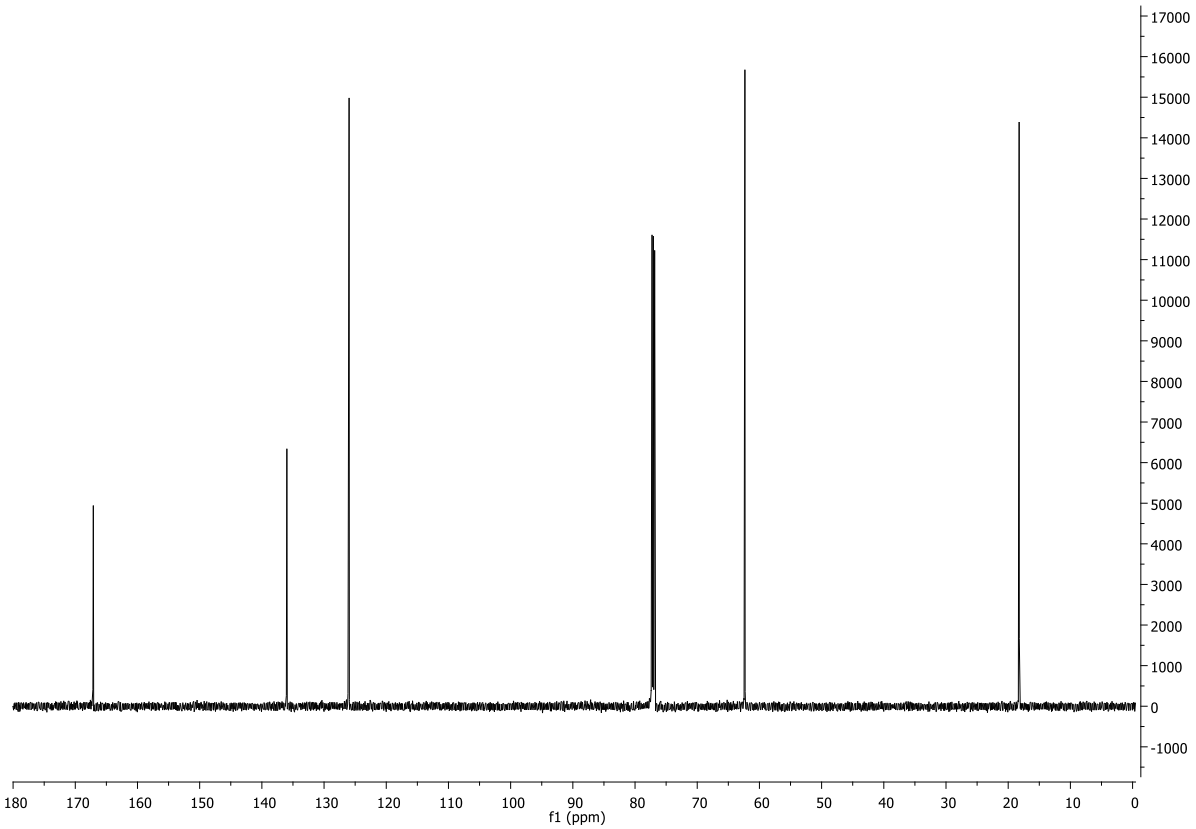

Figure 3.7 ^{13}C-NMR spectrum of **11** in $CDCl_3$

NMR analyses of compounds 1-10

The signals of **11** in Figure 3.6 and Figure 3.7 are divided into three regions for both ^{1}H-NMR and ^{13}C-NMR, and can be observed and applied in the subsequent NMR analyses of **1**-**10** and **12**-**14**. The NMR regions correspond to the positioning of the hydrogen or carbon under investigation and its location on the mono-ester, di-ester or tri-ester molecule, which can be used to identify signals and predict their location on their respective product molecules. These regions are allocated according to the illustration in Figure 3.8 below, with the numbered positions on the mono-ester and di-ester products. The regions are as follow for ^{1}H-NMR: region A (structure positions 1 & 2 / 6.5 – 5.5 ppm), region B (structure positions 4, 4' & alcohol-containing structure position / 4.5 – 2.5 ppm) and region C (structure positons 5 – 6 & 5' – 8' / 2.2 – 1.2 ppm). The regions for ^{13}C-NMR are as follow: region A' (structure position 3 / 175 – 165 ppm), region B' (structure positions 1 & 2 and alcohol-containing structure position / 135 – 125 ppm) and region C' (positons 5 – 6 & 5' – 8' / 70 – 10 ppm). The three

structures depicting di-ester compounds are grouped according to their symmetrical patterns. **1**, being the only product with no hydrogen or carbon position further in the molecule than position 4, thus it is identified individually and is depicted in the topmost structure. **3** & **5**, both have two CH_2-positions located adjacent to position 4, however, **3** having one and **5** having two, they remain equivalent and were expected to produce a single signal differing only in integration. **3** & **5** signals expected are represented by the di-ester structure containing positions 1-5 in Figure 3.8.

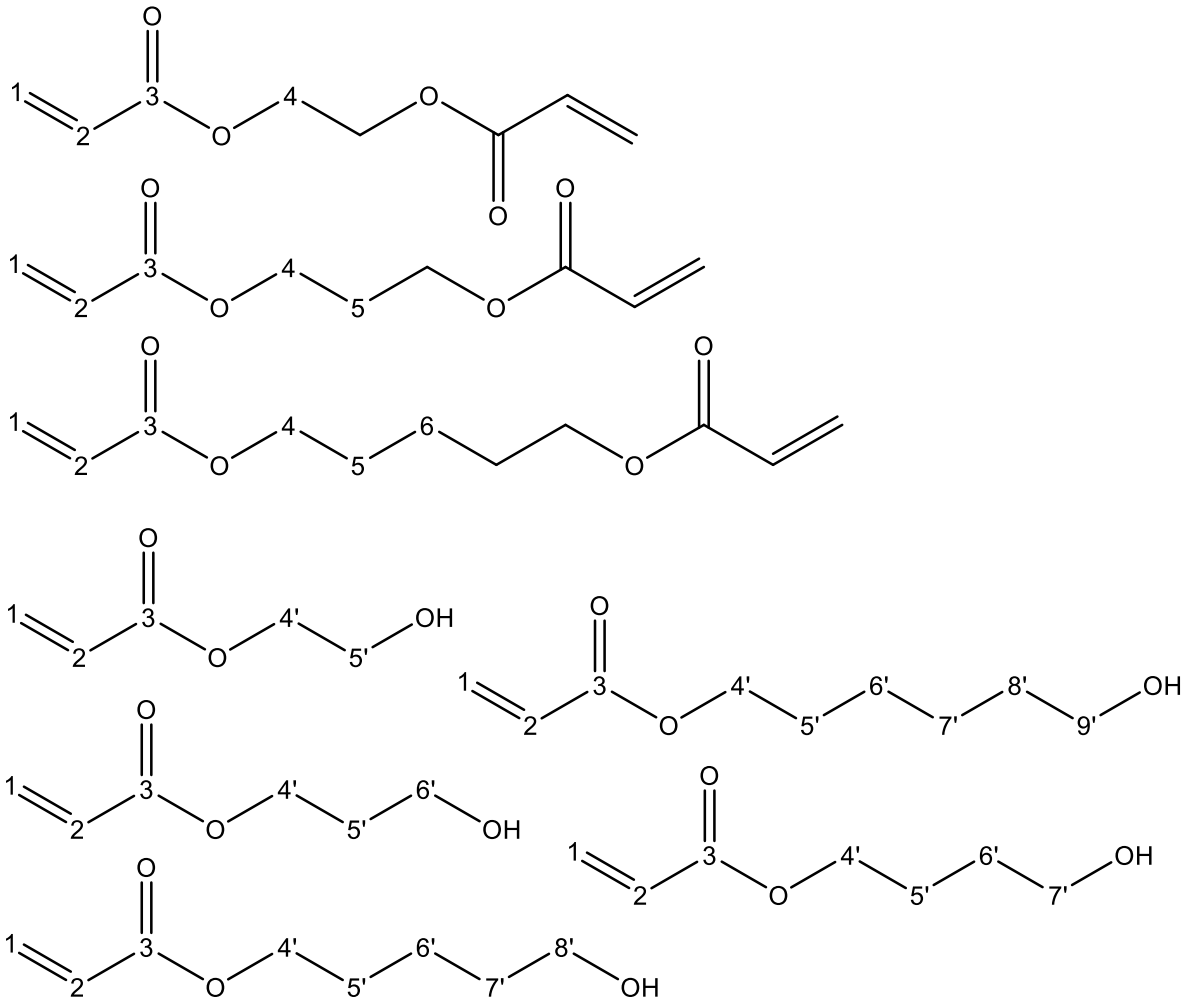

Figure 3.8 Numbering of carbon atoms of compounds **1**-**10** for NMR analyses.

Similarly, **7** & **9** are depicted by the di-ester structures in Figure 3.8 containing positions 1-6, due to their three CH_2 positions found adjacent to the ester group, symmetrical from both terminal positions. **7** & **9** were also expected to produce identical signals, only differing in integration. The carbons in the mono-ester products:

2, **4**, **6**, **8** & **10** are labelled similarly to that of the di-ester products, however, when ascribing numerical allocations to the CH_2 positions on the original diol chain, the positions are numbered from the ester-adjacent group outward to the alcohol baring group as seen in Figure 3.8.

^{1}H-NMR analyses of compounds 1-10

The ^{1}H-NMR spectra of compounds **1**-**10** are available in the supporting information in the appendices. The positions numbered from 1-6 and 4'-9' were allocated signals that appear in the ^{1}H-NMR spectra obtained for the products and are presented in Table 3.3 and Table 3.4.

^{1}H-NMR analysis of **1**-**14** all showed similar alkene proton signals at chemical shift values of 6.43, 6.14 and 5.86 ppm, representing position 1 vicinal cis proton relative to position 2, position 2 and position 1 vicinal trans proton relative to position 2 proton, respectively. The proton signals for both position 1 protons exhibited splitting patterns of doublets and secondary multiplet splitting patterns. For **1** & **2**, the vicinal cis structure position 1 at 6.40 ppm, produced overlaid spectra of a doublet of doublets and a doublet signal at 6.44 ppm. The splitting observed for 1 vicinal trans was similar in pattern, however, smaller splitting values shows the unique environment in contrast to the 1 vicinal trans position. Similar to that of 1 vicinal cis, 1 vicinal trans possess additional signals at 5.86 ppm that do not form part of the described signals expected.

The signals observed in region A for **1**-**10** are formed by the protons of positions 1 vicinal cis (6.38 – 6.31 ppm), 2 (6.10 – 6.00 ppm) and 1 vicinal trans (5.85 – 5.70 ppm), with doublet of doublets, doublet of multiplets and doublet of doublets splitting patterns ascribed to the positions, respectively. The signals are identified as predicted theoretically and as described in literature. The observed coupling and coupling constants for positions 1 vicinal cis (6.38 – 6.31 ppm), 2 (6.10 – 6.00 ppm) and 1 vicinal trans are 3J (0.003 ppm) and 2J (0.028 ppm), 2J (0.028 ppm) and 2J (0.018 ppm), and 3J (0.003 ppm) and 2J (0.018 ppm), which are seen consistently for all spectra. Overlaying signals were caused by the mono-ester and di-ester signals yielding near-identical split and shift signals for positions 1 vicinal cis, 2 and 1 vicinal trans. Some of the product spectra signals showed multiplicity to the degree that a fine splitting

structure could not be clearly assigned, possibly due to additional alkene baring products such as dimers. However, the chemical shift value and integration value of the combined signal, being identical, were used to identify the signals as the structure positions in question.

Table 3.3 ^{1}H-NMR signals of products **1**, **3**, **5**, **7**, **9** & **11**. The positions are described with their chemical shift values and splitting patterns. The splitting patterns are: s = singlet, dd = doublet of doublets, t = triplet and m = multiplet.

11	Position	1-cis	1-trans	2	4	5	6
	δ (ppm)	6.1	5.6	-	4.4	2.0	-
	Splitting	dd	dd	-	s	s	-
1	Position	1-cis	1-trans	2	4	5	6
	δ (ppm)	6.4	5.8	6.1	4.3	-	-
	Splitting	dd	dd	m	t	-	-
3	Position	1-cis	1-trans	2	4	5	6
	δ (ppm)	6.5	5.9	6.1	4.3	2.2	-
	Splitting	dd	dd	m	t	m	-
5	Position	1-cis	1-trans	2	4	5	6
	δ (ppm)	6.5	5.9	6.2	4.2	1.8	-
	Splitting	dd	dd	m	t	m	-
7	Position	1-cis	1-trans	2	4	5	6
	δ (ppm)	6.4	5.8	6.1	4.1	1.7	1.4
	Splitting	dd	dd	dd	t	m	m
9	Position	1-cis	1-trans	2	4	5	6
	δ (ppm)	6.4	5.8	6.1	4.1	1.7	1.4
	Splitting	dd	dd	dd	t	m	m

Table 3.4 ^{1}H-NMR signals of product structures **2**, **4**, **6**, **8** & **10**. The positions are described with their chemical shift values and splitting patterns. The splitting patterns are: s = singlet, dd = doublet of doublets, t = triplet, td = triplet of doublets, p = pentet and m = multiplet.

2	Position	1-cis	1-trans	2	4'	5'	6'	7'	8'	9'
	δ (ppm)	6.4	5.8	6.1	4.5	3.7	-	-	-	-
	Splitting	dd	dd	m	t	m	-	-	-	-
4	Position	1-cis	1-trans	2	4'	5'	6'	7'	8'	9'
	δ (ppm)	6.5	5.9	6.1	4.4	2.0	3.7	-	-	-
	Splitting	dd	dd	m	t	p	t	-	-	-
6	Position	1-cis	1-trans	2	4'	5'	6'	7'	8'	9'
	δ (ppm)	6.5	5.9	6.2	4.2	1.8	1.7	3.7	-	-
	Splitting	dd	dd	m	t	p	p	t	-	-
8	Position	1-cis	1-trans	2	4'	5'	6'	7'	8'	9'
	δ (ppm)	6.4	5.8	6.1	4.2	1.7	1.5	1.6	3.7	-
	Splitting	dd	dd	dd	t	m	m	m	t	-
10	Position	1-cis	1-trans	2	4'	5'	6'	7'	8'	9'
	δ (ppm)	6.4	5.8	6.1	4.2	1.7	1.4	1.4	1.6	3.7
	Splitting	dd	dd	dd	td	m	m	m	m	td

Signals observed in region B for **1**-**10** were formed by the protons located on positions 4, 4', 5' (**2**), 6' (**4**), 7' (**6**), 8' (**8**) and 9' (**10**), equating to the ester-adjacent position for all di-esters (4.45 – 4.22 ppm), the ester-adjacent position for all mono-esters (4.45 – 4.22 ppm) and the alcohol baring CH_2 position (5'-9') for all mono-esters (3.70 – 3.55 ppm). Positions 4 and 4' are closely located to one another and were expected to differ slightly, with position 4' expected to be the more downfield of the two signals. In addition to the expected signals for positions adjacent to the ester and alcohol baring CH_2 groups, signals were observed for nucleophilic addition dimers, observed in the MS spectra. These signals were consistently located at 4.45 – 4.40 ppm and 2.75 – 2.65 ppm and were equal in both integration and having triplet splitting patterns due to being vicinal located to a single CH_2 group. The chemical shift values ascribed to

the signals of positions 5'' and 4'' observed are as shown in Figure 3.9, with the two CH_2 positions: ester-adjacent (4.45 – 4.40 ppm) and the carbonyl adjacent (2.75 – 2.65 ppm) forming the triplet signals, described respectively. Positions 1 vicinal trans, position 2 and position 1 vicinal cis of the dimer form signals in near-identical positions to that of **1**-**11**.

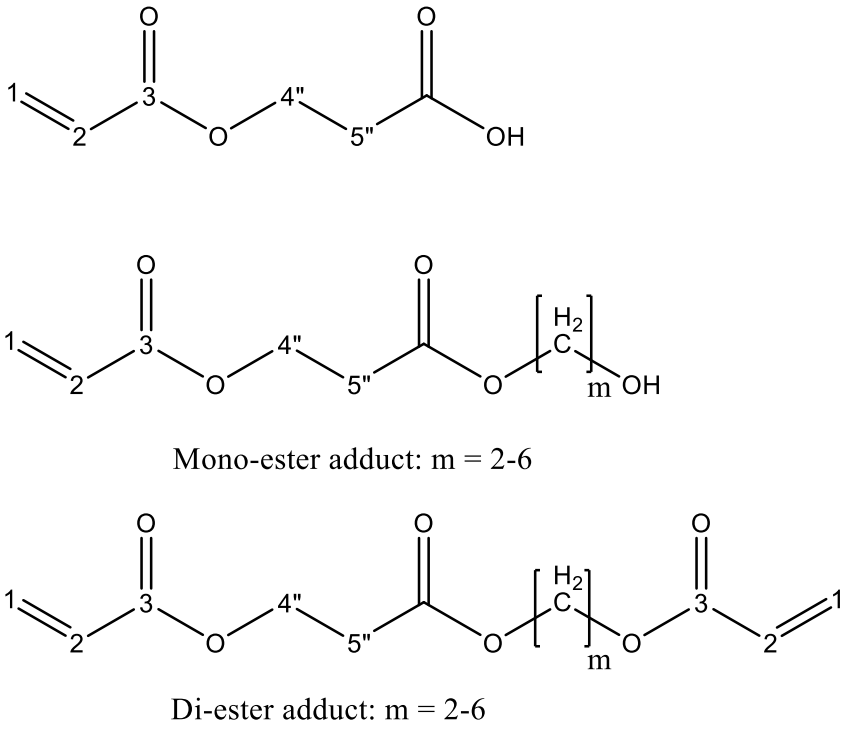

Figure 3.9 DAA dimeric form of AA, and mono-ester and di-ester adducts, with m = 2-6 for products **1**-**10**.

Region C contains the signals of the central CH_2 protons, former diol CH_2 positions, numbered 5, 6 and 5', 6', 7' & 8' that are alcohol-adjacent. The integration values for these positions are dependent on the chain length and the point of symmetry in the di-esters. Splitting patterns expected were multiplets such as pentets (3-J) due to location between two CH_2 groups, however, increased complexity was seen due to further coupling (4-J) and non-ideal symmetry. Symmetry changes could occur due to dimer formation and the formation of mono-esters. The signal shifted downfield with increasing proximity to the ester and alcohol groups, with the ester having the greatest deshielding effect.

Thus, position 5 was located the furthest downfield and the central protons on positions 6, 6' & 7' being the most shielded and upfield. The furthest upfield signals show increased overlapping of signals ascribed to positions similar in a chemical environment, with the integration values of the overlapping signals serving as support. However, the values were non-indicative of specific position identification due to overlapping signals causing integrational variation from the expected integration values. In some cases, the presence of a hydroxyl signal was seen in region C, which correlated with **2**, **4**, **6**, **8** & **10**. However, the signal was only observed in the spectra of the **7** & **8** and **9** & **10** mixes. Thus the impression of a predominant mono-ester formation is given, which was also seen in the MS data and yield percentage obtained.

^{13}C-NMR analyses of compounds 1-10

The ^{13}C-NMR analysis of **1**-**10** was carried out and were allocated according to the numbered positions of **1**-**10** in Table 3.5 and Table 3.6, as shown in Figure 3.8. The ^{13}C-NMR spectra of compounds **1**-**10** are available in the supporting information in the appendices.

The carbonyl signal at position 3 was the only signal observed in region A', however, differing numbers of and positions for the position 3 signal was observed. For **1** & **2** there were three carbonyl peaks observed and two for **3** & **4** and **5** & **6**, which was indicative of the mixture expected and also observed in the MS data. There are four potential carbonyl baring groups that could form the observed signals. These are the di-ester carbonyl, the mono-ester carbonyl, the nucleophilic addition dimer carbonyl and PAA carbonyl groups (COOH). From the MS data it is clear that most of the products were expected to contain mono-ester, di-ester and dimer compounds, however, the possibility of polymerization to some degree could not be ignored.

Theoretical signal chemical shift values expected for the di-ester and mono-ester carbonyl signals of **1**-**10** were 166.1 and 166.5 ppm, respectively. The theoretical carbonyl signals expected for PAA carboxylic acid carbonyls were 180.3 ppm, and for the dimer carbonyls were respectively 163.6 (ester) and 174.7 ppm (carboxylic acid). Thus, the ester carbonyl will almost indefinitely overlap with or appear exceptionally close to that of the di-ester carbonyl at position 3. However, the more downfield 174.7

ppm signal was easily distinguishable as seen in **1** & **2**. The CH_2 group protons of the dimer product were observed in all spectra of products **1**-**10**. However, the ester carbonyl signals were difficult to distinguish. In region A' there also appeared a signal at 170.74 ppm in the spectra of **1** & **2** and **5**-**10**, which was of unknown origin.

Table 3.5 ^{13}C-NMR analysis of products **1**, **3**, **5**, **7**, **9** & **11**. The numbered positions are described by the chemical shift values and degree of carbon substitution (C subs.).

11	Position	1	2	3	4	5	6
	δ (ppm)	126.1	136.1	167.2	62.3	18.2	-
	C subs.	CH_2	CH	C	CH_2	CH_3	-
1	Position	1	2	3	4	5	6
	δ (ppm)	131.1	128.2	166.5	62.3	-	-
	C subs.	CH_2	CH	C	CH_2	-	-
3	Position	1	2	3	4	5	6
	δ (ppm)	130.9	128.2	166.1	61.3	27.9	-
	C subs.	CH_2	CH	C	CH_2	CH_2	-
5	Position	1	2	3	4	5	6
	δ (ppm)	130.8	128.3	165.9	64.1	25.3	-
	C subs.	CH_2	CH	C	CH_2	CH_2	-
7	Position	1	2	3	4	5	6
	δ (ppm)	130.7	128.3	165.7	64.3	28.3	22.3
	C subs.	CH_2	CH	C	CH_2	CH_2	CH_2
9	Position	1	2	3	4	5	6
	δ (ppm)	130.7	128.3	165.7	64.5	28.5	25.4
	C subs.	CH_2	CH	C	CH_2	CH_2	CH_2

Region B' refers to the chemical shift values as seen in the chemical shift range of 135 – 125 ppm, which correspond to the shift values expected from the alkene carbons on positions 1 & 2. Thus, two signals were expected, due to the alkene groups on the mono-ester di-ester and dimer product being identical and theoretically appear at

131.1 ppm for position 1 and 128.0 ppm for position 2, which is seen. There were, however, small signals observed 0.28 ppm downfield from the position 1 signal and 0.26 ppm upfield from the position 2 signal, which was most likely due to slight differences between the mono-ester, di-ester or dimer alkene carbon signals. The internal carbons from the original linear diol reagents were expected to appear in region C'.

Table 3.6 ^{13}C-NMR analysis of products **2**, **4**, **6**, **8** & **10**. The numbered positions are described by the chemical shift values and carbon substitution (C subs.).

2	Position	1	2	3	4'	5'	6'	7'	8'	9'
	δ (ppm)	131.1	128.2	166.5	59.8	33.6	-	-	-	-
	C subs.	CH_2	CH	C	CH_2	CH_2	-	-	-	-
4	Position	1	2	3	4'	5'	6'	7'	8'	9'
	δ (ppm)	130.9	128.2	166.1	61.5	31.7	59.2	-	-	-
	C subs.	CH_2	CH	C	CH_2	CH_2	CH_2	-	-	-
6	Position	1	2	3	4'	5'	6'	7'	8'	9'
	δ (ppm)	130.8	128.3	165.9	64.4	25.1	29.0	62.3	-	-
	C subs.	CH_2	CH	C	CH_2	CH_2	CH_2	CH_2	-	-
8	Position	1	2	3	4'	5'	6'	7'	8'	9'
	δ (ppm)	130.7	128.3	165.7	64.5	28.5	22.5	32.3	62.6	-
	C subs.	CH_2	CH	C	CH_2	CH_2	CH_2	CH_2	CH_2	-
10	Position	1	2	3	4'	5'	6'	7'	8'	9'
	δ (ppm)	130.7	128.3	165.7	64.5	28.6	25.6	25.8	32.6	62.8
	C subs.	CH_2	CH	C	CH_2	CH_2	CH_2	CH_2	CH_2	CH_2

The chemical shift values were expected to increase in shift values, upfield with increasing proximity to the ester and alcohol groups, and oppositely the chemical shift values decrease toward the centre of the linear hydrocarbon chain. The expected values for positions 4, 5 and 6 were approximately 65.0 – 63.5 ppm, 30.0 – 28.0 ppm and 26.0 – 25.0 ppm, respectively with slight differences depending on whether one or two CH_2 groups make up positions 5 and 6. For the mono-ester compounds with

positions 4'-9', the values decreased in the order of first the ester-adjacent CH_2 (4' at 64.4 – 62.0 ppm) followed by the alcohol-containing CH_2 (62.5 – 60.0 ppm) then the β-CH_2 adjacent to the ester and alcohol positions (33.0 – 28.0 ppm), with the β-position adjacent to the alcohol being more downfield than ester β-position and finally the most upfield values were ascribed to the centre most carbon positions located on positions 6' and 6' & 7' for **8** and **10**, respectively, which range between 26.0 – 22.0 ppm.

NMR analyses of glycerol and 1,2,3-Propanetriol triacetate

Glycerol is the only reagent of **12**-**14**, the analysis of which is shown in Figure 3.10 and Figure 3.11.

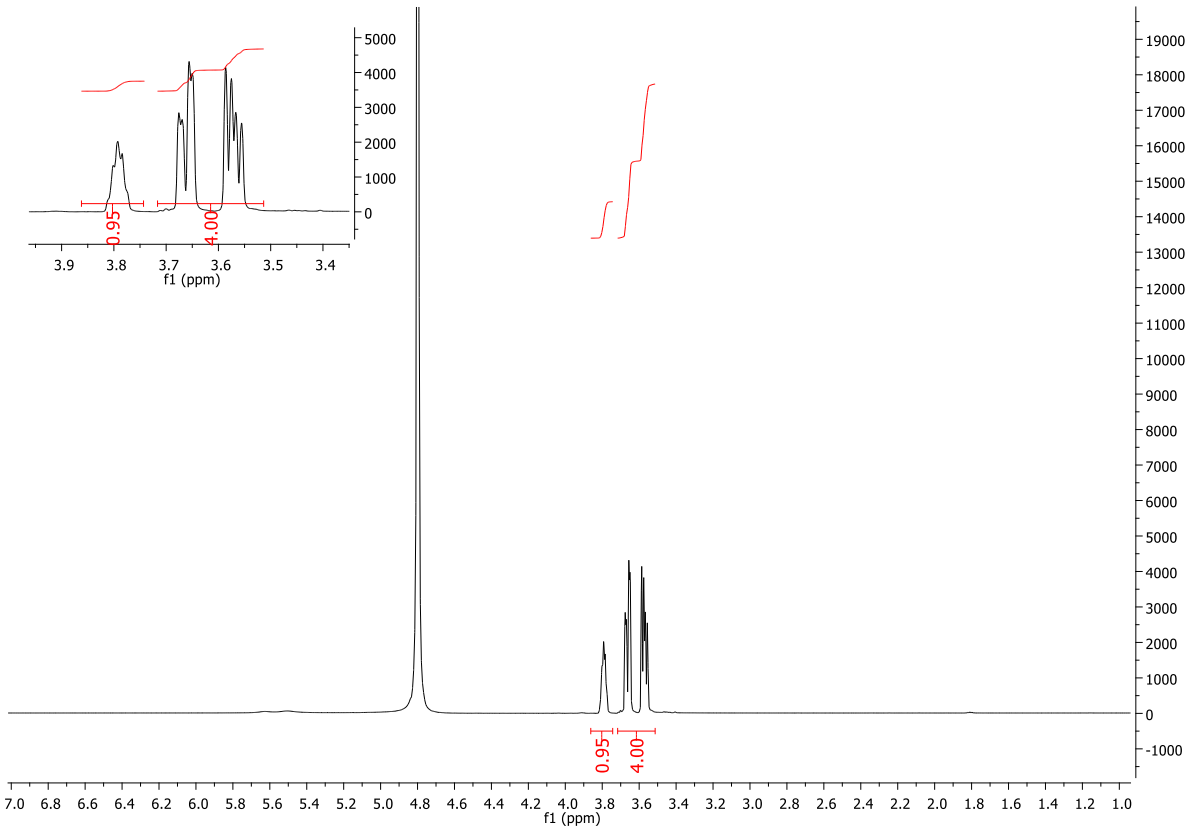

Figure 3.10 ^{1}H-NMR spectrum of glycerol with D_2O as solvent (4.65 ppm).

From the ^{1}H-NMR analysis of glycerol in Figure 3.10, it is clear that symmetric characteristics were observed for the CH_2 protons located terminally at 3.61 ppm, while the central CH proton was singled out and appeared the most downfield at 3.78 ppm. A key characteristic observed from the spectra of glycerol is that the CH_2 signal of the total of four protons formed a large doublet of doublets splitting pattern that stretches across an area of nearly 0.2 ppm. This signature splitting pattern was due to the configurational state of the molecule, with perfect symmetry achieved infrequently, causing the observed splitting. Thus, 2-J coupling of geminal located protons on the same carbon could contribute to the observed splitting pattern.

The signals in the ^{13}C-NMR of glycerol indicated in Figure 3.11, was similar to that observed with ^{1}H-NMR, with the signal of the central CH structure position appearing downfield at 27.1 ppm to that of the terminal CH_2 structure positions at 61.2 ppm, which due to symmetry appeared as a single signal.

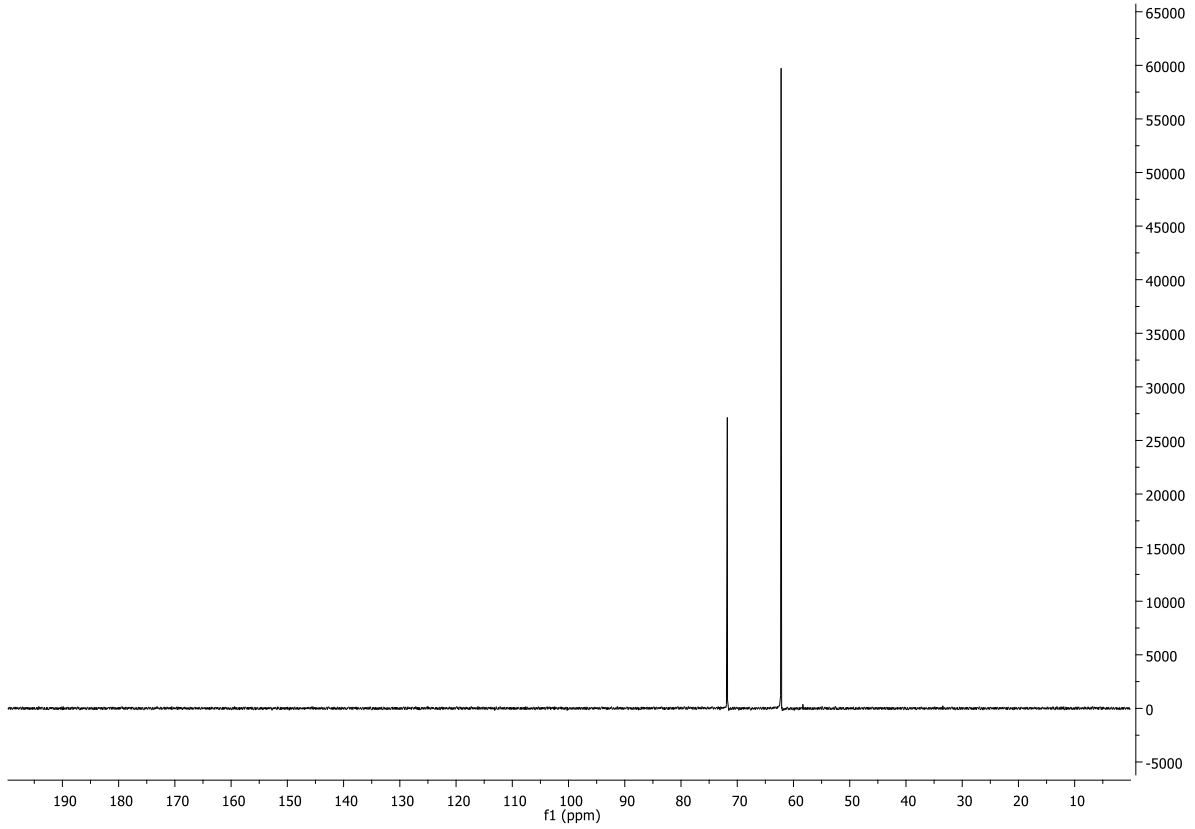

Figure 3.11 ^{13}C-NMR spectrum of glycerol in D_2O.

Figure 3.11The signals appearing in glycerol correlates with the central hydrocarbon positions located in products **12**-**14** and served as a reference for identifying the same position in product mixtures.

The ^{1}H-NMR signals observed in Figure 3.12, for 1,2,3-Propanetriol triacetate served as reference and were the closest to the signals observed for the tri-ester product **12** of glycerol and AA, with the chemical shift and splitting patterns correlating with glycerol and signals in similar regions in the product spectra of **12**-**14**. The unique tri-ester signal at 5.16 ppm in the spectra of 1,2,3-Propanetriol triacetate replicated that of position 5 of **12**, which was used to potentially quantify the product formation. A similar signal was observed for the terminal CH_2 positions, similar to glycerol and position 4 of **12**-**14**. The wide splitting pattern with a large doublet and finer splitting, doublets of doublets for glycerol and 1,2,3-Propanetriol triacetate, was observed at 4.20 ppm.

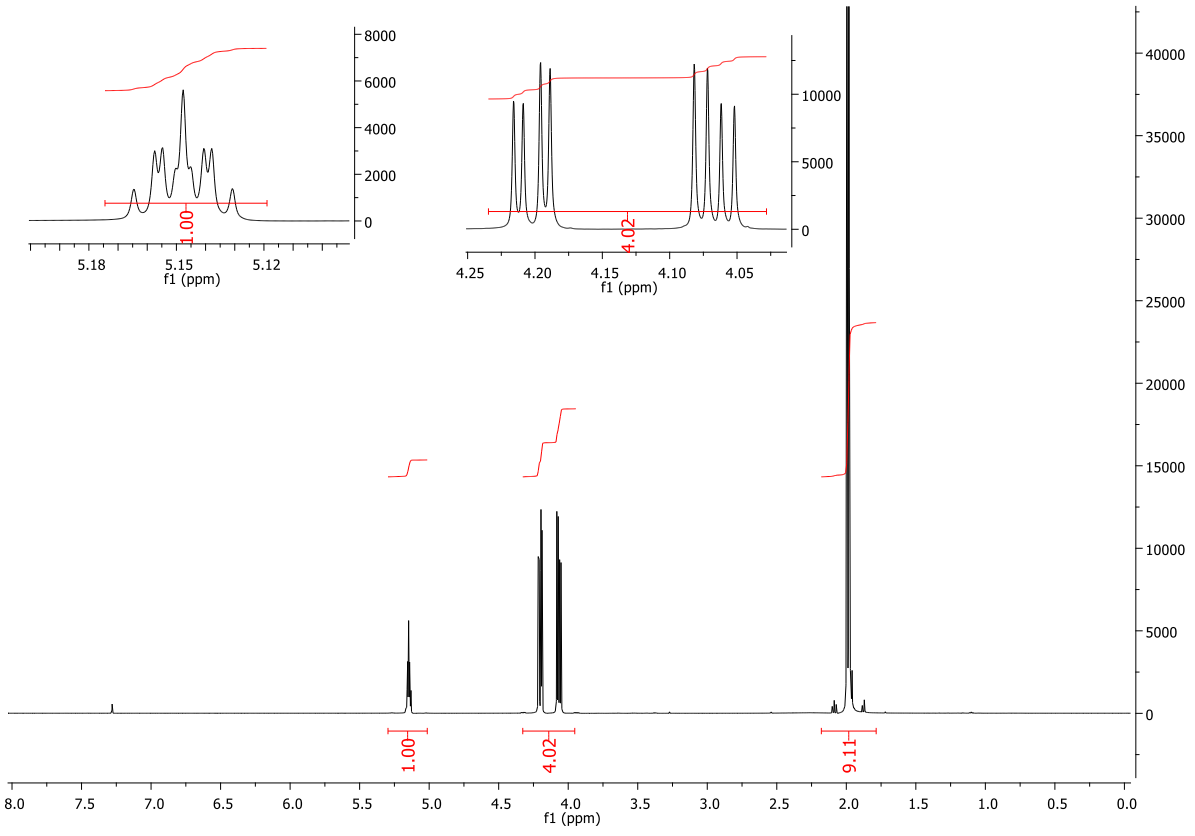

Figure 3.12 ^{1}H-NMR spectrum of 1,2,3-Propanetriol triacetate in $CDCl_3$.

Figure 3.12This chemical shift value moved downfield when hydroxyl groups (3.75 ppm) were substituted for ester groups (4.20 ppm), however, the splitting pattern remained similar and indicative of the CH_2 positions. The singlet observed at 2.00 ppm for 1,2,3-Propanetriol triacetate resulted from the CH_3 hydrogens of the acetate groups attached to the central and terminal positions. The signal observed is comprised of two singlets that nearly overlap, which was due to the near-identical chemical environments for the central and terminal acetate groups attached to the glycerol structure. This small difference in the shift, depending on the terminal or central positioning, can be used to describe overlapping of signals ascribed to groups located outside the central glycerol structure. Such groups include alkene CH and CH_2 signals for positions 1 and 2, and positions 4" and 5" of dimer groups.

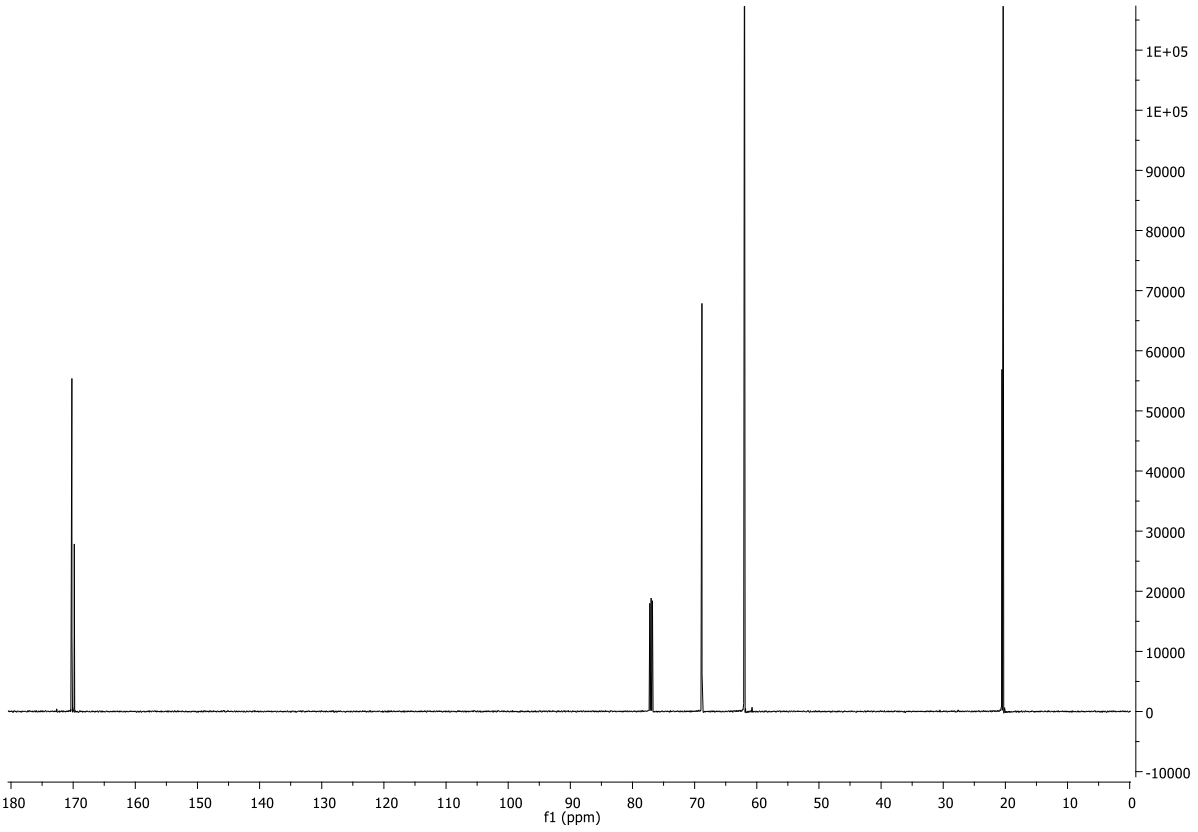

Figure 3.13 ^{13}C-NMR spectrum of 1,2,3-Propanetriol triacetate in $CDCl_3$.

The signals in the ^{13}C-NMR spectra, as shown in Figure 3.13, of 1,2,3-Propanetriol triacetate are similar to that expected of the **12**-**14** and serves as reference, with a carbonyl signal at 169.9 ppm, the central CH and CH_2 positions' signals at 69.3 and 62.4 ppm respectively, and the CH_3 acetate signal at 21.0 ppm.

^{1}H-NMR analyses of compounds 12-14

The analysis of **12**, **13** & **14**, products of glycerol, were expected to primarily form three products, the mono-ester, di-ester and tri-ester. These three ester products were shown by MS and IR analysis of the ester mixture obtained, however, with dimer formation occurring throughout. Thus, expected signals in the ^{1}H-NMR spectra were according to the product structures below, with numbered positions indicating carbons and protons being analysed.

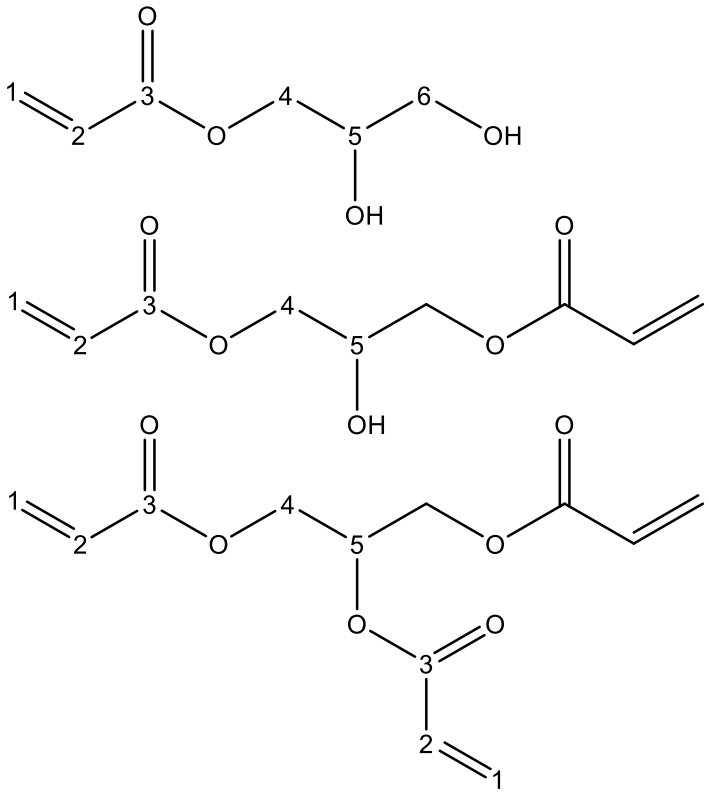

Figure 3.14 Numbered structures of **14**, **13** & **12** for ^{1}H-NMR and ^{13}C-NMR analysis characterisation.

The numbered positions from 1-4 were expected to produce signals with similar chemical shift values and splitting patterns for all ester products. The signals of positions 1-4 will follow similar trends to that observed in Figure 3.12 and Figure 3.13, however, these signals may potentially overlap. The primary differences between the product structures that were expected to be used for identification and quantification, are the positions 5 and 6 on **12** & **14**, respectively. Structure **13** was also expected to show a unique signal for position 5, however, the signal was expected to have a near-exact chemical environment and resulting shift value to that of position 5 of **14**. These unique positions with theoretically unique chemical shift values could be used for this purpose. The complete NMR spectra of **12**-**14** are used to complete Table 3.7. Figure 3.15Figure 3.16Figure 3.17Figure 3.18Figure 3.19Figure 3.20Figure 3.14

Table 3.7 ^{1}H-NMR signal chemical shift values and splitting patterns allocated to the numbered structures of **12**-**14**. The splitting patterns are described by combination of splitting notations: s = singlet, d = doublet, t = triplet and m = multiplet.

14	Position	1-cis	1-trans	2	4	5	6
	δ (ppm)	6.43	5.87	6.14	4.25	4.13	3.78
	Splitting	dd	m	dd	m	m	m
13	Position	1-cis	1-trans	2	4	5	6
	δ (ppm)	6.43	5.87	6.14	4.25	4.13	-
	Splitting	dd	m	dd	m	m	-
12	Position	1-cis	1-trans	2	4	5	6
	δ (ppm)	6.43	5.87	6.14	4.25	5.16	-
	Splitting	dd	m	dd	m	p	-

The complete spectra of the **12**-**14** product mixture include; the ^{1}H-NMR spectrum in Figure 3.15, the ^{1}H-NMR COSY spectrum in Figure 3.16, the ^{13}C-NMR spectrum in Figure 3.17, the HSQC spectrum in Figure 3.18, the HMBC spectrum in Figure 3.19 and the DEPT 135 spectrum in Figure 3.20, showed signals that identified positions present in the structures of the glycerol products, as shown in Figure 3.14, The spectra in Figures 3.21-3.26 are explained shown and used for elucidation as needed in subsequent paragraphs.

The ^{1}H-NMR spectra obtained for the ester product mixture of glycerol, as shown in Figure 3.15 yielded a proton spectra similar to that of products **1**-**11**, with the hydrogen positions of 1 vicinal cis, 2 and 1 vicinal trans being located in region A. These signals displayed similar splitting patterns associated with doublets with finer splitting also visible, for positions 1 vicinal cis and 1 vicinal trans, and overlaid triplet signals in the form of a multiplet for position 2.

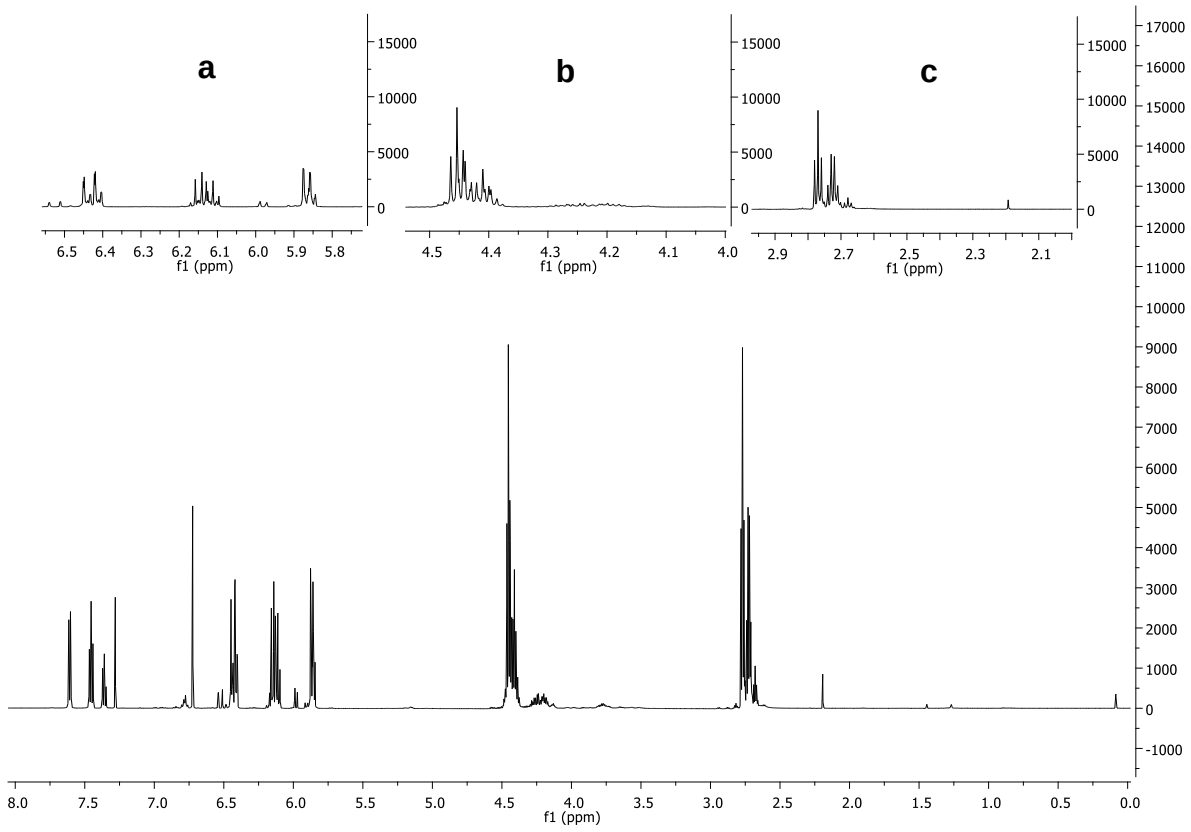

Figure 3.15: (**a)** (Top Left) ^{1}H-NMR spectrum of **12**-**14** in $CDCl_3$, in region A range 6.50 - 5.50 ppm; (**b**) (Top Centre) ^{1}H-NMR spectrum of **12**-**14** in $CDCl_3$, in the range 4.50 – 4.00 ppm; (**c**) (Top Right) ^{1}H-NMR spectrum of **12**-**14** in $CDCl_3$, in range 2.90 – 2.10 ppm.

Figure 3.15 **b** & **c** show a nearly identically chemical shift value for position 4 with the wide splitting pattern also observed in glycerol and 1,2,3-Propanetriol triacetate, however, there is a large overlay of signals present. The overlay of signals is due to similar CH_2 protons adjacent to an ester group in each of the ester structures, however, with the possibility of slight chemical environmental differences causing the multiplet

observed. Positions 5 and 6 of **12** and **14** are theoretically expected to appear at chemical shift values of 5.06 (5.16 ppm according to 1,2,3-Propanetriol triacetate) and 3.50ppm, respectively. The aforementioned unique signals of positions 5 for **13** was seen at 4.22 ppm and position 6 for **14** was seen at 3.78 ppm, with position 5 of **12** downfield at 5.16 ppm. The large signal overlays described in the ranges of 4.50 - 4.45 ppm and 2.80 – 2.65 ppm were attributed to positions 5 and 4 located on dimer groups, as shown in Figure 3.14.

The positions described in the regions of 4.50 - 4.45 ppm and 2.80 – 2.65 ppm were henceforth described by 4.47 and 2.75 ppm, respectively for simplified explanation. The multiple possibilities for dimer, trimer or other oligomer formation was depicted clearly in the APCI-MS analysis of **12**-**14**, however due to near identical theoretical chemical shift values caused overlaying signals. The integration values of the aforementioned ranges do, however, equal one another; thus, being consistent with the 1:1 ratio of protons on positions 4'' and 5'' as seen in the dimer product. Due to the ester group adjacent positions of CH_2 and CH positions in **12**-**14**, none were shielded in central long linear CH_2 chains like that of **3**-**10**; thus no signals were expected upfield in Figure 3.15 region C. There were, however some signals present in region C that might have been a result of impurities or by-products, as seen in Figure 3.15 **c**.

For the identification of the product specific signals, 2-D COSY analysis was employed to determine which signals in the overlaid signal regions fit which product. The analysis, as shown below in Figure 3.16, elucidated that the large integral signals at 4.47 ppm were indeed associated with the signal range at 2.75 ppm. The only theoretical positions expected at chemical shift values in the range of 2.75 ppm were that of dimer by-products, which was proven to have formed, as shown in the MS analysis of the same ester mixture. The signal positions expected for the predominant identification of **12**-**14** were very small in comparison to the signals at 4.47 ppm, expected position 4'' of the dimer, and 2.75 ppm, expected position 5'' of the dimer.

The signals at 5.16, 4.25 and 3.78 ppm could, however, be associated with other signals present in the ^{1}H-NMR spectra. The tri-ester identified signal at 5.16 ppm was associated with signals located at 4.25 and 3.78 ppm. The signal at 4.25 ppm could be ascribed to position 4. The signal at 4.25 ppm also associated with signals at 5.16, 4.25, 4.22, 3.78 and 2.75 ppm. The wide range of associations that 4.25 ppm made

showed its identification as position 4 was accurate. Position 4 is closely positioned to positions 5, 6 and also to dimer positions 4'' and 5''. Thus, the wide range of associations could be ascribed to the mixture of ester products and the formation of dimers.

^{13}C-NMR of 12, 13 & 14

The ^{13}C-NMR analysis of **12**-**14** was theoretically expected to form in regions A' (175 - 165 ppm), B' (135 - 125 ppm) and C' (70 - 10 ppm) as for linear diol esters, with carbonyl signals expected in region A', alkene signals in region B' and central positions 4, 5 and 6 appearing in region C'. The multiple carbonyl signals in region A' were expected due to **12-14** differing in their carbonyl chemical environment, most of all the third central carbonyl depicted in **12,** which should differ to a small degree from the terminal carbonyl peaks. This deviation between central groups and terminal groups were seen in the spectrum of 1,2,3-Propanetriol triacetate, which caused deviation for ester groups and dimer groups attached. Similarly, as seen in the ^{1}H-NMR in Figure 3.15 spectra the amount of dimer associated signals made it clear that dimeric forms of the products were present, which was supported by the MS data; thus, carbonyls associated with the dimeric forms of **12-14** were expected, adding to the number of carbonyl signals expected.

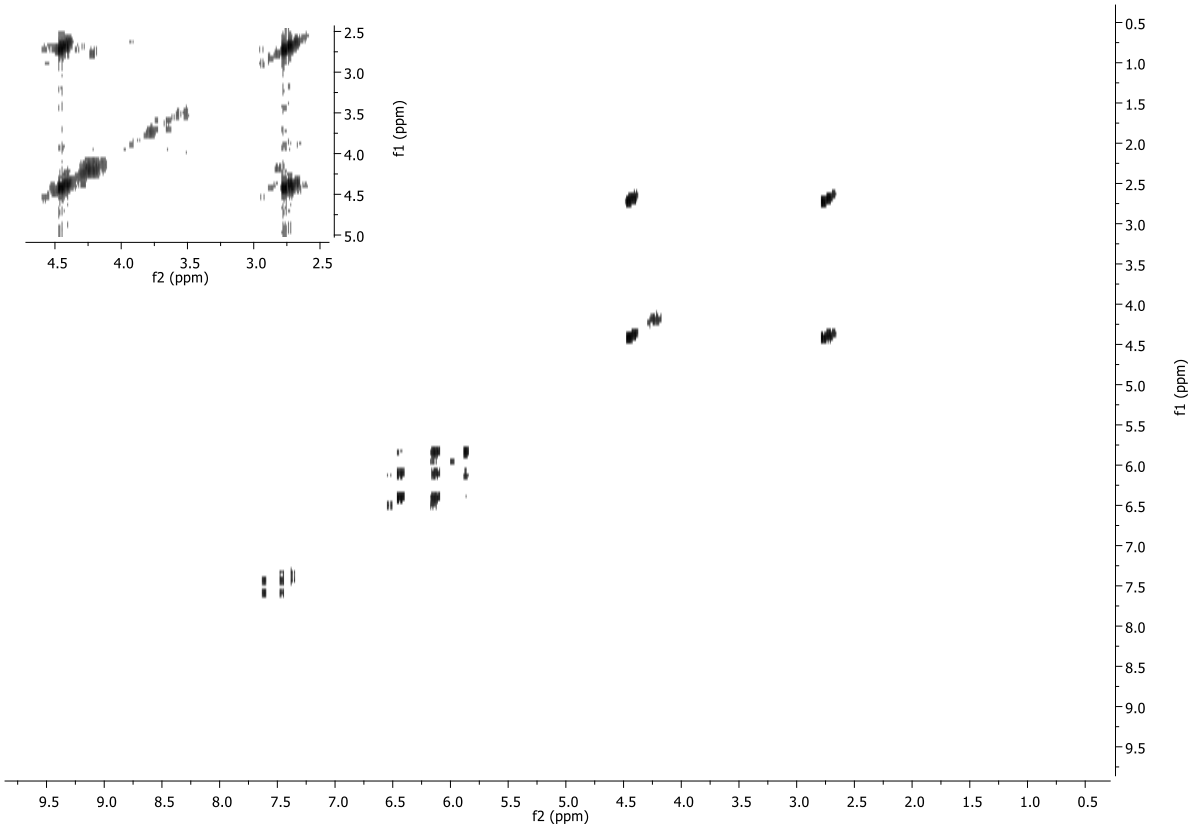

Figure 3.16 ^{1}H-NMR COSY spectrum of **12**-**14** in $CDCl_3$ with the full spectrum below and an enlarged spectrum above.

The multiple carbonyl signals in region A' were expected due to carbonyls present in **12**-**14** differing in expected chemical shift values, most of all position 3 (central) in **12**, which should differ to a small degree from the terminal carbonyl peaks. This deviation between central groups and terminal groups were seen in the spectrum of 1,2,3-Propanetriol triacetate, which caused deviation for ester groups and dimer groups attached. Similarly, as seen in the ^{1}H-NMR spectra the amount of dimer associated signals made it clear that dimeric forms of the products were present, which was supported by the MS data; thus, carbonyls associated with the dimeric forms of **12**-**14** were expected, adding to the number of carbonyl signals expected. The signals observed in the ^{13}C-NMR spectra were ascribed to the numbered structures of **12**-**14** and tabulated in Table 3.8.

Table 3.8 ^{13}C-NMR signal allocation to the numbered positions on **12**-**14**, in addition to chemical shift and carbon substitution (C subs.).

14	Position	1	2	3	4	5	6
	δ (ppm)	131.1	128.0	166.0	65.3	68.4	66.9/61.0
	C subs.	CH_2	CH	C	CH_2	CH	CH_2
13	Position	1	2	3	4	5	6
	δ (ppm)	131.1	128.0	166.0	65.3	68.4	-
	C subs.	CH_2	CH	C	CH_2	CH	-
12	Position	1	2	3	4	5	6
	δ (ppm)	131.1	128.0	166.0	65.3	72.5	-
	C subs.	CH_2	CH	C	CH_2	CH	-

The most downfield signal expected for any carbonyl group was that of the carboxylic acid group of the dimer, if unattached to an alkene group, expected at 174.7 ppm, which was similar to signals observed at 176.2, 176.0 and 175.7 ppm. The remaining signals observed in region A' could be ascribed to the remaining dimer carbonyl signal (ester) and the ester carbonyl signals of the products **12**-**14**. These carbonyl signals were expected to theoretically form at 163.6 and 166.1 ppm, respectively. In Figure 3.17 the ^{13}C-NMR spectrum of **12**-**14** is shown and used to determine the chemical shift value of signals of the glycerol ester product mixture. The theoretical product ester carbonyl signal was matched exactly at 166.0 ppm in the region A', as shown in Figure 3.17 **a**. However, the other signal was observed at 170.5 ppm and could thus potentially be that of the dimer ester carbonyl.

The signals associated with positions 1 and 2 were theoretically expected to appear at chemical shift values of 131.1 and 128.0 ppm, which are represented by the signals observed at 131.4 and 128.0 ppm. The central alkene group attached to the structure of **12** was expected to yield a signal for position 2 that differs slightly from similar terminal positions. This signal was expected to appear at 129.2 ppm, and a similar signal was observed at 128.75 ppm that could potentially be ascribed to this structure position. The signals appearing at 127.17, 127.27 and 128.76 ppm were formed by the internal standard used in the ester mixture (biphenyl) for quantification of **12**-**14**, and were therefore not a result of the ester compounds formed. The signal observed

at 116.16 ppm was not expected theoretically and was most likely due to an impurity in the ester mixture.

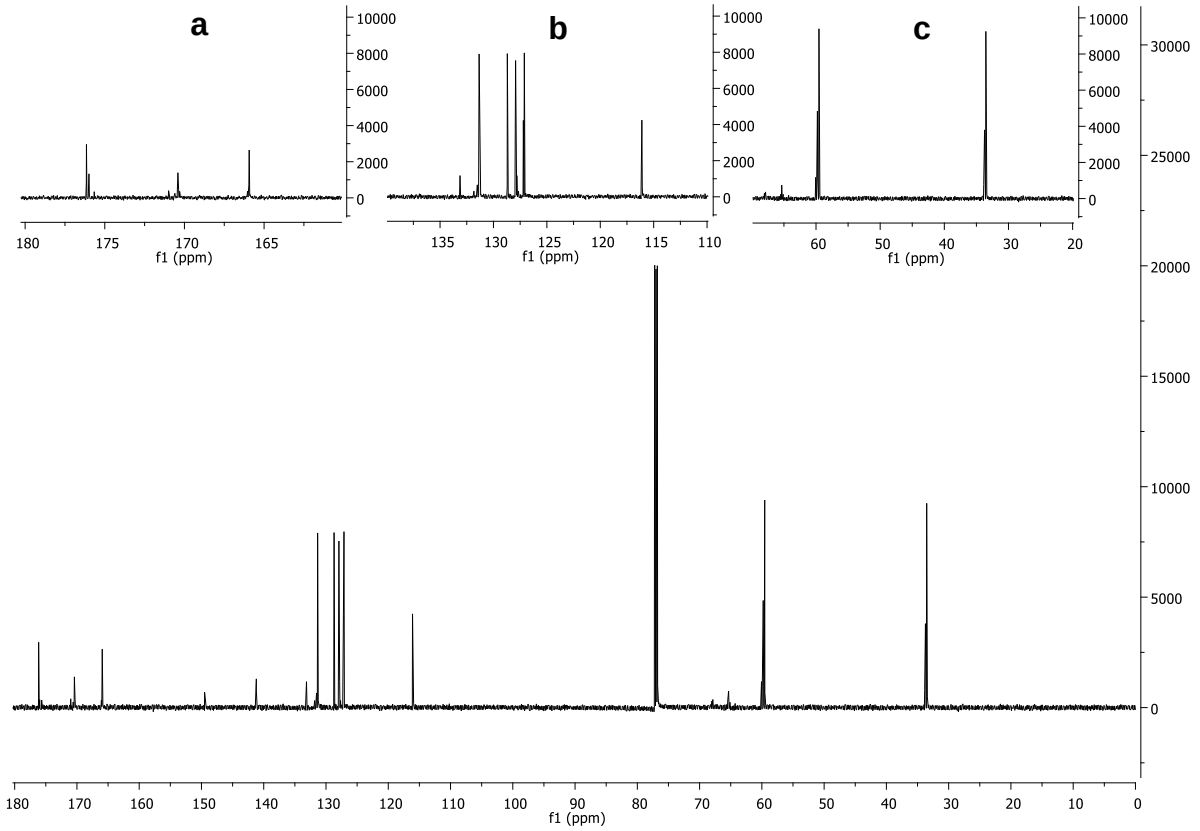

Figure 3.17 ^{13}C-NMR spectrum of **12**-**14** in $CDCl_3$, with (**a**) in region A' 180.0 - 160.0 ppm, (**b**) in region B' 140.0 - 110.0 ppm and (**c**) in region C' 70.0 - 20.0 ppm

The signals ascribed to the interior positions 4, 5 and 6 are located in region C', with signals expected at values from 72.0 – 60.0 ppm for compounds **12**-**14**. The unique signals expected were that of the central CH of **12,** which was expected to have the most downfield signal appearing at 72.0 ppm. Other signals observed were at 67.96, 65.41, multiple signals at 59.87 and multiple signals at 33.71 ppm. These signals were likely to be that of the central positions 4-6, and can be observed in Figure 3.17 **c**.

Analysis via HSQC and HMBC, as shown in Figure 3.18 and Figure 3.19, were used to identify and verify the proton to carbon coupling certainty the carbon signal and correlate it with a known ^{1}H-NMR signal to conclusively assign the ^{13}C-NMR and ^{1}H-NMR data to positions on the product structures.

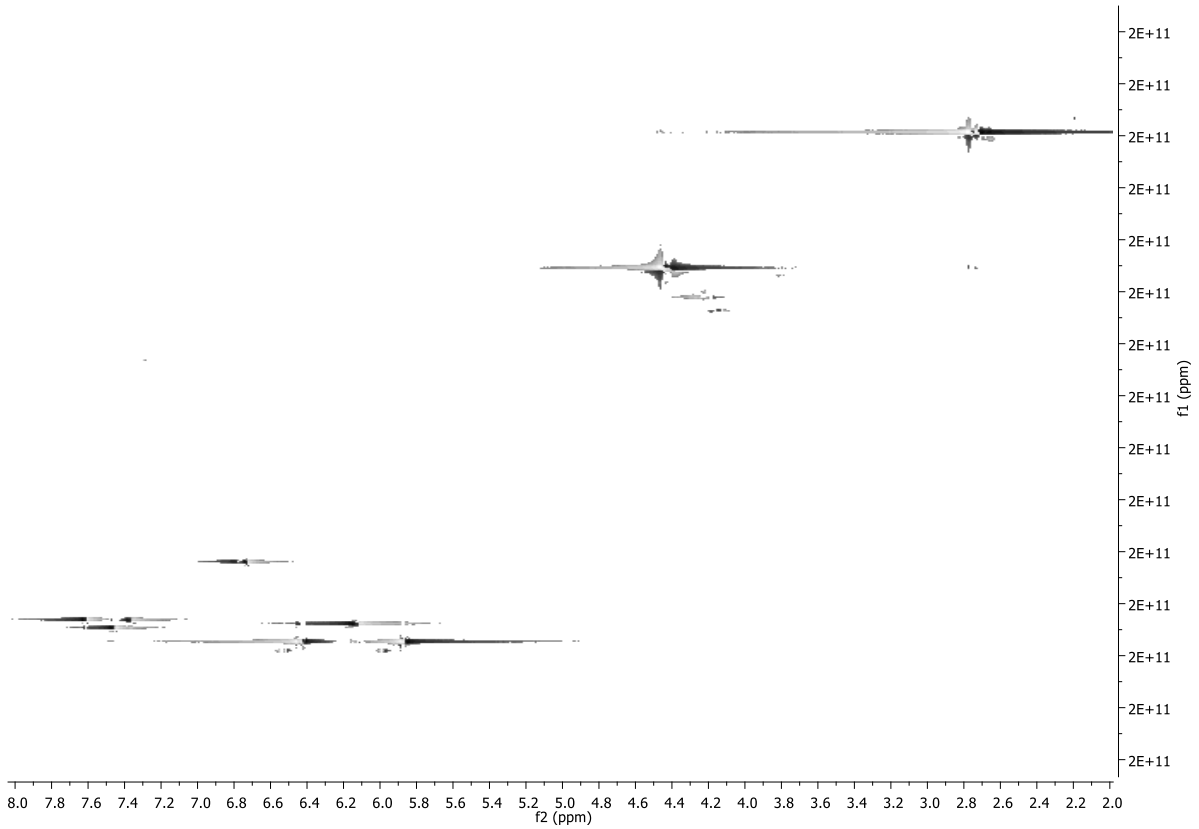

Figure 3.18 HSQC spectrum of **12**-**14** in $CDCl_3$.

The lack of corresponding signals from the ^{1}H-NMR spectra to the ^{13}C-NMR signals in region A' confirmed their suspected carbonyl identity. According to the HSQC data the signals at 5.87, 6.14 and 6.43 ppm, in the ^{1}H-NMR spectra correlated to the signals at 131.0 and 128.0 ppm, in the ^{13}C-NMR. These signals were expected to correspond due to the fact that they were the carbon and hydrogen signals of positions 1 and 2. There is another set of ^{1}H-NMR signals that correspond to a single ^{13}C-NMR signal, being that of 6.53 and 5.99 ppm, in the ^{1}H-NMR spectra, that corresponds to the signal at 133.13 ppm in the ^{13}C-NMR spectra. The signal at 133.13 ppm was previously not thought part of the 131.0 and 128.0 ppm signal distribution expected, and its corresponding ^{1}H-NMR signals were also not expected. Thus it can be concluded that it was a result of a by-product or from dimer formation.

HSQC data in region C' showed that the signals at 5.16, 4.47, 4.25 ppm, 4.13, 3.78, 3.54 and 2.78 ppm in the ^{1}H-NMR spectra could be ascribed to signals in the ^{13}C-NMR spectra. The position 6 on **12** signal at 5.16 ppm is attributed to a carbon signal in the ^{13}C-NMR spectra at 72.5 ppm that cannot be seen on the ^{13}C-NMR spectra, however,

is visible on the HSQC spectra and correlated with the theoretical expected ^{13}C-NMR signal of 72.0 ppm. The signals of 67.96, 66.6, 65.41, 61.1, the multiple signals at 59.87 and the multiple signals at 33.71 ppm, in the ^{13}C-NMR spectra correlated with the ^{1}H-NMR signals of 4.15, 3.78, 4.23, 3.78, 4.47 and 2.75 ppm, respectively and are tabulate in Table 3.7 and Table 3.8. From this, it could be concluded that the signal obtained at 2.75 and 33.5 ppm, in ^{1}H-NMR and ^{13}C-NMR respectively, were as a result of dimer formation.

Similarly, the large signal overlay observed at 4.47 ppm in the ^{1}H-NMR spectra could be correlated to the ^{13}C-NMR multiple signals at position 54.9 ppm, which was also deduced to be position 4'' on the dimer formation product. Supporting the assignment of the aforementioned signals in the ^{1}H-NMR and ^{13}C-NMR spectra to that of dimer products is that, according to the COSY data, the ^{1}H-NMR signals at 4.47 and 2.75 ppm were predominantly influenced by one another. Nearly identical integration values, across all signals in these specific ranges, served as further proof of dimer formation, due to dimer positions 4'' and 5'' being expected to have identical integration values. The signal at 5.16 ppm in the ^{1}H-NMR spectra was conclusively shown to be that of the tri-ester **12**; thus, can be used for quantification in further NMR analysis.

The HSQC analysis showed that the signals, considered to be overlay of multiple signals, at 4.25 ppm was, in fact, a large doublet signal that corresponds to the ^{13}C-NMR signal at 65.45 ppm, which is in line with the position 4 in the compounds **12**-**14**. There was some uncertainty regarding the identity of the signal at 3.78 ppm, believed to be **14** (mono-ester) specific, due to it correlating to signals in the ^{13}C-NMR at 61.2 and 66.5 ppm, both of which are possible chemical shift values for position 6. However, 3.78 is most similar to that of the theoretical 3.49 ppm, whilst also corresponding to the signals at 4.25 (position 4 / 5 of **13** & **14**) and 5.16 ppm (position 5 of **12**), it was assigned to position 6 of **14**. The most difficult position to distinguish was that of position 5 for **13** & **14**, due to their theoretical chemical shift values expected to be nearly identical to that of position 4. The inseparable nature of the signals was supported by the overlaid nature of the signal described as 4.25 ppm. However, HSQC and ^{1}H-NMR data both showed a signal at 4.13 ppm which correlated closely to the theoretical 4.10 ppm chemical shift expected. COSY data, however, showed no direct correlation with the signals at 3.78 ppm, but a correlation to the position 4 signals at 4.25 ppm was observed.

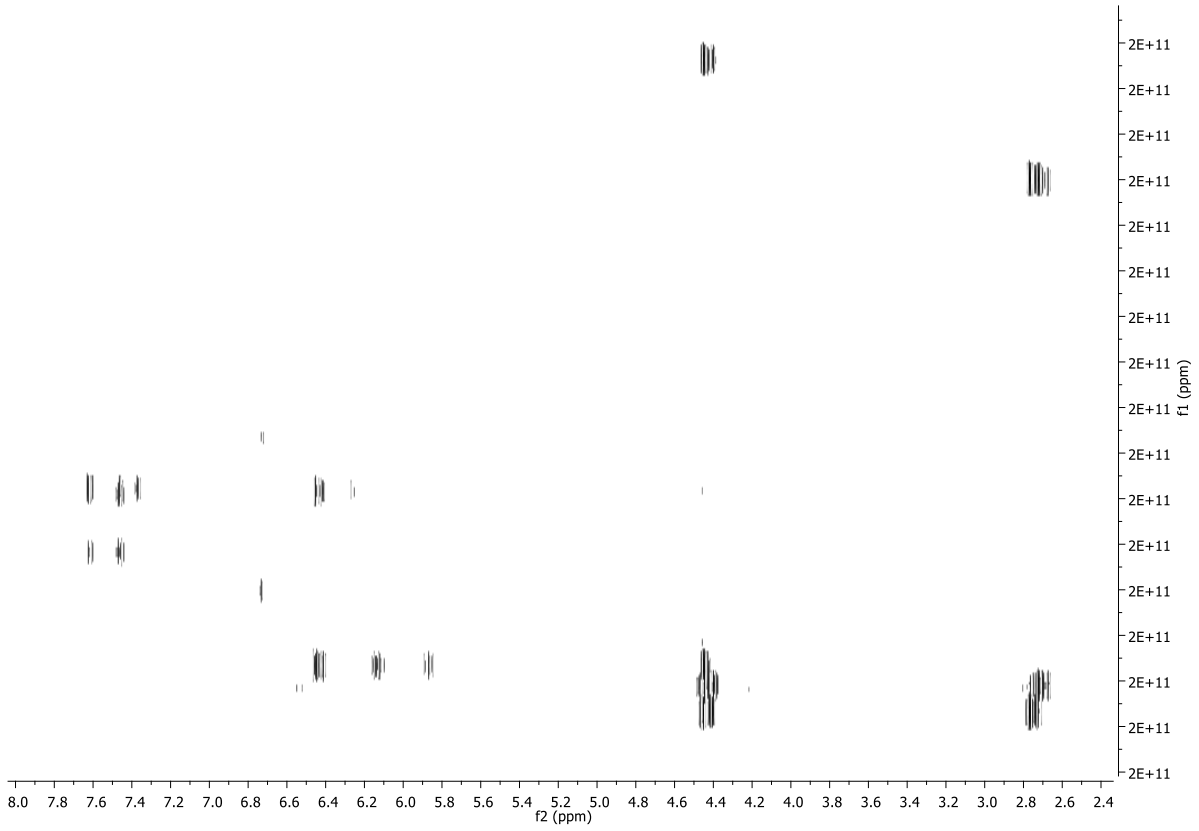

Figure 3.19 HMBC spectrum of **12**-**14** in $CDCl_3$.

Similarly a ^{1}H-NMR signal-to-signal integrational ratio of approximately 1:2.6 (4.13 ppm : 3.78 ppm) was observed, which was near the expected value, with the deviation from an exact 1:2 ratio being ascribed to 4.13 ppm serving as position 5 for both products **13** & **14**. From the HMBC analysis of **12**-**14,** as shown in Figure 3.19 a clearer depiction can be made of the structures obtained. From the HMBC data obtained it was clear that the signal 166.1 ppm is the primarily recognized carbonyl in position 4 for the ester product mixture, due to it being the only carbonyl signal that corresponded to the ^{1}H-NMR signals of positions 1 and 2. The carbonyl signals at 176.4, 170.5 and 166.1 ppm all corresponded to the signals at 4.47 and 2.75 ppm, apart from 166.1 ppm not corresponding to 2.75 ppm.

The aforementioned carbonyl signals allowed for the deduction that the signals at 176.4 and 170.5 ppm were solely dimer signals. Similarly, carbon signals 59.9 and 34.0 ppm corresponded to the oppositely located ^{1}H-NMR signals of 2.75 and 4.47 ppm, which confirmed their structure positions being located adjacent to one another

as in positions 4'' and 5'' of the dimer product as shown in Figure 3.9. The signals at 5.16 and 3.78 ppm did not correspond to any carbon signals on the HMBC spectra, however, the signal at 66.9 ppm does correspond to the position 4 carbon signal 4.25 ppm, which was expected due to the position 6 carbon signal (66.9 ppm) being located near the position 4 carbon. From the DEPT135 analysis in Figure 3.20 of the ^{13}C-NMR spectra, the allocations of the signals expected for carbon positions on the structures of **12**-**14** becomes apparent. All signals in the ^{13}C-NMR spectra shown in region A' have a substitution character of a non-hydrogen baring (quaternary) carbons, which is in accordance with carbonyl positions.

Secondly, region B' signals at 131.1 and 128.0 ppm display substitutions of CH_2 and CH/CH_3, respectively. These substitutions were expected due to the CH_2 being the only possibility for position 1, being part of the alkene group, however, possessing only hydrogen groups attached. The carbon in position 2 was expected to have a CH substitution, and therefore, the CH/CH_3 substitution is appropriate, and also served to confirm the assignment of ^{1}H-NMR signals to both ^{13}C-NMR signals. Lastly, the signals of positions 4-6 are shown in region C', with the signals at 68.37 (position 5 of **14** & **13**), 66.9 (position 6 of **14**), 65.28 (position 4 of **12**-**14**) and 61.0 ppm (position 6 of **14**) showing substitutions matching that of the structures in Figure 3.15. The carbon substitution of position 5 on product **12** can, however, not be discerned due to the signal only being visible on the HSQC. Further elucidation of the dimer positions 4'' and 5'' are shown in the DEPT135 spectra, which determined their substitution to be that of CH_2, as expected.

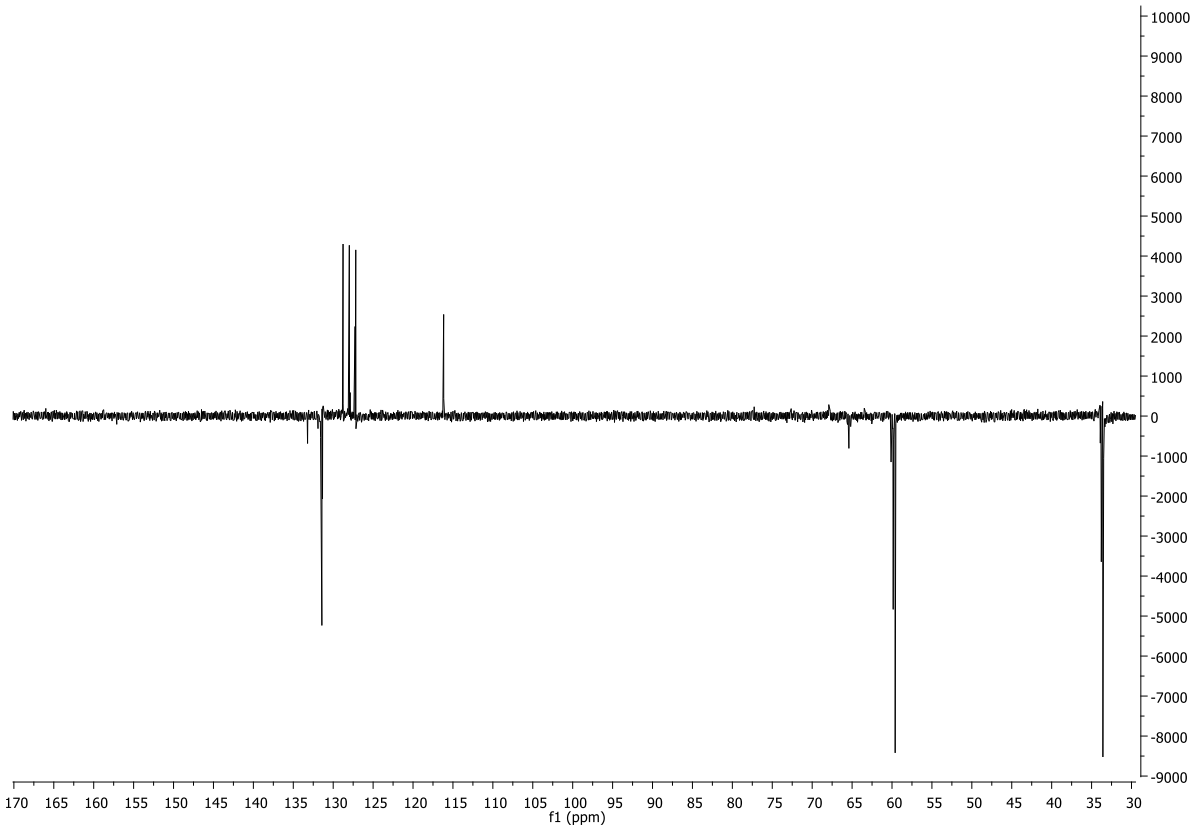

Figure 3.20 DEPT 135 spectrum of **12**-**14** in $CDCl_3$ for carbon substitution determination of carbon signals.

3.4.6 Quantification of ester mixtures components

Quantification of ester mixes is used to primarily determine the ratio of ester products that formed relative to each other, i.e. mono-ester relative to di-ester for **1**-**10**, and mono-ester relative to di-ester and tri-ester for **12**-**14**. This ratio was determined by quantifying the integration values of the mono-ester, di-ester and tri-ester specific signals observed for each product and calculating their relative ratios in relation to a known internal standard of biphenyl. The total mass of mono-ester, di-ester and tri-ester product obtained for each product was used to determine the amount of combined ester product that formed for each linear diol ester mixture and that of glycerol.

Signals used for quantification of di-ester and mono-ester products in products **1**-**10** were the position 4 signals at approximately 4.15 for the di-esters and of the position 5', 6', 7', 8' and 9' signals for mono-ester products; **2**, **4**, **6**, **8** & **10**, respectively.

Glycerol quantification was done by determination of the mono-ester, position 6, the di-ester, position 4 or 5, and the tri-ester, position 5, for comparison and ratio determination. The signals had unique chemical shift values apart from the di-ester, thus attempted mono-ester and tri-ester signal quantification and their use in determining the ratio of the di-ester, was attempted. This was, however, not possible due to the overlapping signals as seen in the Figure (HNMR). Thus, the quantification of glycerol ester products could not be done and neither could a ratio be determined. The mixture, however, was used as is for further application in Chapter 4.

Biphenyl was chosen as the internal reference for quantification due to its signals appearing at more downfield chemical shift values than any expected for those of **1**-**14** in both ^{1}H-NMR and ^{13}C-NMR. The signals obtained from biphenyl were well known and easily identifiable, and any of the three ^{1}H-NMR signals obtained could be used to serve as a reference. The signal chosen primarily for quantification was that of the most downfield signal, i.e. that of the ortho-position at 7.65 ppm with an integration value composed of four protons.

From Table 3.9, it is clear that significantly more of mono-ester was formed, with a mono-ester to di-ester ratio being approximately 3.5:1. However, in the cases of **3** & **4** and **5** & **6** a deviation from the aforementioned ester ratio was observed. Products **3** & **4** formed more di-ester than others and nearly equalling the amount of mono-ester. The opposite was observed for **5** & **6**, with the mono-ester in far excess of the di-ester. In addition to the trends and variations observed, attention should be brought to the standard deviation of the values obtained by repeating the esterification reaction three times. The standard deviations observed were noticeably large in comparison to the average values obtained, with some indicating standard deviation values equating to half the average value. Thus, the reactions, although favouring mono-ester formation, was easily influenced by reaction conditions or were highly susceptible to human error.

Table 3.9 Ester percentage composition quantification of ester mixtures

Ester mixture	Mono-ester (Comp.)	Standard deviation (Mono)	Di-ester (Comp.)	Standard deviation (Di)	Total ester (Comp.)	Standard deviation (Total)	Mono:Di Ratio	Standard deviation (Ratio)
1 & **2**	51.4%	19.81%	14.86%	6.8%	66.2%	23.7%	4.0	2.3
3 & **4**	39.88%	8.07%	31.9%	9.4%	71.8%	4.2%	1.4	0.8
5 & **6**	65.47%	24.48%	4.14%	1.2%	69.6%	25.7%	15.6	1.4
7 & **8**	71.12%	9.94%	21.6%	0.6%	92.7%	10.3%	3.3	0.4
9 & **10**	66.11%	10.23%	20.1%	3.0%	86.2%	9.6%	3.4	0.9
12-14	-	-	-	-	-	-	-	-

The quantification of the glycerol products, **12**-**14**, was not possible and is not shown in Table 3.9. The mono-, di- and tri-ester specific signals for positions 4, 5 and 6 were not distinguishable and occurred within overlapping regions as seen in Figure 3.15 **b.** The overlapping signal range as shown in Figure 3.15 **b** made signal integration inaccurate and thus quantification impossible.

3.5 Conclusion

From the syntheses performed and the products obtained, characterization showed that product formation occurred with di-ester and mono-ester products for all linear diol and glycerol reagents used. Linear diols reacted to form predominantly mono-ester compared to di-ester. However, in all cases, both ester products were formed. Glycerol showed a slightly increased formation of products, however, due to the di-ester being the desired product tri-ester masses increased the yield. Only 1,2-ethanediol and glycerol ester mixtures formed in excess of 50% product formation, thus the reactions are not ideal for eventual application in industry

The low product formation and the large degree of standard deviation prove that the method employed is not ideally suited for a Dean-Stark acid resin catalysed esterification method. Dimer formation was confirmed to take place in every product. However, linear diols showed reduced dimer formation in comparison to the glycerol ester mixture. Product purification could not be achieved via conventional separation methods including TLC and column separation. Post-esterification yielded pure samples containing multi-ester mixtures with inevitable dimer formation. Washing is, however, expected to have attributed to the low product yield by removal of potential product molecules, such as mono-ester products being more water soluble.

Another possibility for the low product yield is that during esterification dimeric or oligomeric forms of an ester product becomes insoluble in the solvent, thus separating from solution and no longer participating in the reaction. Analysis of the product with FTIR, MS and NMR techniques showed the formation of the desired products and made their characterisation possible. However, quantification was limited due to the inability to separate and quantify individual compounds. Thus mono-ester and di-ester ratios were calculated based on pure mixtures. Glycerol's ester composition could, however, not be determined due to the NMR spectra showing overlapped signals at chemical shift values necessary for quantification. However, ester identification could be done for both linear diols and glycerol.

Chapter 4

Polymerization and characterisation of PAA and cross-linked PAA polymer under ideal conditions

4.1 Introduction and objectives

Polyacrylic acid (PAA) and polymethacrylic acid (PMA) are the polymers that result from acrylic acid (AA) and methacrylic (MA) polymerization.[70] The chemical structure of PAA and PMA polymers contains carboxylic acid substituted ethylene polymer chains. PMA, opposed to PAA, is substituted by a methyl group on the carboxylic acid bearing carbon at every second carbon position; thus altering the polymeric structure and packing efficiency, but retaining identical chemical reactivity.[61] Acrylate and methacrylate monomers have limited solubility in water, and their respective polymeric products are also weakly soluble. Due to their solubility, water-based free radical polymerization is the conventional method of forming PAA and PMA.[51]

Free radicle initiation of acrylate and methacrylate polymerization is generally carried out by the addition of peroxides such as hydrogen peroxide.[71] The initiation of the reaction is achieved by thermal decomposition of the radicle generator or radiation exposure of the reaction mixture.[72] An advantageous characteristic for comparing PAA polymer coatings with different cross-linkers is that, according to Kricheldorf et al.,[51] "The behaviour of the various acrylates and methacrylates in copolymerization is independent of the nature of the ester group." Thus, using both ethylene glycol dimethacrylate (EGDM), which is methacrylate based, and acrylate-based cross-linkers should not adversely affect the polymerization behaviour to such a degree that incomparable products are obtained. The only differing factor is thus the length of the cross-linker chain.

Similar to the di-ester products described by Kricheldorf et al.[51] that are formed by the esterification of multi-alcohol baring molecules and linear diols and glycerol, the cross-linkers proposed are derived similarly. Although the behaviour of the acrylates and

methacrylates do not differ significantly based on the ester group, it is found that acrylic derivatives polymerize approximately three times faster than the corresponding methacrylates.[51, 73] To facilitate complete polymerization and high conversion of monomers, conditions proposed by Mohammed,[15] are imposed for the pre-coating characterisation of the polymer. In this study investigations done on the polymer pre-coating and its effect once acting as a coating was compared via Thermogravimetric Analysis (TGA) and was correlated to solution rate results. According to literature the thermal, physical and chemical properties of acrylate polymers are greatly affected by the presence and type of cross-linking.[74]

The uncross-linked polymer products are not ideal for application as a coating, thus in this study cross-linking will be employed whilst having an uncross-linked polymer serving as a reference. Polymerization of the reference uncross-linked and cross-linked PAA was carried out under ideal conditions in an aqueous solution. However, for coating, a solvent-less reaction was used due to water causing runoff and dispersion of the monomer solution. Industrial-scale polymerization of acrylates and methacrylates done solvent-less and are ideal for the encapsulation of fertilizer pellets.[76] Cross-linking agents are additives to the monomeric mixture prior to polymerization that promote covalent bond formation between polymer chains.[70] Cross-linking occurs by the incorporation of the cross-linking agent into the monomeric solution, which reacts similarly to acrylates and methacrylates.

The effects of cross-linking vary greatly, which are based on the type of cross-linker and the degree of its composition of the resulting polymer. Cross-linkers cause, by the intermolecular linking of polymers, the formation of a three-dimensional mesh-like structure with differing characteristics to the uncross-linked polymer chains. These altered characteristics may include reduced solubility, increased thermal stability and changes in chemical reactivity, which among other applications, are ideal for coating due to its increased adhesive ability.[71, 77] The inability to dissolve most cross-linked polymers acts to prohibit dissolution of the polymer layer applied, thus retaining its shape and function as a barrier. The mechanically stronger cross-linked structure also acts to increase its abrasion resistance, which acts to protect it from mechanical removal that is ideal when used as a coating. However, the three-dimensional mesh-like structure allows for increased water adsorption to the pellet and absorption into the polymeric structure.[15, 47] The inter-polymeric spaces caused by cross-linking acts

to increase porosity and form an amorphous structure that can be penetrated by water.[47]

As mentioned previously in Chapter 2, a physical barrier coated fertilizer is the predominant and most promising method; thus a similar method is utilized in this study. The use of biodegradable coatings has in the past served as a programmed-release method due to its degradation time, thus planning the release in accordance to the degradation of the coating.[19] When using cross-linked PAA, itself biodegradable and non-toxic,[2] to form a physical barrier, encapsulating the pellet will act to slow the release of fertilizer ions. The act of serving as a physical barrier is due to the ability of cross-linked PAA to adsorb water readily into the inter-polymeric spaces of the three-dimensional structure leading to eventual penetration through the barrier to the fertilizer within.[44-45]

An amorphous polymer coating on fertilizer pellets will allow water absorption to take place when applied in the soil; the hydrophilic nature of PAA will cause adsorption and penetration of the capsule by the water to the inner core. Solution of the fertilizer occurs inside the encapsulated pellet; however, its release is slowed by traversing the polymer matrix to the surrounding environment. The release of the fertilizer is thus gradual and systematic compared to the simple solution of a salt-like substance such as KNO_3 and monoammonium phosphate (MAP). The controlled-release of fertilizer to the surrounding environment could theoretically be suited to the requirements of the crop nutritional demand.[78] Determination of optimal cross-linking and the amount of coating is done by the variation of the cross-linker percentage presence and the mass percentage of polymer applied to a fertilizer batch.

In this study potential ‘programming’ of the release rate was determined by evaluating experimental data, which was subsequently used to plan coating compositions based on its composition of cross-linker, amount of coating and the number of layers applied.[78] Multiple-layered coatings are commonly employed in various studies to slow the release rate of fertilizers. However, the amount of coating applied to fertilizers differs substantially, similarly, the type of coating in each layer is also frequently varied.[79] Multiple coating layers were attempted, however, limited to two types of cross-linked PAA due to logistical and time constraints.

The aim of this study was to evaluate the potential application of synthesized PAA cross-linkers as cross-linked PAA coatings on fertilizer pellets. The effect of the coating on controlled-release characteristics was determined by evaluating the solution rate of fertilizer pellets, with and without coatings. An additional investigation into the altered effect that the cross-linkers have on the properties of PAA was done to match thermogravimetric data to release rates.

The objectives of this Chapter is:

- Ideal condition polymerization of uncross-linked and cross-linked PAA to determine the effect of cross-linker introduction on the thermogravimetric characteristic of the polymer.
- Application of PAA and cross-linked PAA on fertilizer pellets to form a coating in various layers and with differing cross-linkers.
- Evaluation of whether controlled-release characteristics were imparted to uncross-linked PAA coatings and with cross-linked PAA coatings.

4.2 Experimental

4.2.1 Materials

AA (Sasol), ammonium ferric sulphate (LabChem), ethylene glycol dimethacrylate (Merck; **11**), , KNO_3 (Omnia), MAP (Omnia) and hydrogen peroxide (Rochelle Chemicals) were used as received from suppliers unless stated otherwise. In addition to the chemicals obtained from suppliers the ester mixtures synthesized in Chapter 3 (i.e. **1** & **2**, **13** & **4**, **5** & **6**, ***7*** & **8**, **9** & **10**, **12** -**14**) were used following the post-reaction work-up. Freshly distilled AA was prepared prior to each reaction or application involving AA. AA distillation occurred under nitrogen and reduced pressure with the addition of hydroquinone prior to distillation.

4.2.2 Analytical techniques

Physical Characterisation – Thermogravimetric and Calorimetric Testing

TGA and DSC analysis of the polymer samples were carried out on uncross-linked and cross-linked PAA samples with cross-linker percentages of 0.5%, 1.0%, 2.0% and 5.0%. The analyses were carried out using a Netzsch STA 449F3 STA449F3A-1386-M with a temperature calibration of 5 K/min, starting at -10.0 °C for 5 min after which the temperature was increased to 100.0 °C and held constant for 2 min, followed by cooling of the sample at 5 K/min to -10.0 °C, which was held constant for 5 min, and again heated at 5 K/min until 800.0 °C was reached. The system was purged with helium throughout the analysis of all samples.

Moisture absorption testing of coated fertilizer pellets

Moisture absorption testing was done in a Memmert CTC 256 climatic test chamber, with a 1 cm high and 6 cm diameter glass Petri dishes A Hairuis data logger, model SSN-22 to verify temperature and humidity was also used. Glass Petri dishes were used for test work By adding enough sample to ensure the bottom of the petri dish

was covered. The weight was noted, and done in triplicate. The samples were placed in a humidity chamber for at least 6 hours. Over the time period the samples were weighed to track the increase in mass that can be attributed to water absorption. For the MAP moisture absorption test, the temperature and humidity were set at 30 °C and 95% respectively, and for the KNO_3 moisture absorption test, the temperature and humidity were set at 30 °C and 90% respectively.

Controlled-release rate determination

Controlled-release evaluation was done by the solution of uncoated and coated, KNO_3 and MAP in deionised water and the continuous measurement of conductance throughout the solution. A batch of 1.0 g pellets was placed in a beaker filled with 1 L of deionised water, while kept at 25 °C. A conductance meter electrode was inserted into the solution and held emplace centrally, 3 cm above the bottom of the beaker, by fixing with a clamp. At the moment of introducing the pellets into the 1 L deionised water solution, the conductance analysis program was activated to analyse the conductance value of the solution at 10 min intervals over a 72-hour period.

Throughout the analysis, the solution was not stirred or moved, due to any physical disturbance acting to stir the solution and causing faster solution of the pellets. An uncoated batch of fertilizer and polymer-only samples were analysed to serve as a reference, giving an indication of solution time and the contribution to conductance by the polymer. The initial change in conductance and the final value, exhibiting significant plateauing, were the key points observed and were used to determine the effectivity of the controlled-release effect.

4.2.3 Synthesis of uncross-linked and cross-linked polymers and coating of fertilizer pellets

Polymerization of AA

Polymerization of uncross-linked and cross-linked PAA was performed under controlled conditions for investigation of the effect of the cross-linker on the polymer. Controlled polymerization was done to negate any potential effect on the polymer not attributed to the cross-linker. Polymerization was done according to the method of Mohammed.[15] For an uncross-linked PAA polymer coating, 2.5 mmol (0.98 g) of $Fe(NH_4)_2(SO_4)_2 \cdot 6H_2O$ was added to 0.347 mole (25 g) of AA, while stirring under nitrogen for 15 min in a 200 mL two neck round bottom flask. Addition of 0.0196 mole (2 mL) 30% H_2O_2 was done by introducing the solution with a gastight syringe through a venting valve, while maintaining nitrogen flow, after which the reaction was heated to 70 °C and continuously stirred for 2.5 hours. Cross-linker incorporation was achieved by introducing the cross-linker in weight percentages with regard to AA, as seen in Figure 4.1.

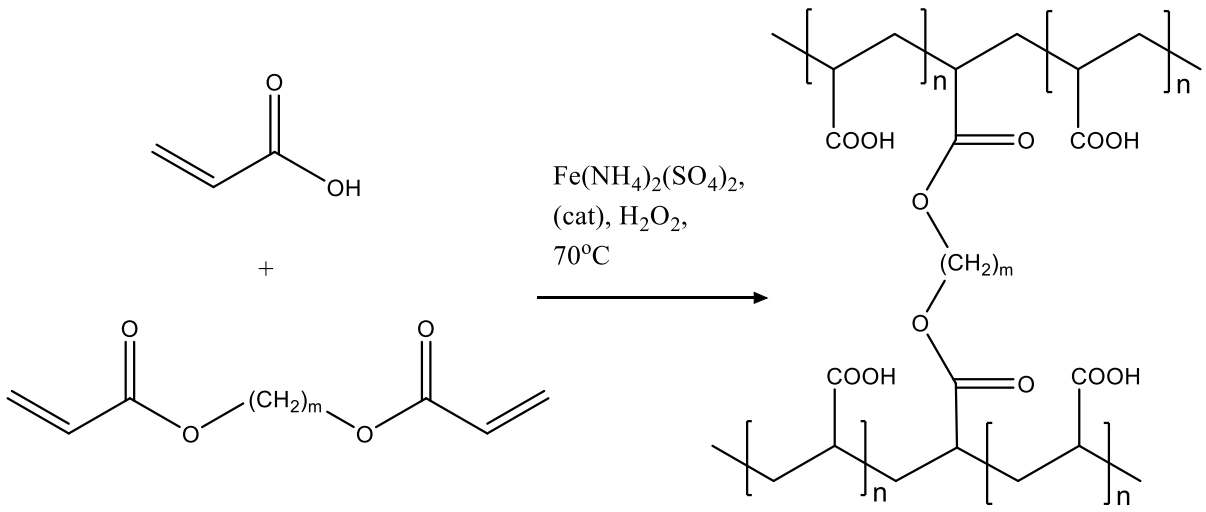

Figure 4.1 Polymerization of AA monomers in the presence of cross-linking di-ester groups, with m = 2-6, will promote the formation of hydrophilic porous polymer structures, used to encapsulate fertilizer pellets.

4.2.4 Variation of cross-linker type and layers applied during fertilizer coating

Honey-Jar coating method

The application of uncross-linked and cross-linked PAA as KNO3 and MAP coating is carried out by cover the pellets being coated and polymerize the polymer on the fertilizer surface. The coating procedure of KNO_3 and MAP fertilizers used 100 g batches of fertilizer placed in a 500 mL container with a screw-on lid. Mass notations were made throughout the coating process to determine the amount of polymer transferred to the fertilizer batch that was used for coating thickness determination. Prior to coating, the monomer solution containing AA and cross-linker was combined with H_2O_2. In the weighed container; 100 g of fertilizer, the monomer and the H_2O_2 mixture were placed, the lid was screwed shut, and with manual shaking for 10 seconds, distribution of the monomer occurred to fully coat the fertilizer pellets. Immediately following the addition of the monomer and H_2O_2 solution, $Fe(NH_4)_2(SO_4)_2 \cdot 6H_2O$ dissolved in H_2O, was added and again the lid was screwed shut and shaking of the container occurred to distribute the catalyst, initiating polymerization.

The coated fertilizer batch was transferred from the container that was weighed post-coating to a pre-weighed metal dish that was placed in an oven at 70 °C for 2.5 hours under nitrogen. The coated fertilizer was removed from the dish, with both weighed and the coated fertilizer stored until solution testing. 5% cross-linker usage was employed throughout testing to ensure comparable testing. Lower cross-linker percentages were not used due to time constraints and high percentages being most likely to encourage controlled-release. All variations in coatings applied were done with a 5 weight-to-weight percentage (w/w%) application of each linear diol, glycerol and EGDM cross-linked coating, uncross-linked PAA served as reference and multi-layered coatings of PAA and **3** & **4** cross-linked coatings were made to test multiple coating effects.

4.3 Results and discussion

4.3.1 TGA and DSC analyses of cross-linked and uncross-linked PAA

Analysis of PAA has been well documented in the literature and was shown by Moharram and Khafagi[80] and Fyfe and McKinnon,[81] the decomposition steps associated with PAA thermal degradation is due to either absorbed compounds released from the polymer matrix or internal degradation of the polymer structure. The released substance in the case of PAA is water, reaching a maximum at 100 °C, with main chain and side chain degradation occurring at higher temperatures. The decomposition of polymeric structures is divided into three separate decomposition steps following one another with some degree of overlap; however, each having a unique maximum temperature for degradation.

Degradation of PAA generally occurs by initial side group elimination, that entails a two-step process during which the polymer chain is first stripped of atoms or molecules, leaving an unsaturated chain, followed by the resulting polyene undergoing scission, aromatisation and char formation.[82] The three theoretically expected, and experimentally observed, decomposition steps, as described by Moharram and Khafagi,[80] are divided into temperature ranges, i.e. (A) 156.8 – 225.3 °C with maximum degradation reached at 196.89 °C and an approximate weight loss percentage of 8.419%; (B) 225.3 – 301 °C with maximum degradation reached at 270.93 °C and an approximate weight loss percentage of 17.74%; and (C) 301 – 476.1 °C with maximum degradation reached at 372.36 °C and an approximate weight loss percentage of 55.87%.

The degradation processes ascribed to these decomposition steps (A, B and C) are a combination of chemical changes and reaction; with the first step being that of a loss of acid functionality and anhydride formation. Carboxylic acid groups located on the polymer chain undergoes anhydride formation. This anhydride formation occurs via a dehydration reaction to form either an open structure isobutaric anhydride, a five-membered succinic anhydride ring or a six-membered dimethylglutaric anhydride ring. The six-membered ring is formed predominantly by cyclization of adjacent carboxylic

acid groups.[81] During the second decomposition step, an increase in aromaticity and dehydrogenation occurs, with the polymer backbone becoming unsaturated.[81]

The final step encompasses the degradation of previously formed anhydride groups, methylene double bond (main chain) cleavage and oxidation of carbonyl and other groups still present.[80-81] Breaking of the polymer chain occurs by double bond cleavage, forming methyl groups present on chain fragments, while oxidation of carbonyl groups leads to CO_2 release and char forming in the heating pan.[80-81]

From the TGA of the varyingly cross-linked PAA presented in Figure 4.2, it became apparent that during the initial heating curve a large mass percentage of entrapped compounds were released with the spectra plateauing, to only again degrade once 100 °C was surpassed. The initial release of entrapped compounds is clearly evident and can be ascribed to the aqueous solvent and atmospheric water absorbed. However, after the cooling period the degradation patterns were similar than described in the literature with three distinct decomposition steps forming. The maximum degradation temperatures for the analysed polymers were determined at the points within the decomposition steps at the steepest points along the TGA line. The temperature ranges of degradation were noted and labelled A, B and C as shown in Figure 4.2 and Table 4.1, following the steps described by Moharram and Khafagi.[80] The mass percentage loss observed for the solvent release, degradation steps A, B and C, and the final residue percentage following analysis is tabulated as shown in Table 4.1. Analysis of the cross-linked PAA showed similar degradation steps with similar ranges and maximum temperatures to those proposed in the literature. The effect of cross-linking on thermogravimetric degradation was limited, and TGA data closely resembled that of the literature PAA [81], which indicates the ineffective cross-linking ability of the ester mixtures applied.

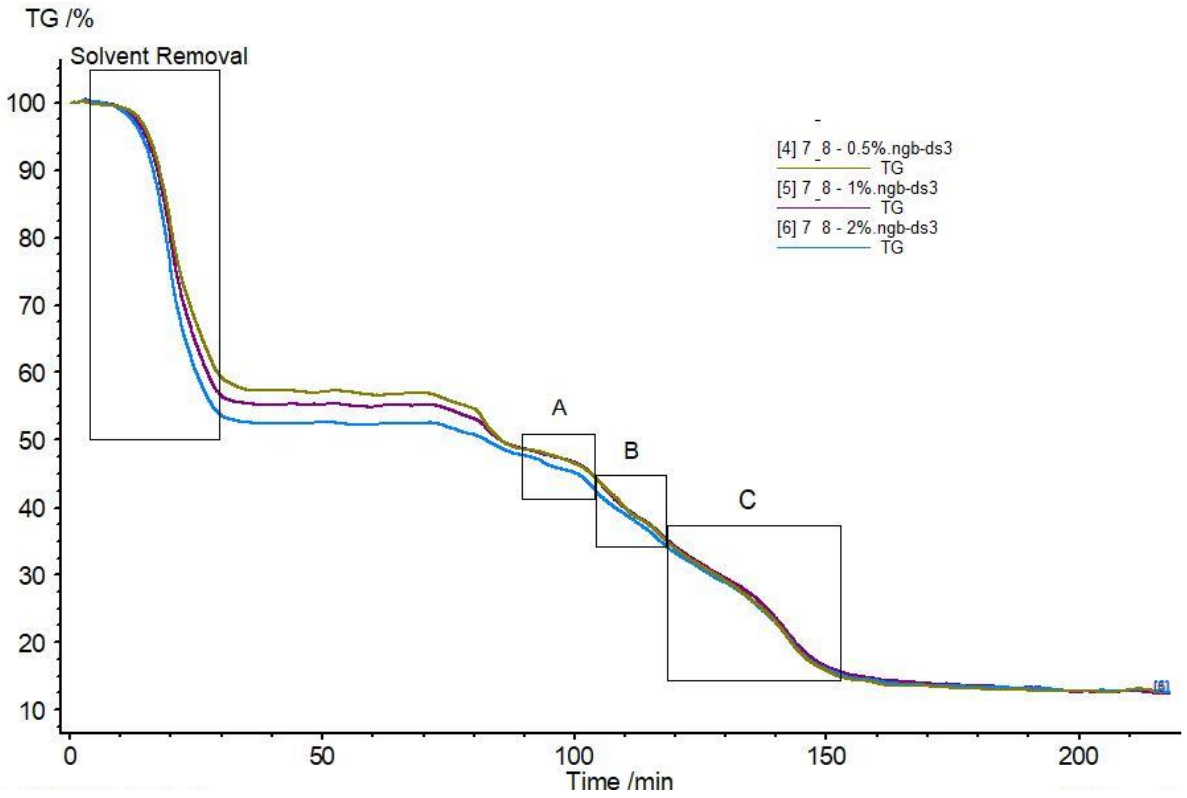

Figure 4.2 TGA of 0.5%, 1.0% and 2.0% cross-linked PAA, employing **7** & **8** cross-linker mixtures. Degradation steps indicated with regions labelled; Solvent removal, A, B and C.

Table 4.1 Thermogravimetric analysis of cross-linked PAA, with percentage incorporation of cross-linkers **1**-**10**. The mass percentage losses noted for the degradation steps observed. The solvent release step and final residue percentage present are also given.

		Cross-linkers												
		1 & **2**			**3** & **4**			**5** & **6**			**7** & **8**			**9** & **10**
Cross-linker Percentage	Degradation Step	0.5	1.0	2.0	0.5	1.0	2.0	0.5	1.0	2.0	0.5	1.0	2.0	1.0
Mass Loss %	≤ 100 °C	27,6	25.9	31.6	41	47.8	46,4	44.9	28.7	40.5	42.6	44.8	47.5	44.8
	A	6.1	5.6	8.2	5.7	7.3	5.0	7.7	7.7	4.7	8.6	6.3	4.5	6.3
	B	21.0	20.2	21.9	14.7	14.5	14.3	15.3	22.3	18.7	17.9	18.6	18.7	18.6
	C	18. 8	21.3	17.7	14.3	13.7	12.6	18.8	22.0	14.0	15.5	14.7	13.5	14.7
Residue %		26.6	27.0	20.6	24.3	16.8	21.7	13.4	19.3	22.2	15.4	15.7	15.9	15.7

The loss of mass prior to the first degradation step at temperatures up to 100 °C due to solvent evaporation, occurred for all cross-linked samples of PAA. However, the amount released from the polymer prior to degradation varied greatly, as seen in Table 4.1. Solvent mass losses were in excess of 40% for most samples, which was to be expected due to the superabsorbent nature of PAA without any drying process being performed prior to analysis. However, the mass of solvent lost for all cross-linker percentages of the **1** & **2** cross-linked PAA and the 2% cross-linker percentage sample of the **5** & **6** cross-linked PAA were less in comparison and were in the range of 20 – 32%, while being significant compared to the mass loss of the remaining sample that was less than other cross-linked samples. The mass percentage of solvent lost can be ascribed to the absorption potential of the polymer matrices and reflects the efficiency of the cross-linker emplace.[17]

The effect of cross-linking under thermogravimetric analysis will not retain the absorbed water similar to mechanical testing, however, the solvent will escape from the matrix when the solvent's boiling point is overcome.[17, 47] Thus, the amount of mass loss was ascribed to the retention capability of the matrix itself and as shown in literature, the retention ability of PAA is indirectly proportional to the degree of cross-linking.[83-84] Due to atmospheric exposure, some water absorption under ambient conditions could have contributed to the mass percentage of water absorbed, indicated by the solvent mass loss during heating while undergoing thermogravimetric analysis. However, varying cross-linker concentrations yielded similar solvent mass loss prior to the decomposition steps. Thus, the overarching effect of solvent absorption was due to the unique cross-linker employed, however, differences between concentrations of similar cross-linkers differed insignificantly, with similar mass losses observed and no clear pattern emerging.

This observation led to the assumption that the cross-linker has an initiatory role in water absorption. However, using less or more of the cross-linker did not significantly alter its effect. The observed insignificant effect of the cross-linker was in contrast to a study done by Katime, de Apodaca and Rodriguez,[84] who proved the effect of cross-linker presence on both the absorption and swelling, by showing an increasing cross-linker presence lessened absorbance and swelling. According to Katime, de Apodaca and Rodriguez,[84] the effect of the cross-linker reached a maximum at a cross-linker

percentage presence of 2%, which is similar to this investigation although employing different cross-linkers to this study. The cross-linking efficiency of cross-linkers employed therefor comes under scrutiny, which was to be expected from the ester product mixtures obtained previously, as shown in Table 3.9. The mono-ester presence was in excess of the di-ester, with the only species capable of cross-linking being the di-ester. Thus, an increased ester product percentage in the polymer was expected to exhibit little to no cross-linker variation due to the limited amount of di-ester present.

However, due to cross-linkers still causing a difference in the thermogravimetric characteristic of the PAA despite limited di-ester present, the effect of the mono-ester and di-ester must be considered when determining the effect of the introduced cross-linker. The introduced cross-linking agent could form structural variations that differ from that of uncross-linked PAA or the packing densities of the polymer is altered due to the ester groups from the mono-ester, dimeric or other oligomeric compounds. These structurally protruding groups would make polymer alignment strained or cause inter-polymeric interactions to take place, accounting for the limited effect of the varied cross-linkers employed.

Comparison of the analysed samples to that of theoretical degradation percentages as given by Moharram and Khafagi,[80] showed a near-identical percentage mass loss at degradation step A and B, however, a significantly lower percentage of mass loss was observed at step C. Step C pertains to the cleavage of the main chain of the polymer by breaking the polyene chain and oxidation of remaining carbon content. The observed mass loss percentage was on average 16.39% which was significantly less than the 55.87% as observed by Moharram and Khafagi.[80] Such a large deviation was uncharacteristic of the final degradation step due to the process of anhydride cleavage and CO_2 formation via oxidation occurring in step C, being dependent on the groups formed in steps A and B. Thus, due to steps A and B being identical in scale to literature values and the mass loss percentage of step C being smaller, the difference must have been due to the presence of cross-linkers or other compounds in the ester mixtures.

4.3.2 Scanning Electron Microscopy (SEM) analyses of cross-linked and uncross-linked PAA

Visual investigation of the coated and uncoated fertilizer pellets served as a reference to determine the coating effectivity by establishing complete coating of the entire surface and by determining the thickness of the coatings applied. Complete coating of the pellet surface is important for achieving effective controlled-release, due to exposed surfaces negating the effect of the coating and resulting in unaltered release rates.[85] The coating thickness of samples will aid in determining the effectiveness of the polymer to serve as a barrier, and is frequently reported in the literature.[85] Coating thickness can be determined by mass calculations, using pellet size and the mass of polymer applied. However, in this study thickness was determined by SEM measurement.

According to Du, Zhou and Shaviv,[86] an increased coating thickness caused the rate of release to slow, however, a greater emphasis was placed on the environmental factors that affect the rate of the solution, in addition to the thickness of the membrane that needed to be traversed for release from the encapsulated pellet. These external environmental factors were controlled during the release rate testing, to minimize effects not ascribable to the coating itself. In addition to the thickness of the applied coating layer, the need for coating efficiency is the largest factor influencing the rate of release for encapsulated fertilizers. Thus, for controlled release of fertilizers, a uniform layer of coating must be achieved, with minimal amounts of deficiencies and exposed surface area, which acts to negate the effect of the coating.[85]

Coated and uncoated samples of KNO_3 fertilizer pellets were analysed with SEM. Analysed micrographs were taken of the uncoated sample in Figure 4.3 **a**, and coated fertilizer samples are shown in Figure 4.3 **b,** which shows an enlarged picture of fertilizer pellets joined together, Figure 4.3 **c** showing a surface coating picture of fertilizer that was partially covered and Figure 4.3 **d**, giving an indication of the coating thickness obtained. The observed smooth surface of the KNO_3 as seen in Figure 4.3 **a,** is due to the fertilizer that is formed industrially. The sizes and masses of such pellets vary greatly, however, the pellets were used as obtained and implemented in industry. The smooth surface may cause difficulty for polymers to adhere to the pellet and remain fixed throughout processing and use. This is due to polymers tending to

collect and adhere to rough surfaces, cavities and protrusions[87] on the surface or between pellets,[12, 88] which is evident as ridges protruding from the surface in Figure 4.3 **b**, showing polymer collection occurring and acting as an adhesive between pellets.Due to the collection of polymer to protrusions, the surface coating becomes less effective as observed in Figure 4.3 **b**. The polymer inevitably collects at a specific point on the fertilizer and spreads; thus, full surface coating is not achieved. Industry-based application of polymers to fertilizers, opposed to the coating method used in this study, usually follows the addition of a coating to fertilizers in a tilted rolling granulator, keeping pellets moving continuously throughout coating that grants sufficient time for the coating to harden and set, similar to the process described in the patent by Hirano, Yamaguchi and Nakamura [89], however, this process is for much larger scale applications than tested in this study.

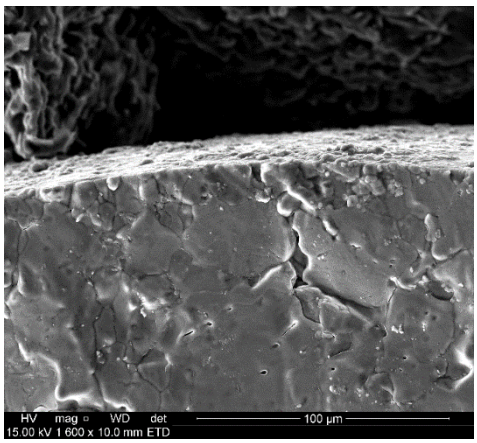

a) Uncoated KNO_3 pellet

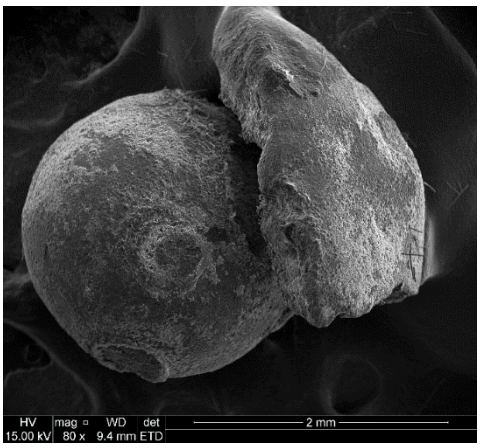

b) PAA coated KNO_3.

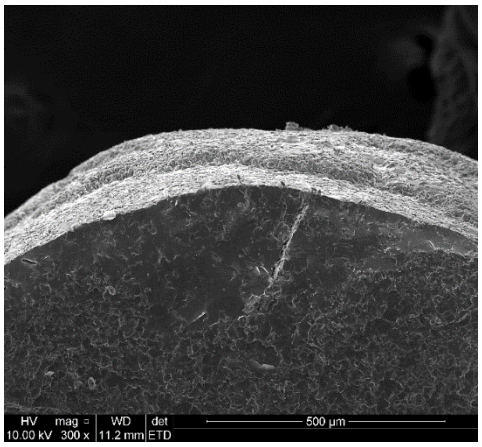

c) Cross-section of single layer PAA coated KNO_3

.

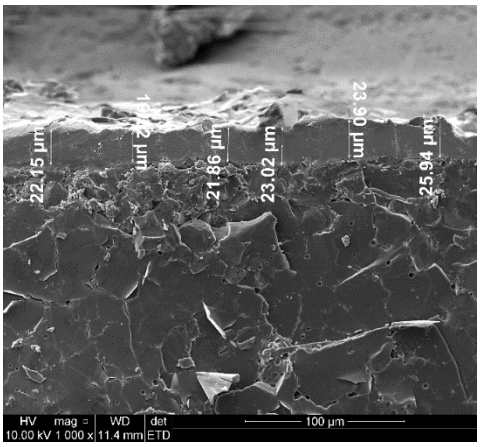

d) Measured cross-section of single-layered cross-linked PAA coating on KNO_3.

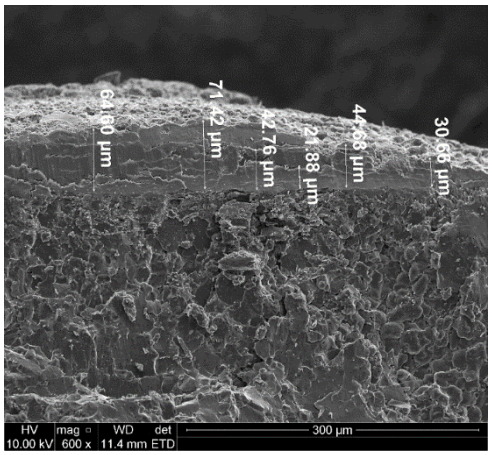

e) Cross-section of multiple-layered cross-linked PAA coating of KNO_3,

Figure 4.3 SEM micrographs of uncoated and coated KNO_3 samples.

Following the description given by Hirano, Yamaguchi and Nakamura,[89] where a 0.5 w/w% coating of polymer, in this case, cross-linked polyurethane, was applied to a 2 kg fertilizer batch compared to 100 g batches as attempted in this study, a coating thickness of 3.1 µm was obtained by Hirano, Yamaguchi and Nakamura.[89] When analysed, after coating of a single coating the thickness of the applied polymer coating measured an average thickness of 22.65 µm, which was expected of a 5.0 w/w% application as is the case for this study as shown in Figure 4.3 **d**.

However, according to Figure 4.3 **c** it shows non-uniform coating and with some of the surface area left uncoated which is due to the ineffective method of application. The collection of the polymer occurred atop layers of the previous application. In Figure 4.3 **d** and Figure 4.3 **e,** the polymer is the smooth layer surface observed above the bottom fertilizer core. Figure 4.3 **e** demonstrates the tendency of secondary and tertiary layers of coating to stack and fill pores created by the previously applied layer, leading to variation in thickness to the layers applied multiple times, as observed in this study. Thus multiple-layered coatings did not cover the fertilizer pellets completely nor form uniform layers, however, instead secondary and tertiary layers collected atop previously applied layers and caused varied thickness to form. The porosity of PAA mentioned earlier, is a good reason for the affinity of secondary and tertiary layers to form atop previous layers.

4.3.3 Moisture absorption testing of coated KNO_3 and MAP fertilizers

Moisture absorption testing occurs by placing fertilizer pellets in a climate-controlled chamber capable of maintaining the humidity and temperature exposed to the fertilizer pellets. The analysis starts by drying the pellets of all moisture and subsequent determination of the moisture absorbed from the experimental ambient conditions. The ability to absorb moisture is directly relatable to the hydrophilicity of the sample, with increasing moisture absorption suggesting increasing solution rates. PAA, will inevitably cause an increase in moisture absorbance, however, the introduction of cross-linkers should limit the water interaction capability of PAA. Increased amounts of cross-linkers used should lower the moisture absorption of the coated pellets and inevitably lead to a reduced rate of solution. Thus, a correlation between the moisture

absorption and the rate of release was determined. Investigation of whether the super absorbance of the polymer increased water interaction and still resulted in increased solution or whether the polymer, although being superabsorbent, remained intact and acted as a barrier surrounding the pellet, was carried out. Since coating fertilizer pellets with polymer was done in an attempt to create a less hydrophilic surface that would cause slowed solution when exposed to water, the implementation of cross-linked polymers was expected to lower the moisture absorption of the fertilizer pellets.

The amount of change brought about by varying cross-linker implementation and the amount of layers applied were used to determine the efficacy of the polymer coatings and to distinguish the best cross-linker for controlled-release coating and the effect of varying numbers of layers. Moisture absorbance testing is predominantly done on fertilizers that are hygroscopic of nature and absorbance testing of KNO_3 and MAP, not particularly prone to exhibiting hygroscopic character, are not commonly analysed by this method. Thus, the application of PAA-based coatings to these fertilizers might act to increase moisture absorbance while also acting to serve as a barrier for controlled-release. From the moisture absorbance trends observed in Figure 4.4, it became clear that most coatings imparted hydrophobicity to the fertilizer pellets.

However, **9** & **10** and **12**-**14** cross-linked samples showed slight increases in moisture absorbance. From the multiple-layered coatings, a lessened effect was observed, with most samples showing similar or increased moisture absorbance, with **11** 50% 5% being the only sample that showed a clear reduction in moisture absorption, as shown in Figure 4.5. The effect caused by the amount of coating was negated, due to the varying absorbance values obtained, with some single-layered coatings resulting in reduced moisture absorption values compared to double or triple coatings. Thus, the effect of moisture absorbance was solely due to the cross-linker type or the efficiency of the coating made, as seen by the double and single-layer coated **3** & **4** cross-linked layer having decreased absorbance compared to the triple-coated sample of **3** & **4**. However, from the multiple **3** & **4** cross-linked coating, the cross-linker effect was removed from consideration due to the same cross-linker being used. Thus, the coating method must be the driving factor for the observed trend. The lowest moisture values obtained were from the single-layer coating of the **11** 50%-5% and the **5** & **6** cross-linked coating, possibly due to possessing the most di-ester compounds or from efficient coating.

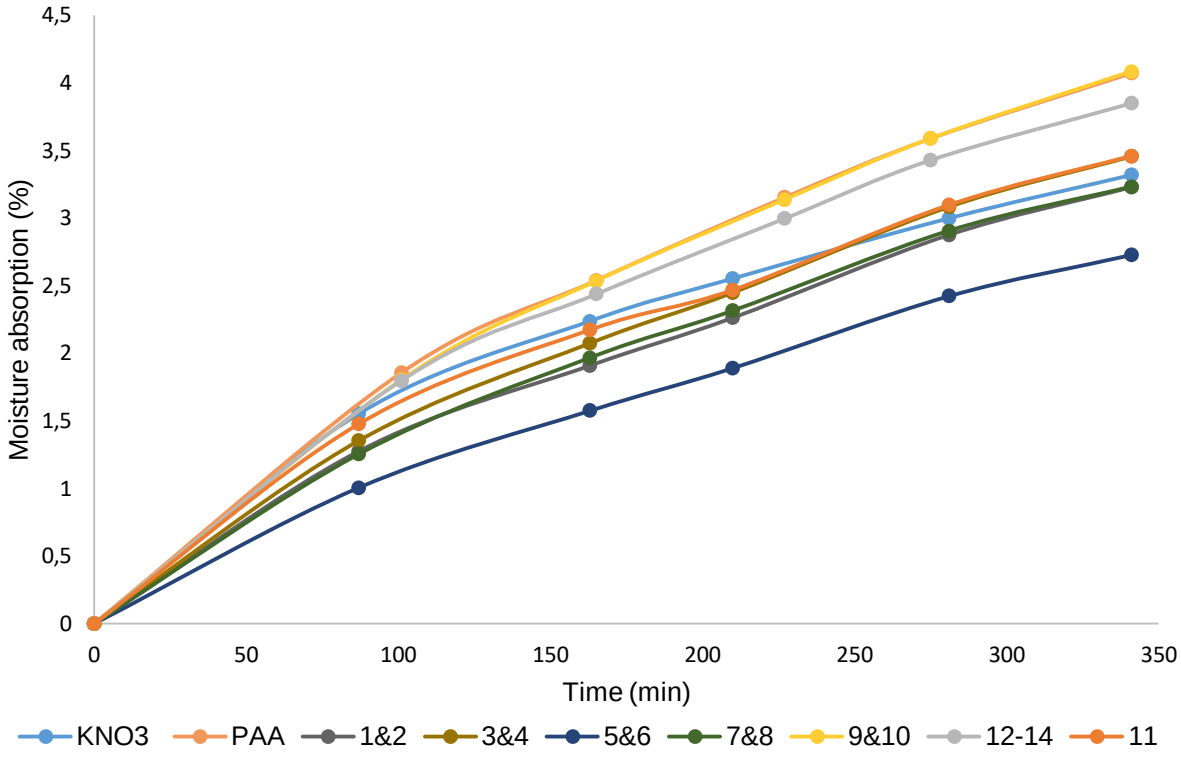

Figure 4.4 Moisture absorption of uncoated and single-layered coatings of KNO_3 fertilizer. Cross-linkers used employed were applied at 5% crosslinked, 5 w/w%.

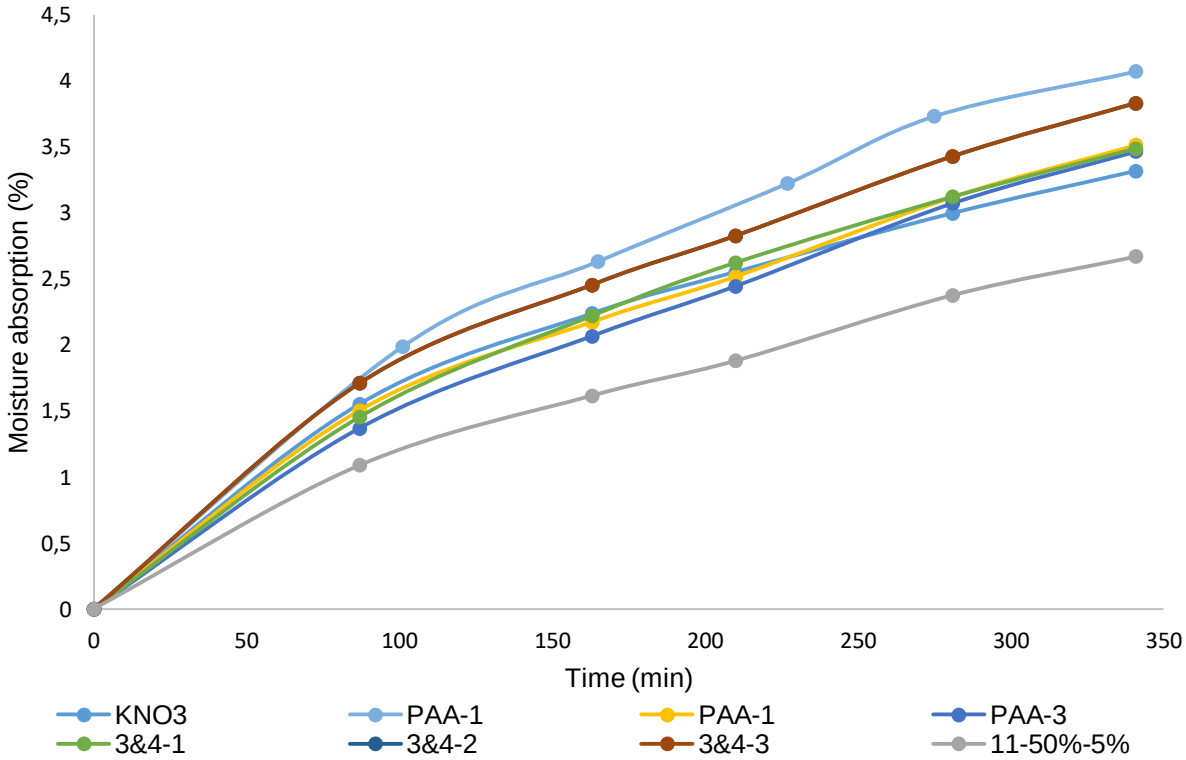

Figure 4.5 Moisture absorption of uncoated and cross-linked multiple-layered coatings of KNO_3 fertilizer. The layers applied: 1 (2 w/w%), 2 (4 w/w%) and 3 (5 w/w%) with a 5% cross-linker presence.

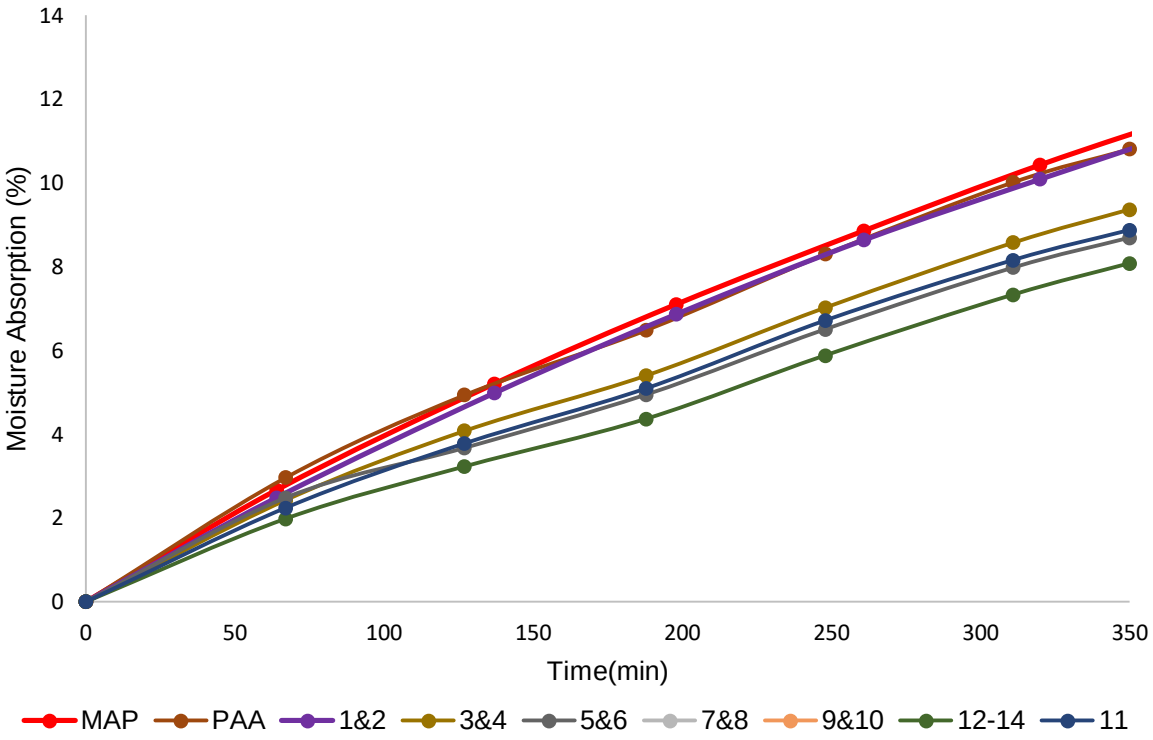

Figure 4.6 Moisture absorption of uncoated and single-layered coatings of MAP fertilizer. Cross-linkers used employed were applied at 5% cross-linked, 5 w/w%.

From Figure 4.7, it is again observed that a multiple-layered application of cross-linked PAA decreased the moisture absorbance of coated samples in comparison to the uncoated sample, with the exception of the double layered PAA coating which showed a large increase compared to the uncoated MAP sample. The effect of the coating application once again became evident, due to the single-layered application of PAA having the lowest absorbance value of all samples tested, and the double-coated PAA sample having the highest absorbance value. The PAA multiple coatings did not employ cross-linkers, and therefore only the presence of a coating and the nature of the fertilizer were considered for an explanation.

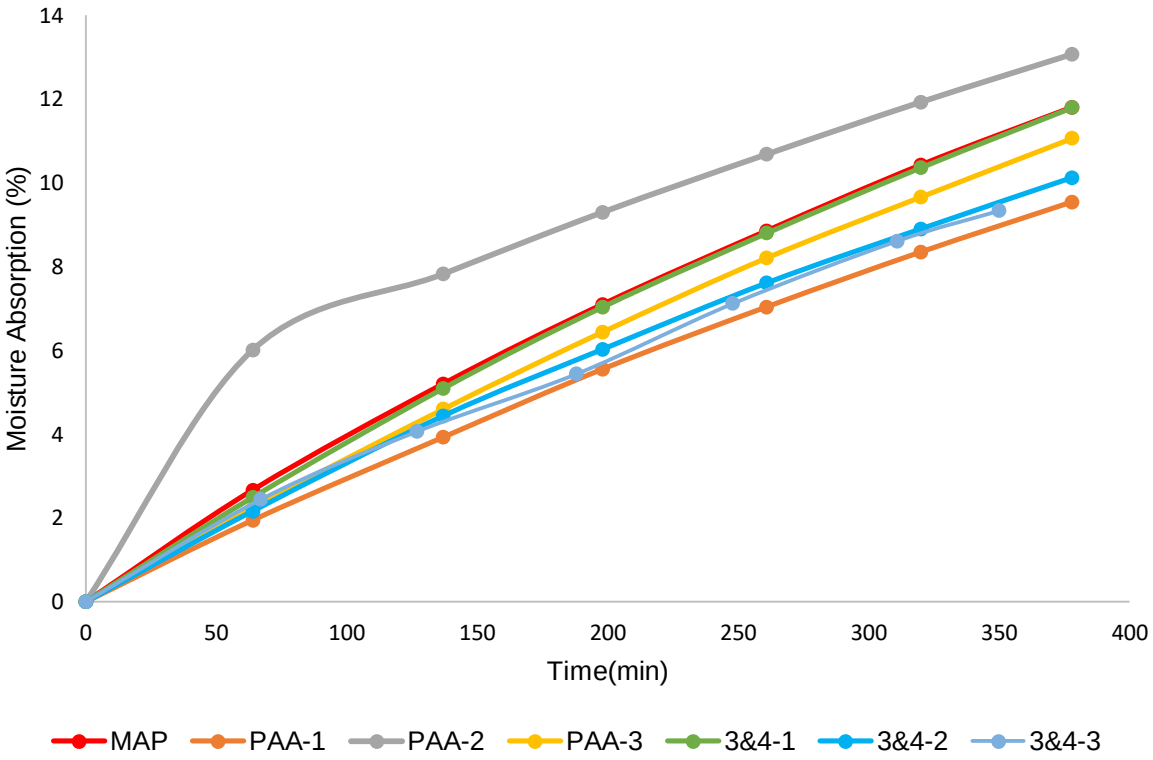

Figure 4.7 Moisture absorption of uncoated and cross-linked multiple-layered coatings of MAP fertilizer. The layers applied: 1 (2 w/w%), 2 (4 w/w%) and 3 (5 w/w%) with 5% cross-linker presence.

4.3.4 Controlled-release testing of coated and uncoated KNO_3 and MAP fertilizers by solution rate determination

Analysis of controlled-release fertilizers generally occurs in soil-based media that are evaluated continuously, or post-release by either fertilizer content determination or analysing the soil or surrounding environment.[19, 79] Analysis of the soil and coated pellets are done by various methods such as conductance measurement or mass difference of the soil, as well as mass difference or UV-vis analysis of the pellets after solution.[19, 90] Generally, the release of controlled-release fertilizer in the soil is carried out over weeks and even moths due to the near-identical conditions to that in agricultural application. However, due to time constraints and additional factors that influence soil release rates, such as soil pH, -water percentage and -composition,[78, 90] the release of coated pellets was done in an aqueous solution and analysed by conductance measurements in this study.

Analysis of the samples showed the formation of initial spikes in conductance values, however, the initial conductance values stabilized over time, hence the gradient of the conductance graph obtained was used in accordance with the final value, defined as the point at which plateauing was observed. The conductance values prior to plateauing followed a steady linear path until a sharp gradient change occurred. This point was made to be the endpoint of the analysis, due to all the following conductional changes being due to the equilibrium settling in the solution mixture.

Analysis of KNO_3 and MAP fertilizers with an uncoated sample served as a reference to single-layered coatings of all the proposed cross-linkers and multiple-layered coatings of selected coatings. Single-layered coatings were analysed with an uncross-linked PAA coated sample serving as a reference, while 5 w/w% coating masses containing 5% cross-linker presence were applied of the linear diols (**1**-**10**), glycerol (**12**-**14**) and EGDM (**11**). Multiple-layered coatings were applied by the addition of a 2 w/w% first coat, 2 w/w% second coat and finally a 1 w/w% third coating, which added together resembled that of single-layered coatings, however, applied systematically.

From the single-layered coating analyses shown in Figure 4.8, it became apparent that the coatings applied all had a relatively small slowing effect on the release rate of KNO_3 apart from the **1** & **2** ester mixture. The time of plateau occurred at lower values for all cross-linkers employed apart from the **1** & **2** and **7** & **8** ester mixtures, however, the gradients prior to plateauing were all below that of the uncoated sample, with the **1** & **2** ester mixture nearly identical to the uncoated sample, thus illustrating a degree of slowed solution.

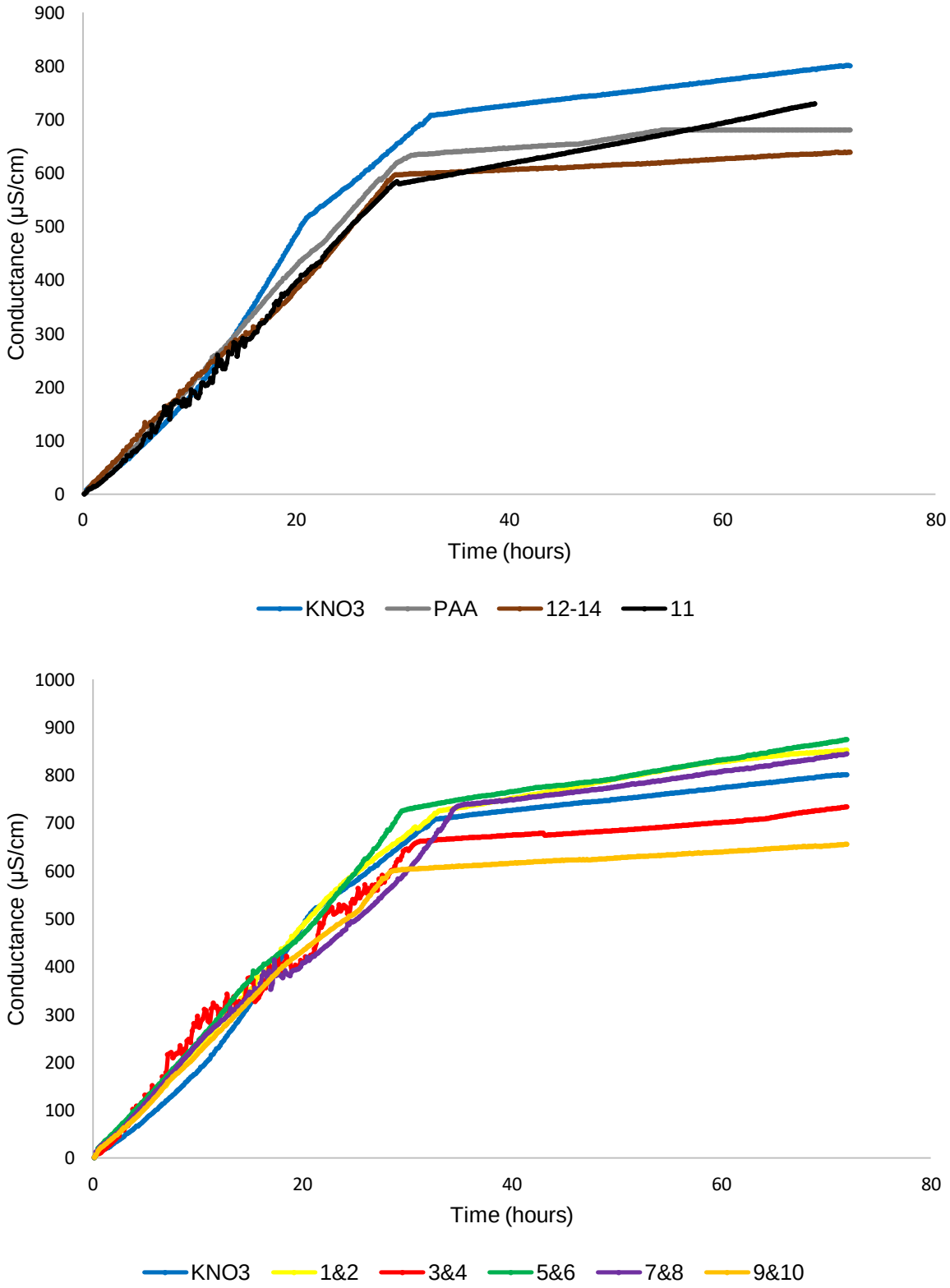

Figure 4.8 Single-layer 5 w/w%, 5% cross-linker presence, coating analysis of KNO_3 fertilizer coated with uncross-linked and cross-linked PAA samples. The uncross-linked PAA, **12**-**14** and ethylene glycol dimethacrylate cross-linked (above) and linear ester mixtures (below) are compared to the solution rate of uncoated KNO_3.

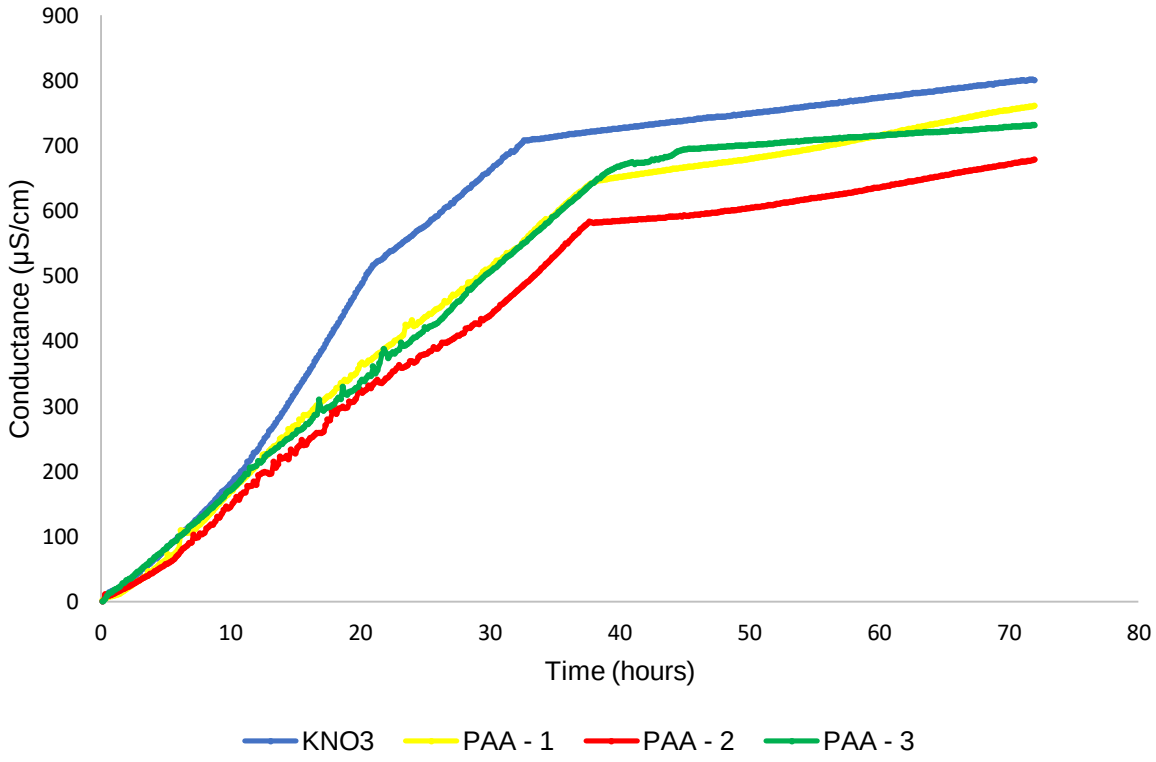

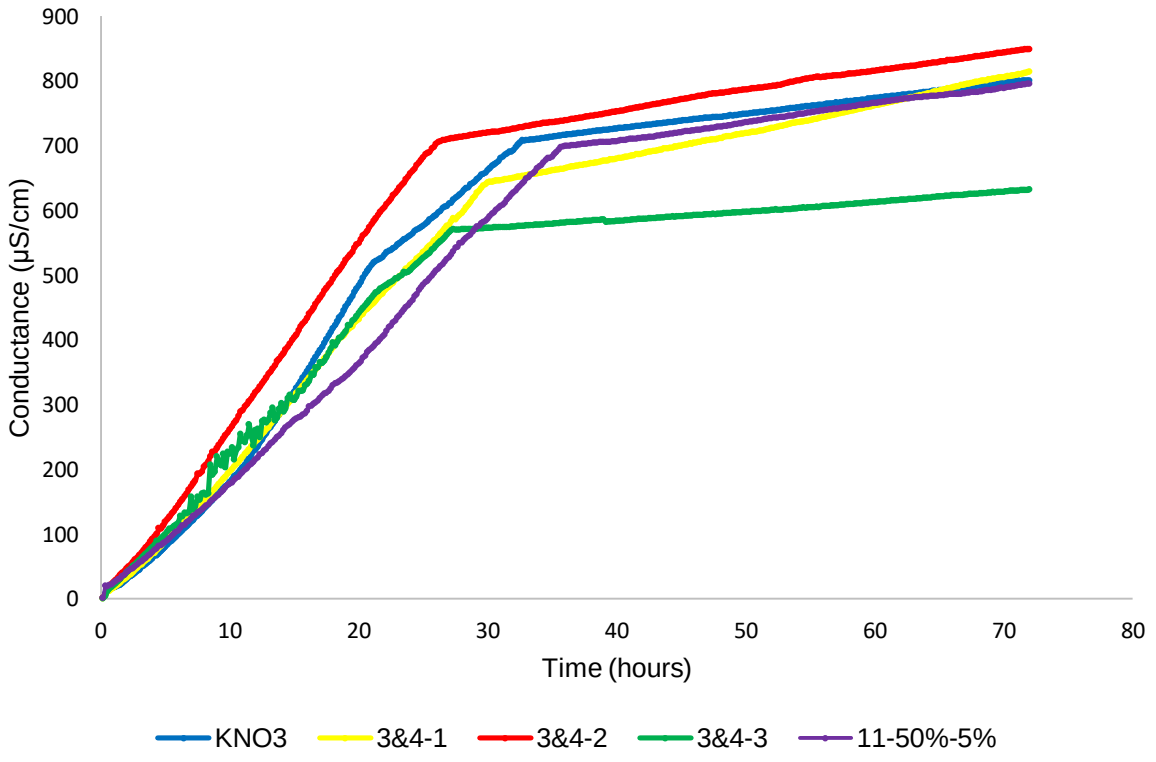

Figure 4.9 Multiple-layered coating of KNO_3 fertilizer with uncross-linked and cross-linked PAA. The uncross-linked multiple layered PAA coatings (above) and cross-linked multiple layered PAA coatings (below) are compared to the solution rate of uncoated KNO_3. The layers applied: 1 (2 w/w%), 2 (4 w/w%) and 3 (5 w/w%) were 5% cross-linked for all samples except 11-50%-5%.

From the analysis of the single layer coatings and multiple layer coatings applied to KNO_3, the times and conductance values at the point of plateau and the initial slopes, determined over the first 24 hours, are tabulated in Table 4.2 and Table 4.3, respectively.

Table 4.2 Solution analysis of KNO_3 and single-layer coated KNO_3, with initial gradient, endpoint time and conductance values.

	KNO_3	PAA	**1** & **2**	**3** & **4**	**5** & **6**	**7** & **8**	**9** & **10**	**12**-**14**	**11**
Time (h)	32.8	30.8	33.2	30.7	29.7	34.3	28.8	29.8	29.3
Conductance (µS/cm)	708	597	727	655	726	732	599	597	581
Gradient (24h)	25.4	21.7	24.7	21.3	23.4	19.8	21.4	18.9	20.2

The **7** & **8** ester mixture maintained a lower gradient than that of the uncoated sample, thus being unaffected by the higher ionic content than the uncoated sample. The smallest gradient and the longest time until a plateau were obtained from the **7** & **8** ester mixture, closely matched by **11** and **12-14** in gradient, however, plateauing occurred earlier.

Table 4.3 Solution analysis of KNO_3 and multiple-layer coated KNO_3, with initial gradient, endpoint time and conductance values. The multiple-layered coatings applied are a **11** 50% and 5% cross-linked double-layered, PAA and **3** & **4** ester mixture applied in the number of layers as indicated. The layers applied: 1 (2 w/w%), 2 (4 w/w%) and 3 (5 w/w%) are indicated as PAA-1, PAA-2, PAA-3 and **3**&**4**-1, **3**&**4**-2, **3**&**4**-3, that respectively correspond to the first, second and third layers applied.

	KNO_3	PAA-1	PAA-2	PAA-3	**3**&**4**-1	**3**&**4**-2	**3**&**4**-3	**11** 50%
Time (h)	32,8	38.5	38,2	40	30	26,3	26,8	36
Conductance (µS/cm)	708	647	582	667	643	706	562	699
Gradient (24h)	25.4	18.8	16.5	17.1	22.3	28.2	21.9	18.6

From Figure 4.10, the endpoint conductance values of the single-layer coated samples varied greatly from that of the uncoated MAP sample, with only the **7** & **8** cross-linked polymer sample resulting in a shorter endpoint time.

This short time coupled with the low 598 µS/cm endpoint conductance value explained the lowered initial gradient, however, the **7** & **8** cross-linked polymer sample remained the best performer at reducing solution. A near-identical gradient was observed for the **3** & **4** single-layer cross-linked coating, however, opposed to that of **7** & **8** it had a significantly higher time of plateau, thus could be considered amongst the best performers for lowering solution rates. The variation in the plateauing height at the endpoint was most likely due to variations in the sample, such as mass or unreacted monomer. The multiple-layered coatings applied to MAP had much less of an effect on the solution of the coated fertilizer, as shown by Figure 4.11.

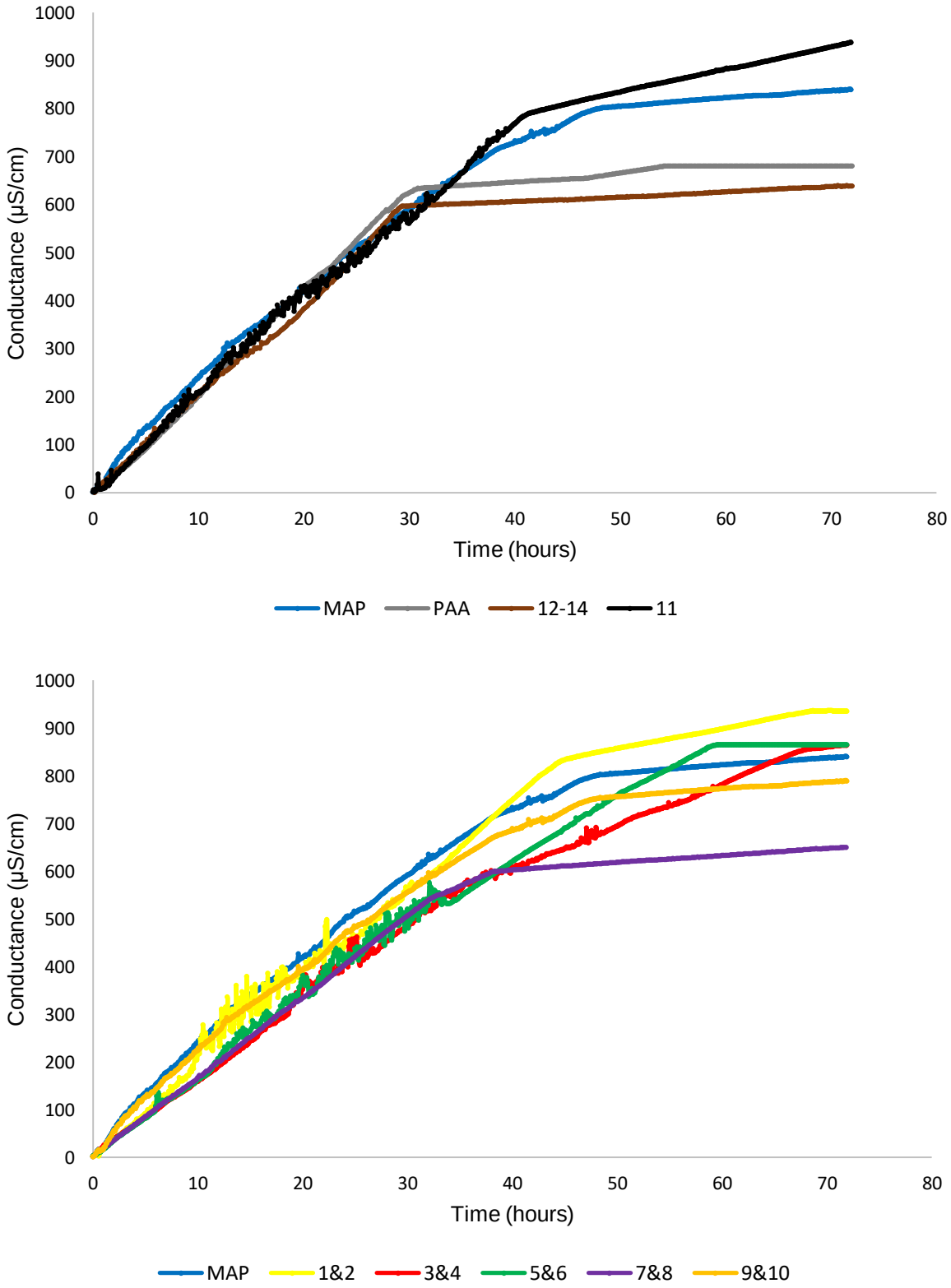

Figure 4.10 Single-layer 5 w/w% coating analysis of MAP fertilizer coated with uncross-linked and cross-linked PAA samples. The uncross-linked PAA, **12**-**14** and ethylene glycol dimethacrylate cross-linked (above) and linear ester mixtures (below) are compared to the solution rate of uncoated MAP.

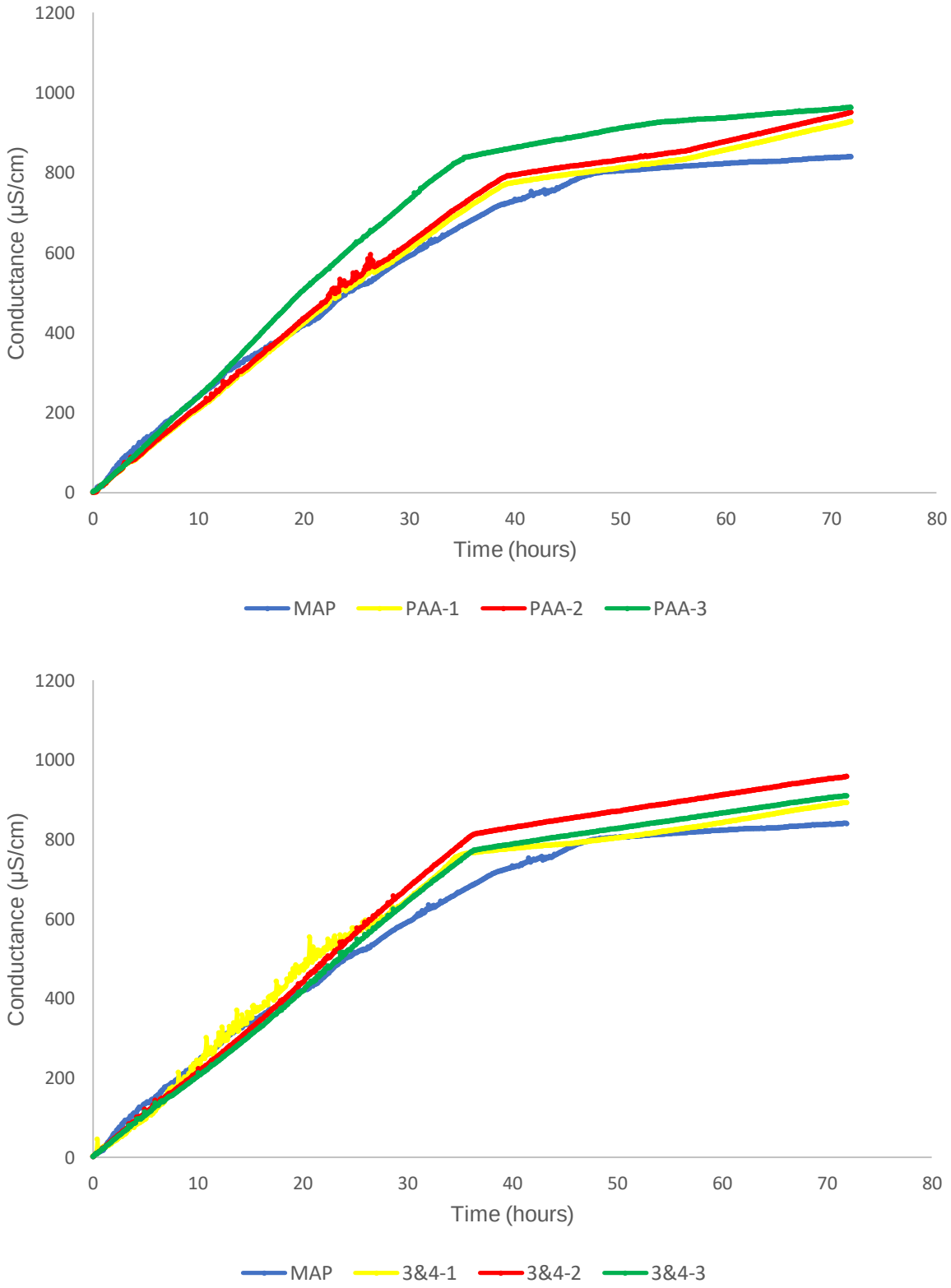

Figure 4.11 Multiple-layered coating of MAP fertilizer with uncross-linked and cross-linked PAA. The uncross-linked multiple layered PAA coatings (above) and cross-linked multiple layered PAA coatings (below) are compared to the solution rate of uncoated MAP. The cross-linker used is the **3** & **4** ester mixture. The layers applied are: 1 (2 w/w%), 2 (4 w/w%) and 3 (5 w/w%) were 5% cross-linked for all samples.

The uncoated MAP sample possessed the lowest gradient for the initial 24-hour period, with the multiple-layered samples all resulting in higher gradient values and shortened endpoint times. From the analysis of the single layer coatings and multiple layer coatings applied to MAP, the times and conductance values at the point of plateau and the initial slopes, determined over the first 24 hours, are tabulated in Table 4.4 and Table 4.5, respectively.

Table 4.4 Solution analysis of MAP and single-layer coated MAP, with initial gradient, endpoint time and conductance values.

	MAP	PAA	**1** & **2**	**3** & **4**	**5** & **6**	**7** & **8**	**9** & **10**	**12**-**14**	**11**
Time (h)	48.3	31	44.75	68.17	59.42	38.5	48.4	29,8	41.1
Conductance (µS/cm)	800	633	831	854	864	598	752	597	787
Gradient (24h)	19.9	21.7	19.9	17.0	17.8	16.7	18.7	18.9	20.7

None of the multiple-layered MAP coatings had slowing effects on the solution rate of the MAP fertilizer, as seen in Table 4.5. The endpoint times were all shorter than that of the uncoated reference sample and reached the endpoint in close proximity to one another. The endpoint conductance measurements were closely situated to 800 µS/cm, thus giving confirmation that the solution content did not show large deviation and thus not having as significant an effect on the gradient or endpoint time. The gradients of the multiple-layered coatings were, as a result, also higher than that of the uncoated sample, supporting its lack of effect on the solution rate. The multiple-layered application of the **3** & **4** cross-linked coating did show a successive decrease in the gradient with an increased number of coatings.

Table 4.5 Solution analysis of MAP and multiple-layer coated MAP, with initial gradient, endpoint time and conductance values. The multiple-layered coatings applied are PAA and **3** & **4** ester mixture applied in the number of layers as indicated. The layers applied: 1 (2 w/w%), 2 (4 w/w%) and 3 (5 w/w%) are indicated as PAA-1, PAA-2, PAA-3 and **3**&**4**-1, **3**&**4**-2, **3**&**4**-3, that respectively correspond to the first, second and third layers applied.

	MAP	PAA-1	PAA-2	PAA-3	**3**&**4**-1	**3**&**4**-2	**3**&**4**-3
Time (h)	48.3	40.3	39.4	35.4	34.1	36.7	36.3
Conductance (µS/cm)	800	776	792	838	766	814	772
Gradient (24h)	19.9	21.3	21.8	25.5	24.3	22.1	21.0

From the observed solution trends it became apparent that despite the application being flawed, decreased rates of solution were observed and achievable, based primarily on a longer time required to reach the endpoint and lowering of the initial conductance change over time. The reason being that the polymer applied was expected to have a lowered interaction with the surrounding water than the fertilizer surface. Lowered water-interaction by the polymer leads to the physical barrier formation described by Shaviv and Mikkelsen,[3] that should theoretically show a delayed initial release, a lowered gradient and a longer time required until plateauing or reaching the endpoint. Some of the coated fertilizer pellets did show a reduced rate of solution, however, no direct correlation between the time until plateau and the gradient prior to plateauing could be made, and the solution test values varied greatly.

The best-perfoming coating was that of a single-layer coating of 5%, **7** & **8** ester mixture cross-linked polymer. Multiple-layered coating of uncross-linked PAA showed promise when coating KNO_3, however, proved ineffective at slowing the rate of release of MAP. These variations in performance could be ascribed to variation in and ineffective coating, however, the similarly cross-linked/uncross-linked polymers showed linear results. During analysis polymer removal from the fertilizer pellets was observed, which was due to the solubility and high affinity of the PAA polymer towards water, thus during the solution of the coated fertilizers, a point was reached when polymer effects were completely negated.

This occurrence was attributed to the ineffective coating method or possible incomplete polymerization, resulting in low molar mass polymerization of the applied

monomer and cross-linker, also due to the coating method. The gradient of most applied coatings to KNO_3 fertilizer showed reduction and was thus seen as a successful attempt at slowing the rate of solution, however, the solution of MAP proved to only be effectively halted by the **7** & **8** ester mixture single-layered coating. Minute variations in the 1 g samples used for testing might account for the differences observed in the conductance values at the plateau. The shape and size of pellet batches vary greatly and in conjunction with coating variations, resulting from exposed surface area and varying coating thickness, accounted for the lessened effect of coating on the rate of release compared to uncoated fertilizers.

4.4 Conclusion

From the thermogravimetric analysis, it became apparent that cross-linkers employed in PAA matrices bring about thermal characteristic changes to the polymer, however, the amount of cross-linker employed had little to no additional effect. From this it can be deduced that the polymer is reacting to the presence of the cross-linker, however, varying cross-linker presence does not bring about expected thermogravimetric characteristic changes, due to the cross-linkers employed varying greatly. Changes in cross-linkers were expected to show decreased solvent absorption with increased cross-linking, shifts in the thermal degradation steps or glass transitional steps being introduced, which were not observed. The thermal degradation steps followed that of uncross-linked PAA closely and showed no significant deviation from the reference polymer, apart from the initial solvent loss that occurs prior to degradation.

SEM investigation of the coated KNO_3 fertilizers, with uncoated coated pellets serving as a reference, were applicable for surface coverage and coating thickness investigation. However, the investigation of the surface areas showed that insufficient coverage occurred from the amount of fertilizer applied.[89] The most prominent problem being that the pellets were not kept moving similar to granulators, and that fertilizer pellets came into contact with one another and provided collecting points for the polymer instead of distributing evenly. Limited time did not allow for reproducing industry coating methods, however, the use of industry coating methods were not used due to the cost and scale involved, and was not practical in this study. Due to environmental effects and coating efficacy being the most important effects on the release rate, in this study the environmental effects were minimized and excluded by standardized and repeatable solution testing, however, incomplete surface coverage was the largest contributor to the ineffective control of the coating on the fertilizer's rate of release.

Moisture absorbance showed an overall decrease in absorbance once fertilizers were coated with single-layers or multiple-layers, thus supporting the expected effect brought about by an applied coating. However, some coatings brought about an increased moisture absorption, which was to be expected due to the super absorbent nature of the PAA used. However, an increased moisture absorption did not indicate

the applied coating's inability to serve as a physical barrier and still maintained a controlled rate of release. From the moisture absorbance values obtained, the effect of efficient coating became apparent due to cross-linker variation having less of an effect than the application of a second or third layer. The best coating according to lower absorbance values was that of the **7** & **8** cross-linked polymer coating, which correlates exactly with the solution analyses.

The effect of the cross-linker on the polymer and the method of application had a significant effect on the polymer's ability to serve as coating and to promote controlled-release. The cross-linker had little effect on the thermogravimetric characteristics of the PAA polymer, thus limiting its effectiveness as a cross-linked mesh-like structure capable of enveloping the pellets. Thus, the limited cross-linking effect decreased the ability of the polymer to adhere to the fertilizer surface and form a physical barrier. A lack of a physical barrier, as shown in the literature, or the ineffective application thereof leads to an unaltered solution rate. The cross-linked polymers employed showed a limited effect on the rate of release, however, the single-layered **7** & **8** ester mixture had the greatest effect of the cross-linkers applied, with limited success also shown from multiple-layered PAA application to KNO_3. Variations were present and caused deviation from expected trends such as an increased endpoint time with that of a decreased initial gradient, and vice versa.

Chapter 5

Conclusions and Recommendations

5.1 Conclusions

In this study investigation into and synthesis of polyacrylic acid (PAA) cross-linkers from esterification products of linear diols and glycerol and acrylic acid (AA) for industrial synthesis was conducted. The application as potential cross-linked PAA fertilizer coatings to facilitate controlled-release has proved beneficial in clarifying such a potential application. The use of these PAA cross-linkers aids in understanding the esterification and cross-linking effect of the products on PAA, and its effect when employed as a fertilizer coating. The aim of the research work was to synthesize the di-ester products of the linear diols and glycerol with AA esterification reactions under milder conditions and without the need for reagent activation, followed by isolation, characterisation and quantification of the products. The products were subsequently used for cross-linking evaluation under ideal conditions and as a potential controlled-release coating for KNO_3 and monoammonium phosphate (MAP) fertilizers.

From the objectives stated in Chapter 1, conclusions to the stated objectives are as follows:

1. The esterification of linear diols and glycerol with AA occurred with marginal success, determined by product mixture yields and ester mixture composition. Isolation of the di-ester products from mono-ester and by-products formed proved difficult and was most effective by washing with a $NaHCO_3$ aqueous solution, which removed by-products without affecting the planned products. The characterisation of the obtained ester product mixtures was done by using Fourier Transform Infra-Red (FTIR), Atmospheric Pressure Chemical Ionization Mass Spectroscopy (APCI-MS)

and Nuclear Magnetic Resonance (NMR) techniques for qualitative product identification. The ester product mixtures were used as obtained following esterification and quantified via NMR spectroscopy by identification of mono-ester and di-ester specific signals in ^{1}H-NMR spectra. The ester product formation favoured the mono-ester and replications of the synthesis showed similar trends for all linear diols with few exceptions of larger mono-ester to di-ester ratios. Quantification of the glycerol ester mixtures was not possible and deemed inaccurate due to ineffective separation by methods available and the inability for distinct quantifiable signals in NMR spectra.

2. Optimization changes made to reaction conditions made an insignificant difference to the formation of multiple ester products, with mono-ester products being the predominant product formed. Reaction times were varied to determine its effect on product formation, however, no significant changes occurred A set reaction time of three hours was thus established and used in all subsequent reactions. The effect of the B-23 Amberlyst and $Al(OSO_2CF_3)_3$ catalyst on product formation was evaluated and based on yield and ease of use; the B-23 Amberlyst catalysed reactions were subsequently performed. Molar ratio variations were extensively implemented to determine the effect of varying molar ratios of AA relative to linear diols and glycerol. However, little effect thereof was observed, and an economically viable and non-wasteful 1:5 alcohol-to-AA molar ratio was used. Solvent variation influenced reaction temperature changes due to the implementation of Dean-Stark reflux removal of the water formed during esterification. The effect of non-benzene solvents only proved to promote polymerization upon removal of solvents following synthesis. Thus benzene was used at a reflux temperature of 95 °C for all reactions.

3. Cross-linker application in PAA had varying degrees of success, with the thermogravimetric analysis of varying cross-linker percentages showing an initial effect upon the introduction of the cross-linker ester mixture. However, from the investigation made by varying the cross-linker percentage, it had little to no additional effect. Thus, the effect of the cross-linkers is potentially only structural with a limited amount of cross-linking brought about by the lack of di-ester compounds present in

the cross-linker mixtures. Moisture absorption showed a predominantly reduced amount of water absorbance by fertilizers coated with any coating. The degree and linear relationship regarding the type of cross-linker and its effect could, however not be established. The lessening of water absorbance was taken as an improved effect on the controlled-release potential of the coated fertilizer. Scanning Electron Microscopy (SEM) analysis of coated KNO_3 samples showed an irregular and ineffective coating process, with uneven coating thickness across the surface of the applied polymer and exposed fertilizer surfaces clearly observed. The effect of multiple-layered coatings was observed to stack atop of one another, and the different layers could be observed. The effectivity of the application process is attributed to being the main influence on ineffective coverage and results in ineffective controlled-release.

4. Solution testing of the coated fertilizer samples showed varied effects on the solution rate during the initial 24 hours and also the time to reach the endpoint. The most effective coating proved that of a single-layer **7** & **8** product ester cross-linked polymer. This application showed significant decreases in the initial rate of increased conductivity and also lengthened the time until plateauing of conductance values. Multiple-layered coatings of PAA had a significant impact on decreasing the solution rate of coated KNO_3, however, showed little to no effect when applied to MAP. The comparison of initial rates to that of the time until plateauing was not always proportional. The comparison depended on the endpoint conductance value of the batch analysed, however, with a decreased initial rate of release a longer time was expected for the reaction to reach the endpoint. From the investigation made into the effect of the cross-linker on the polymer used as a coating for controlled-release, it is unclear if programmed controlled-release is possible. Thus the cross-linkers synthesized and employed in this study would require further investigation.

5.2 Recommendations

Based on the results obtained from this study, the following recommendations are made for future research endeavours:

1. The selective synthesis of the required di-ester, due to cross-linking ability, from linear diols was not possible under the mild conditions proposed in this study. The altered reaction for increased selectivity and increased product yield must be employed and investigated. Activation of the reagents is required for increased esterification and the selection of specific products such as the di-ester product. A proposed method is acrylic anhydride formation or procurement for esterification, based on a test reaction used to identify the tri-ester of glycerol. The investigation was done using acetic anhydride and formed, following esterification, primarily the tri-ester product. Thus, anhydrides could potentially be used for esterification of acrylic anhydride with linear diols and glycerol. Other methods of acrylic acid activation are possible by acryloyl chloride formation and subsequent implementation for esterification, which should potentially result in increased product formation and improved product selection.

2. Batch esterification is a possible alternative that could serve to obtain the required di-ester and tri-ester products. The avoidance of washing by performing batch esterification reactions is an option to negate the removal of products following synthesis. Batch esterification is done by undergoing esterification under conditions of AA excess, while the esterification reaction will form the required product and remain in sufficient quantity to serve for polymerization application. By employing said reaction, an increased ease of industrial application is achieved, and steps involved from synthesis to application are lessened.

3. Increased product formation and specific product formation would negate or limit the need for product isolation and purification. A more effective separation method must be identified, which would allow accurate product quantification and make pure product testing possible. A proposed method is GC analysis utilizing analysis conditions that do not induce polymerization. High-performance liquid chromatography separation of ester compounds could be used for qualitative and quantitative analysis of the ester composition of the product mixtures.

4. An industrially similar method of coating must be used to ensure better control of the coating process to ensure no exposed surfaces on the fertilizer and to ensure a uniform coating thickness. Such a coating process is possible with an industrial granulizer suited to match the coating conditions required in this study. Such equipment and processes already exist and could be enlisted to ensure improved coating.

5. The solution testing method used in this study must be evaluated by using fertilizer pellets proven to possess the controlled-release ability. It is necessary for setting a benchmark to determine the correlation between deionised water solution and soil-based solution testing. An alternative method includes the analysis of future controlled-release coated fertilizers similar to the literature soil based solution methods.

References

1. Tilman, D.; Cassman, K. G.; Matson, P. A.; Naylor, R.; Polasky, S., Agricultural sustainability and intensive production practices. *Nature* **2002,** *418*, 671-7.
2. Flieger, M.; Kantorova, M.; Prell, A.; Rezanka, T.; Votruba, J., Biodegradable plastics from renewable sources. *Folia Microbiol (Praha)* **2003,** *48*, 27-44.
3. Shaviv, A.; Mikkelsen, R. L., Controlled-Release Fertilizers to Increase Efficiency of Nutrient Use and Minimize Environmental Degradation - a Review. *Fertilizer Research* **1993,** *35*, 1-12.
4. Rodriguez, E.; Sultan, R.; Hilliker, A., Negative effects of agriculture on our environment. *The Traprock* **2004,** *3*, 28-32.
5. Shavit, U.; Shaviv, A.; Shalit, G.; Zaslavsky, D., Release characteristics of a new controlled release fertilizer. *Journal of Controlled Release* **1997,** *43*, 131-138.
6. Boyd, C. E., Solubility of granular inorganic fertilizers for fish ponds. *Transactions of the American Fisheries Society* **1981,** *110*, 451-454.
7. Thawornchaisit, U.; Polprasert, C., Evaluation of phosphate fertilizers for the stabilization of cadmium in highly contaminated soils. *Journal of Hazardous Materials* **2009,** *165*, 1109-13.
8. Maeda, M.; Zhao, B.; Ozaki, Y.; Yoneyama, T., Nitrate leaching in an Andisol treated with different types of fertilizers. *Environmental Pollutantion,* **2003,** *121*, 477-87.
9. Arora, Y.; Juo, A., Leaching of Fertilizer Ions in a Kaolinitic Ultisol in the High Rainfall Tropics: Leaching of Nitrate in Field Plots under Cropping and Bare Fallow 1. *Soil Science Society of America Journal* **1982,** *46*, 1212-1218.
10. Mikkelsen, R. L., Using Hydrophilic Polymers to Control Nutrient Release. *Fertilizer Research* **1994,** *38*, 53-59.
11. Jarosiewicz, A.; Tomaszewska, M., Controlled-release NPK fertilizer encapsulated by polymeric membranes. *Journal of Agricultural and Food Chemistry* **2003,** *51*, 413-417.

12. Bortoletto-Santos, R.; Ribeiro, C.; Polito, W. L., Controlled release of nitrogen-source fertilizers by natural-oil-based poly (urethane) coatings: The kinetic aspects of urea release. *Journal of Applied Polymer Science* **2016,** *133,* 1-8.
13. Goertz, H. M. In *Technology developments in coated fertilizers*, Proceedings: Dahlia Greidinger Memorial International Workshop on Controlled/Slow Release Fertilizers, Technion-Israel Institute of Technology, Haifa, **1993**; pp 7-12.
14. Herron, C. M.; Dean, W. L., Individualized cellulosic fibers crosslinked with polyacrylic acid polymers. US Patent 5549791, **1996**.
15. Mohammed, A. D. Synthesis and characterisation of high performance flocculants and superabsorbents from chemically modified starch and glycerol. PhD Thesis, North West University, **2015**.
16. Wiederkehr, H. In *Examples of process improvements in the fine chemicals industry*, Tenth International Symposium on Chemical Reaction Engineering, **1988**; pp 1783-1791.
17. Cauich-Rodriguez, J. V.; Deb, S.; Smith, R., Effect of cross-linking agents on the dynamic mechanical properties of hydrogel blends of poly(acrylic acid)-poly(vinyl alcohol-vinyl acetate). *Biomaterials* **1996,** *17*, 2259-64.
18. Ha, H.; Shanmuganathan, K.; Ellison, C. J., Mechanically stable thermally crosslinked poly (acrylic acid)/reduced graphene oxide aerogels. *ACS Applied Materials & Interfaces* **2015,** *7*, 6220-6229.
19. Huett, D. O.; Gogel, B. J., Longevities and nitrogen, phosphorus, and potassium release patterns of polymer-coated controlled-release fertilizers at 30 degrees C and 40 degrees C. *Communications in Soil Science and Plant Analysis* **2000,** *31*, 959-973.
20. Chmelir, M., Cross-linked synthetic polymers having a porous structure, a high absorption rate for water, aqueous solutions and body fluids, a process for their production and their use in the absorption and/or retention of water and/or aqueous liquids. US Patent 5856370, **1999**.
21. Hart, M. R.; Quin, B. F.; Nguyen, M. L., Phosphorus runoff from agricultural land and direct fertilizer effects: a review. *Journal of Environmental Quality* **2004,** *33*, 1954-72.

22. Long, S. P.; Marshall-Colon, A.; Zhu, X.-G., Meeting the global food demand of the future by engineering crop photosynthesis and yield potential. *Cell,* **2015,** *161*, 56-66.
23. Kanno, S. S. H., Use of polyolefin-coated fertilizers for increasing fertilizer efficiency and reducing nitrate leaching and nitrous oxide emissions, *Fertilizer Research*, **1994**, 2, 147-152.
24. Shaviv, A.; Mikkelsen, R., Controlled-release fertilizers to increase efficiency of nutrient use and minimize environmental degradation-A review. *Fertilizer Research* **1993,** *35*, 1-12.
25. York, U. O. Fertilizers. http://www.essentialchemicalindustry.org/materials-and-applications/fertilizers.html (accessed 2018/01/25).
26. Bergström, L.; Brink, N., Effects of differentiated applications of fertilizer N on leaching losses and distribution of inorganic N in the soil. *Plant and Soil* **1986,** *93*, 333-345.
27. Conijn, J.; Bindraban, P.; Schröder, J.; Jongschaap, R., Can our global food system meet food demand within planetary boundaries? *Agriculture, Ecosystems & Environment,* **2018,** *251*, 244-256.
28. Kleinman, P. J.; Sharpley, A. N.; Moyer, B. G.; Elwinger, G. F., Effect of mineral and manure phosphorus sources on runoff phosphorus. *Journal of Environmental Quality* **2002,** *31*, 2026-33.
29. Ward, R. C. What is fertilizer other than nutrients? http://www.sdnotill.com/Newsletters/Fertilizer.pdf, (accessed 2018/04/03).
30. CropNutrition, Mosaic. Potassium Nitrate. https://www.cropnutrition.com/potassium-nitrate (accessed 2019/02/25).
31. Del Pilar Cordovilla, M.; Ligero, F.; Lluch, C., Effects of NaCl on growth and nitrogen fixation and assimilation of inoculated and KNO3 fertilized Vicia faba L. and Pisum sativum L. plants. *Plant Science* **1999,** *140*, 127-136.
32. Broschat, T. K., Nitrate, Phosphate, and Potassium Leaching from Container-Grown Plants Fertilized by Several Methods. *Hortscience* **1995,** *30*, 74-77.
33. Nutrition, M.-C. Monoammonium Phosphate. https://www.cropnutrition.com/monoammonium-phosphate (accessed 2019/02/25).

34. Drew, M. C., Comparison of the Effects of a Localised Supply of Phosphate, Nitrate, Ammonium and Potassium on the Growth of the Seminal Root System, and the Shoot, in Barley. *New Phytologist* **1975,** *75*, 479-490.
35. Effect of chicken compost or ammonium phosphate and solarization on pathogen control, rhizosphere microorganisms, and lettuce growth. *Plant Diseases,* **1993** *77,* 886-891.
36. Wiedenhoeft, A. C., *Plant nutrition*. Infobase Publishing. Chelsea House Publishers: **2006**.
37. Baligar, V.; Bennett, O., NPK-fertilizer efficiency—a situation analysis for the tropics. *Fertilizer Research* **1986,** *10*, 147-164.
38. Shoji, S.; Delgado, J.; Mosier, A.; Miura, Y., Use of Controlled Release Fertilizers and Nitrification Inhibitors to Increase Nitrogen Use Efficiency and to Conserve Air Andwater Quality. *Communications in Soil Science and Plant Analysis* **2007,** *32*, 1051-1070.
39. Hanafi, M. M.; Eltaib, S. M.; Ahmad, M. B., Physical and chemical characteristics of controlled release compound fertiliser. *European Polymer Journal* **2000,** *36*, 2081-2088.
40. Liang, R.; Liu, M., Preparation and properties of a double-coated slow-release and water-retention urea fertilizer. *Journal of Agricultural and Food Chemistry* **2006,** *54*, 1392-8.
41. Ni, B.; Liu, M.; Lü, S., Multifunctional slow-release urea fertilizer from ethylcellulose and superabsorbent coated formulations. *Chemical Engineering Journal* **2009,** *155*, 892-898.
42. Cleaver, G., Biodegradable Polymers. Agilent Technologies, I., Ed. Agilent Technologies: USA, **2015,** https://www.agilent.com/cs/library/applications/US5990-6920EN.pdf, (accessed 2019/02/24).
43. Saotome K., Process for improving awater absorbent polyacrylic acd polymer and an improved polymer produced by said process. US Patent 4783510, **1988**.
44. Sonenstein, G. G., Water soluble films of polyvinyl alcohol and polyacrylic acid and packages comprising same. US Patent 4692494, **1987**.

45. Azeem, B.; KuShaari, K.; Man, Z. B.; Basit, A.; Thanh, T. H., Review on materials & methods to produce controlled release coated urea fertilizer. *Journal of Controlled Release* **2014,** *181*, 11-21.
46. J.R. Witono, I. W. N., H.J. Heeres, L.P.B.M. Janssen, Water absorption, retention and the swelling characteristics of cassava starch grafted with polyacrylic acid**,** *Carbohydrate Polymers*, **2013**, 103, 325-332
47. Elliott, J. E.; Macdonald, M.; Nie, J.; Bowman, C. N., Structure and swelling of poly(acrylic acid) hydrogels: effect of pH, ionic strength, and dilution on the crosslinked polymer structure. *Polymer,* **2004,** *45*, 1503-1510.
48. He, S.; Yaszemski, M. J.; Yasko, A. W.; Engel, P. S.; Mikos, A. G., Injectable biodegradable polymer composites based on poly(propylene fumarate) crosslinked with poly(ethylene glycol)-dimethacrylate. *Biomaterials* **2000,** *21*, 2389-94.
49. Choi, J.; Kwak, S. Y.; Kang, S.; Lee, S. S.; Park, M.; Lim, S.; Kim, J.; Choe, C. R.; Hong, S. I., Synthesis of highly crosslinked monodisperse polymer particles: Effect of reaction parameters on the size and size distribution. *Journal of Polymer Science Part a-Polymer Chemistry* **2002,** *40*, 4368-4377.
50. Ju, H.; McCloskey, B. D.; Sagle, A. C.; Kusuma, V. A.; Freeman, B. D., Preparation and characterization of crosslinked poly(ethylene glycol) diacrylate hydrogels as fouling-resistant membrane coating materials. *Journal of Membrane Science* **2009,** *330*, 180-188.
51. Kricheldorf, N. S., *Handbook of Polymer Synthesis*. 2nd ed., CRC Press, ISBN 9780824754730, **2005**.
52. Olson, D. A.; Sheares, V. V., Preparation of unsaturated linear aliphatic polyesters using condensation polymerization. *Macromolecules* **2006,** *39*, 2808-2814.
53. Pfeifer, C. S.; Shelton, Z. R.; Braga, R. R.; Windmoller, D.; Machado, J. C.; Stansbury, J. W., Characterization of dimethacrylate polymeric networks: A study of the crosslinked structure formed by monomers used in dental composites. *European Polymer Journal* **2011,** *47*, 162-170.

54. Mota, C. J.; Silva, C. X. d.; Gonçalves, V. L., Gliceroquímica: novos produtos e processos a partir da glicerina de produção de biodiesel.. *Química Nova* **2009,** *32*, 639-648.
55. Knothe, G.; van-Gerpen, J.; Pereira, L.; Krahl, J., *Manual de biodiesel*. 978-85-212-0405-3, São Paulo (Brasil). **2006**. 340
56. Wang, Z. X.; Zhuge, J.; Fang, H.; Prior, B. A., Glycerol production by microbial fermentation: a review. *Biotechnology Advances* **2001,** *19*, 201-223.
57. Hansen, A. C.; Zhang, Q.; Lyne, P. W., Ethanol-diesel fuel blends - a review. *Bioresource Technology* **2005,** *96*, 277-85.
58. Janigova, I.; Lacik, I.; Chodak, I., Thermal degradation of plasticized poly(3-hydroxybutyrate) investigated by DSC. *Polymer Degradation and Stability* **2002,** *77*, 35-41.
59. Zhou, C. H. C.; Beltramini, J. N.; Fan, Y. X.; Lu, G. Q. M., Chemoselective catalytic conversion of glycerol as a biorenewable source to valuable commodity chemicals. *Chemical Society Reviews* **2008,** *37*, 527-549.
60. Greenberg, A.; Kusy, R., Influence of crosslinking on the glass transition of poly (acrylic acid). *Journal of Applied Polymer Science* **1980,** *25*, 1785-1788.
61. Morita, R. Y., Síntese de acrilatos de glicerina e aplicação como agente de reticulação para obtenção decopolímeros com metacrilato de metila, Brazil, Thesis, **2011**.
62. Neises, B.; Steglich, W., Simple method for the esterification of carboxylic acids. *Angewandte Chemie International Edition in English* **1978,** *17*, 522-524.
63. Iqbal, J.; Srivastava, R. R., Cobalt(Ii) Chloride Catalyzed Acylation of Alcohols with Acetic-Anhydride - Scope and Mechanism. *Journal of Organic Chemistry* **1992,** *57*, 2001-2007.
64. Bartoli, G.; Bosco, M.; Dalpozzo, R.; Marcantoni, E.; Massaccesi, M.; Sambri, L., Zn (ClO4) 2· 6H2O as a powerful catalyst for a practical acylation of alcohols with acid anhydrides. *European Journal of Organic Chemistry* **2003,** *2003*, 4611-4617.
65. Nemec, J.; Bauer Jr, W., Acrylic acid and derivatives. *Kirk-Othmer encyclopedia of chemical technology* **1978,** Wiley Online Library, 330-354.

66. Hajjar, A. B.; Nicks, P. F.; Knowles, C. J., Preparation of monomeric acrylic ester intermediates using lipase catalysed transesterifications in organic solvents. *Biotechnology letters* **1990,** *12*, 825-830.
67. Kautter, C. T.; Baumann, U.; Riemann, K. H., Esterification of acrylic acid. US Patent 3458561, **1969**.
68. Jan C.J. Bart, Stefano Cavallaro, Biodiesel Science and Technology, **2010**.
69. Canevarolo, J., SV Ciência dos Polímeros 2nd Edition, *Editora Artliber* **2006**.
70. RABELLO, M. Aditivação de Polímeros, Ed. Artliber LTDA, São Paulo, **2000,** p. 133.
71. Mano, E. B.; Mendes, L., Introdução a Polímeros, 2nd Edition. *Editora Edgard Blucher* **1999**.
72. Francis, L.; McCormick, A.; Vaessen, D.; Payne, J., Development and measurement of stress in polymer coatings. *Journal of Materials Science* **2002,** *37*, 4717-4731.
73. Okay, O., Macroporous copolymer networks. *Progress in Polymer Science* **2000,** *25*, 711-779.
74. Billmeyer, J. F. W., Textbook of polymer science. **1984**.
75. Marinho, J. R. D., *Macromoléculas e polímeros*. Manole: **2005**.
76. Coutinho, F.; Aponte, M. L.; Barbosa, C. C.; Costa, V. G.; Lachter, E. R.; Tabak, D., Resinas sulfônicas: síntese, caracterização e avaliação em reações de alquilação. *Polímeros: Ciência e Tecnologia,* **2003,** *13*.
77. Oertli, J.; Lunt, O., Controlled Release of Fertilizer Minerals by Incapsulating Membranes: I. Factors Influencing the Rate of Release 1. *Soil Science Society of America Journal* **1962,** *26*, 579-583.
78. Wu, L.; Liu, M. Z., Preparation and properties of chitosan-coated NPK compound fertilizer with controlled-release and water-retention. *Carbohydrate Polymers* **2008,** *72*, 240-247.
79. Moharram, M. A.; Khafagi, M. G., Thermal behavior of poly(acrylic acid)-poly(vinyl pyrrolidone) and poly(acrylic acid)-metal-poly(vinyl pyrrolidone) complexes. *Journal of Applied Polymer Science* **2006,** *102*, 4049-4057.

80. Fyfe, C.; McKinnon, M., Investigation of the thermal degradation of poly (acrylic acid) and poly (methacrylic acid) by high-resolution carbon-13 CP/MAS NMR spectroscopy. *Macromolecules* **1986,** *19*, 1909-1912.
81. Crompton, T., *Thermal methods of polymer analysis*. Smithers Rapra Publishers, **2013**.
82. Hamidi, M.; Azadi, A.; Rafiei, P., Hydrogel nanoparticles in drug delivery. *Advanced Drug Delivery Reviews* **2008,** *60*, 1638-49.
83. Katime, I.; de Apodaca, E. D.; Rodriguez, E., Effect of crosslinking concentration on mechanical and thermodynamic properties in acrylic acid-co-methyl methacrylate hydrogels. *Journal of Applied Polymer Science* **2006,** *102*, 4016-4022.
84. Mulder, W. J.; Gosselink, R. J. A.; Vingerhoeds, M. H.; Harmsen, P. F. H.; Eastham, D., Lignin based controlled release coatings. *Industrial Crops and Products* **2011,** *34*, 915-920.
85. Dave, A. M.; Mehta, M. H.; Aminabhavi, T. M.; Kulkarni, A. R.; Soppimath, K. S., A review on controlled release of nitrogen fertilizers through polymeric membrane devices. *Polymer-Plastics Technology and Engineering* **1999,** *38*, 675-711.
86. Detmer, O.; Mueller, H.; Seibt, H.; Jung, J., Method of preparing polymer coated fertilizer particles from a solvent free system and product. US Patent 3365288, **1968**.
87. Nakamura, Y. H. Y. Granular coated fertilizer and method for producing the same. US Patent 6231633, **2001**.
88. Du, C. W.; Zhou, J. M.; Shaviv, A., Release characteristics of nutrients from polymer-coated compound controlled release fertilizers. *Journal of Polymers and the Environment* **2006,** *14*, 223-230.
89. Oertli, J., Controlled-release fertilizers. *Fertilizer Research* **1980,** *1*, 103-123.

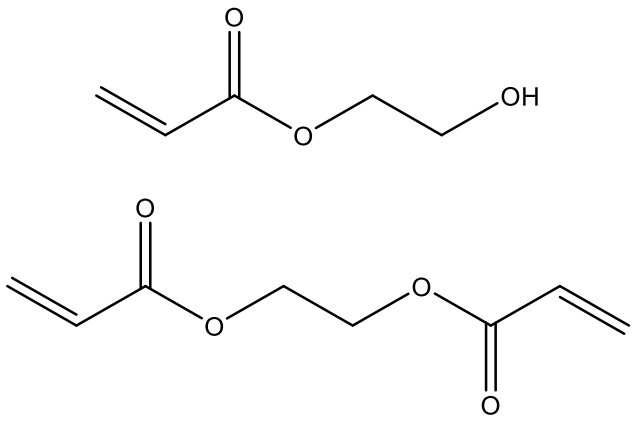

Figure S1: 1,2-ethanediol, mono-ester (**2**) and di-ester (**1**) product.

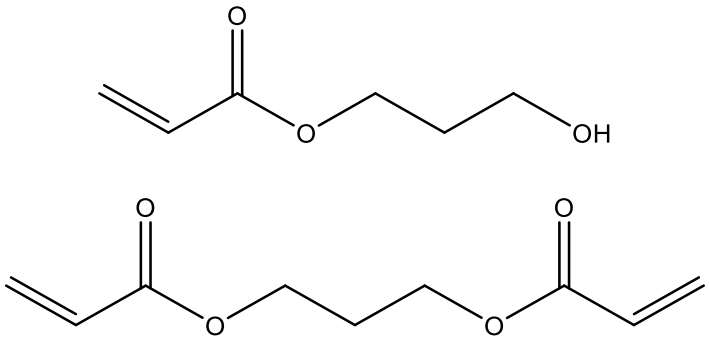

Figure S2: 1,3-propanediol, mono-ester (**4**) and di-ester (**3**) product.

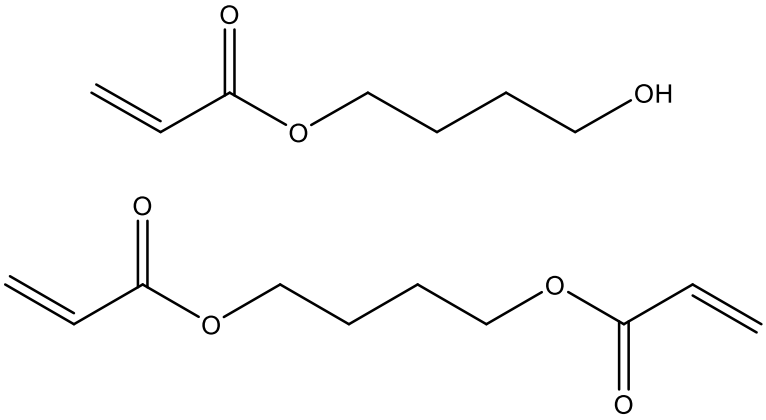

Figure S3: 1,4-butanediol, mono-ester (**6**) and di-ester (**5**) product.

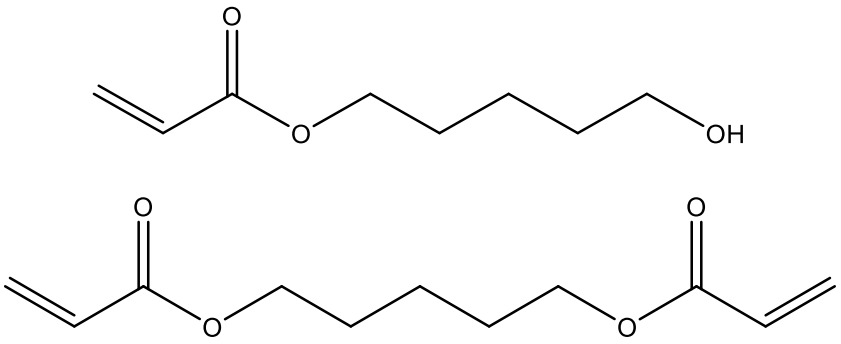

Figure S4: 1,5-pentanediol, mono-ester (**8**) and di-ester (**7**) product.

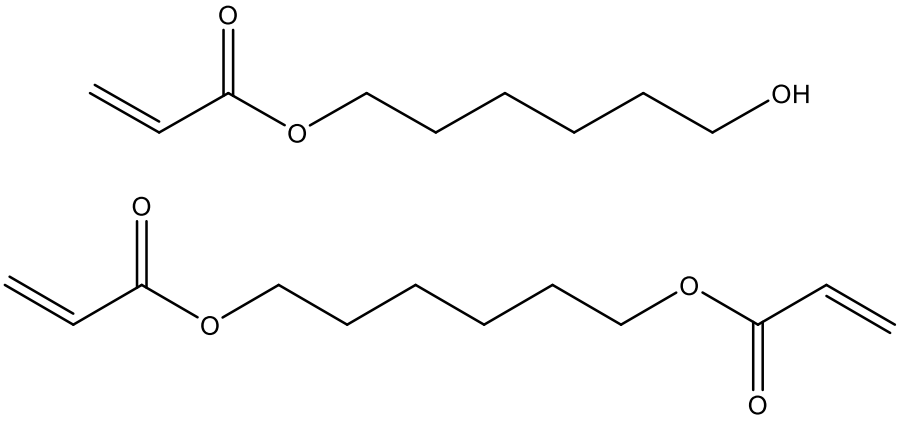

Figure S5: 1,6-hexanediol, mono-ester (**10**) and di-ester (**9**) product.

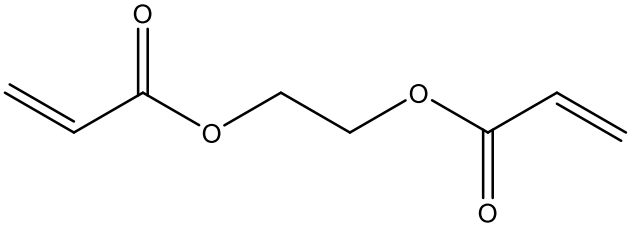

Figure S6: Ethylene glycol dimethacrylate (EGDM), reference di-ester **11**

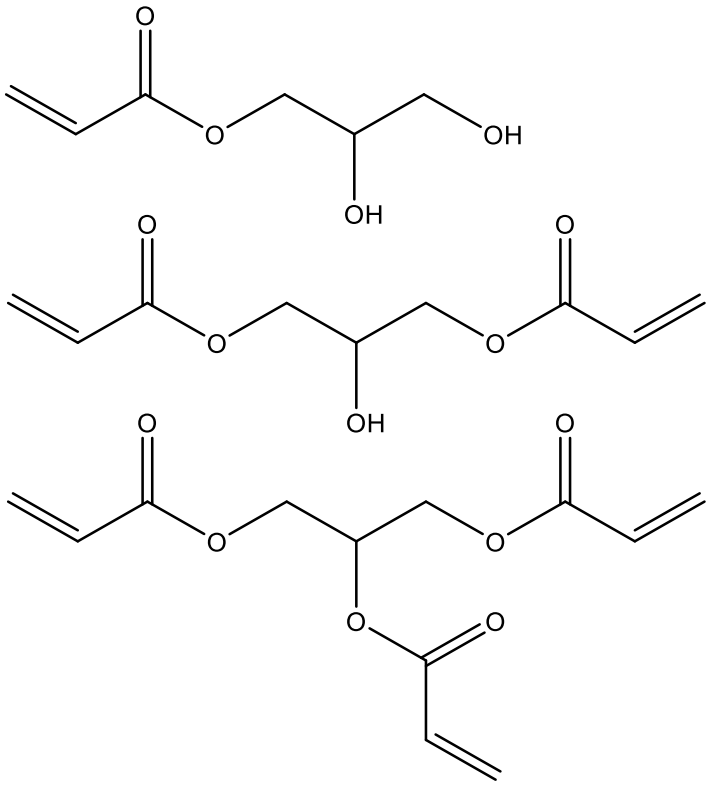

Figure S7: Glycerol mono-ester (**14**), di-ester (**13**) and tri-ester (**12**) products formed.

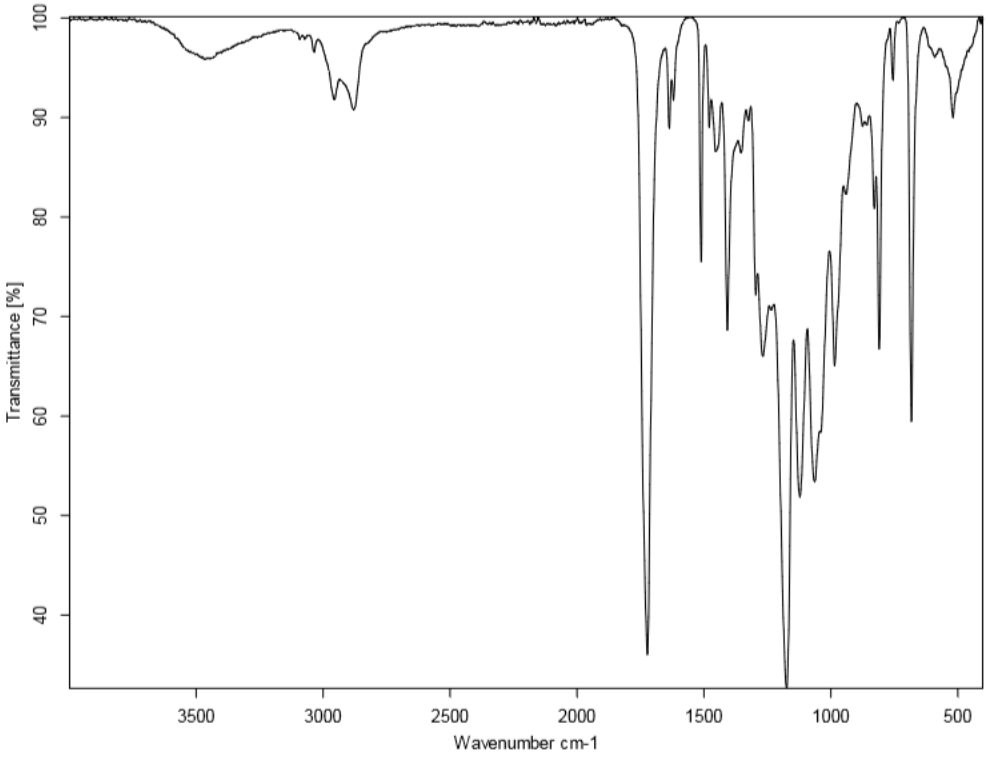

Figure S8: **1** & **2** ester product IR analysis.

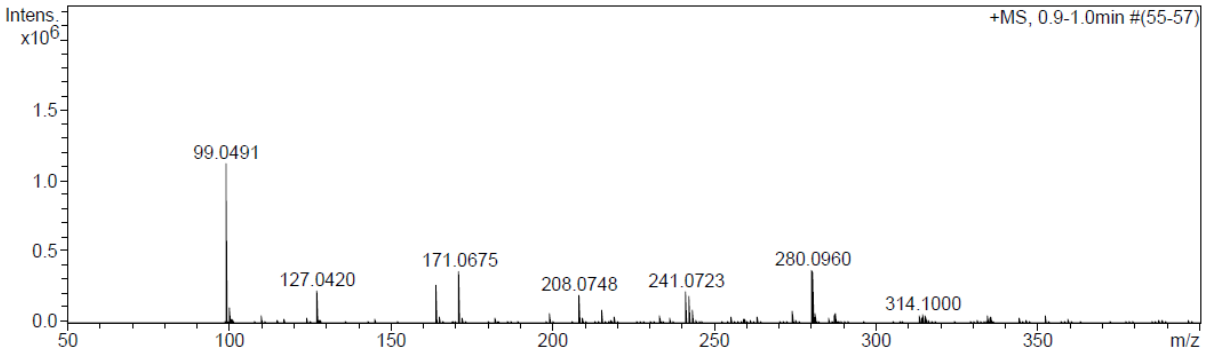

Figure S9 APCI-MS spectrum of **1** & **2** mixture formed from AA and 1,2-ethanediol esterification.

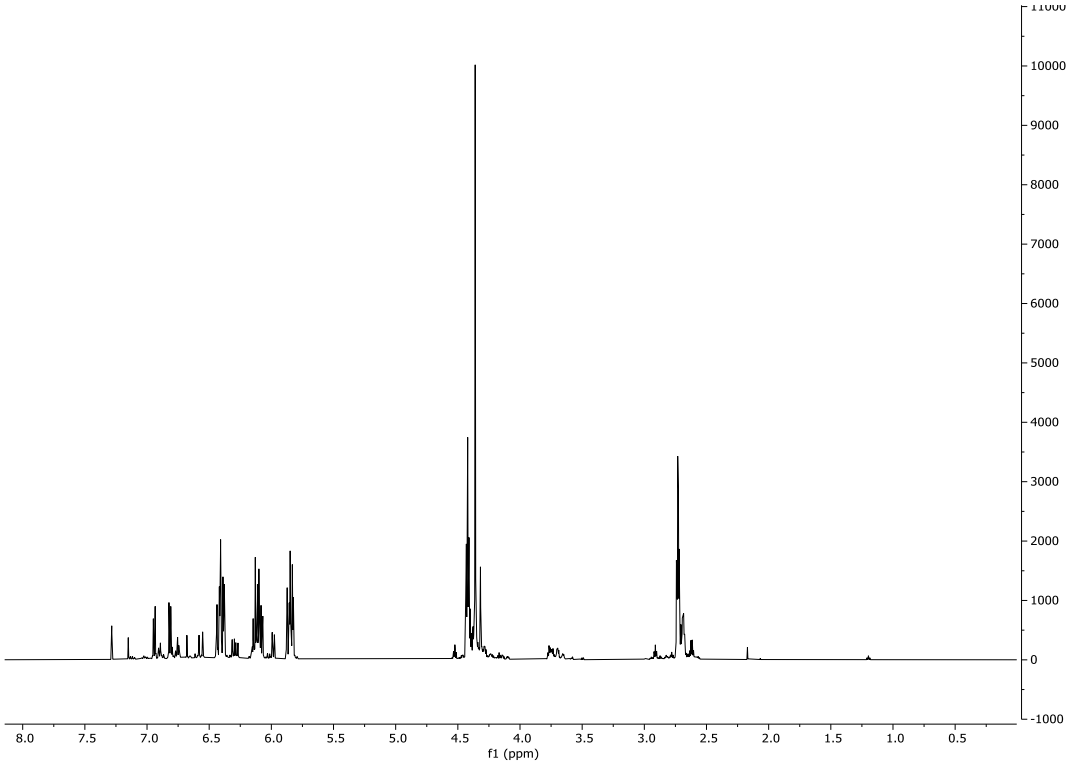

Figure S10: ^{1}H-NMR of **1** & **2** ester product in $CDCl_3$.

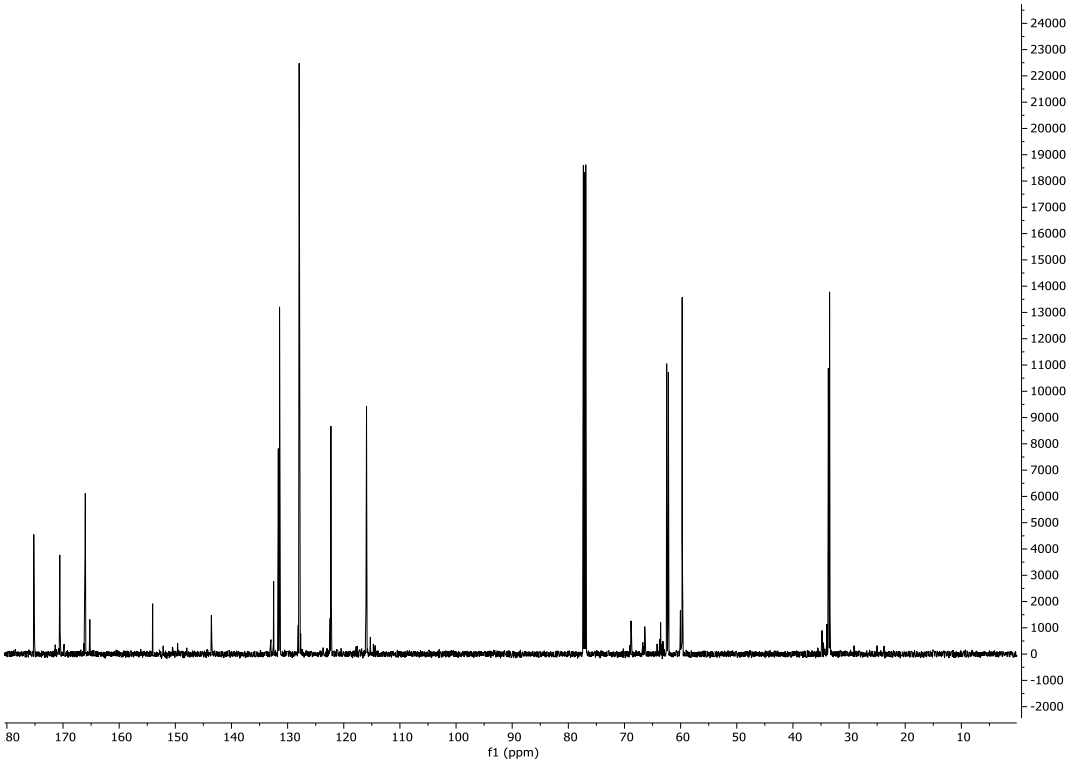

Figure S11: ^{13}C-NMR of **1** & **2** ester product in $CDCl_3$.

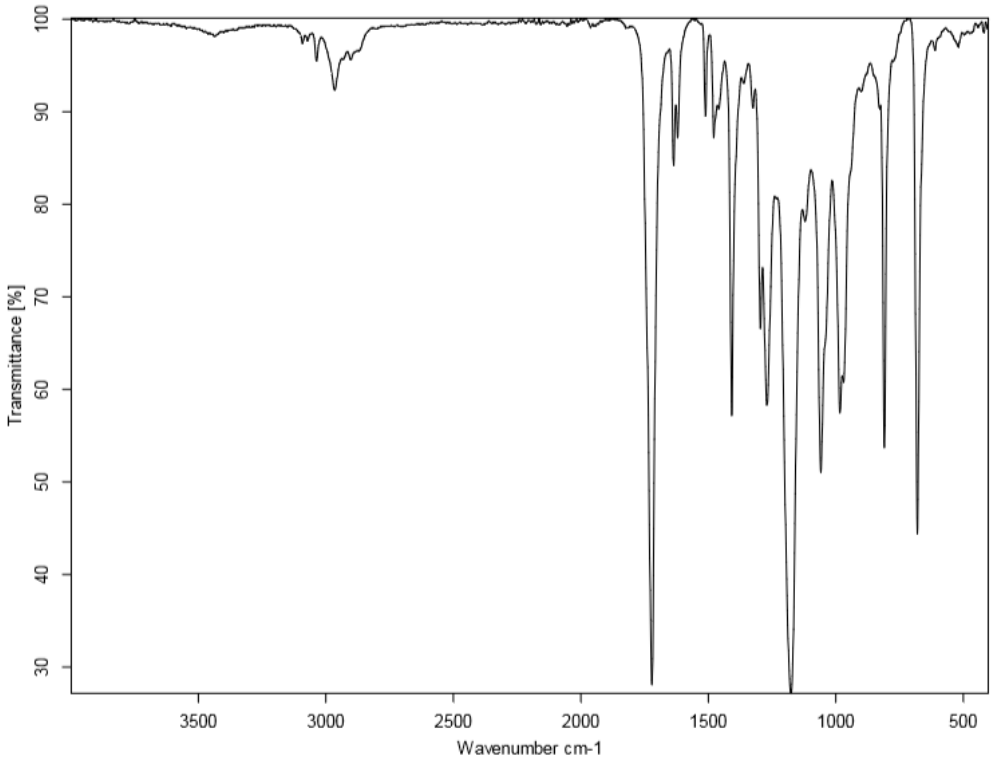

Figure S12: **3** & **4**, ester product IR analysis.

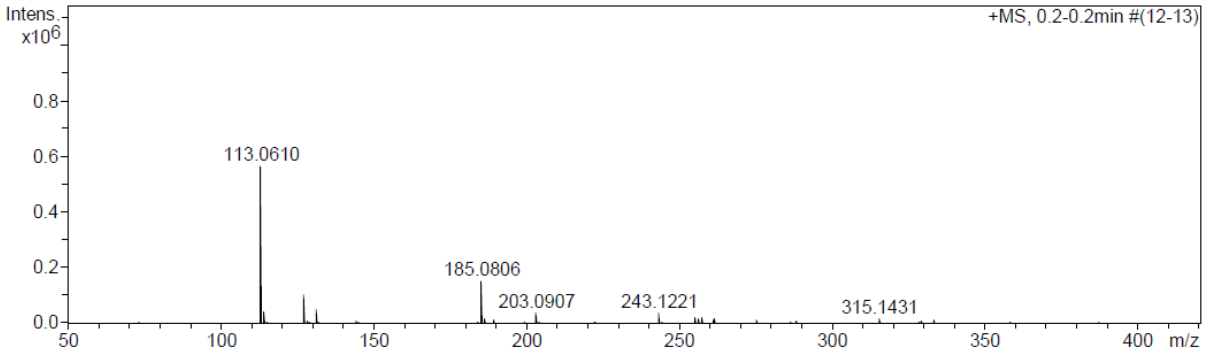

Figure S13 APCI-MS spectrum of **3** & **4** mixture formed from AA and 1,3-propanediol esterification.

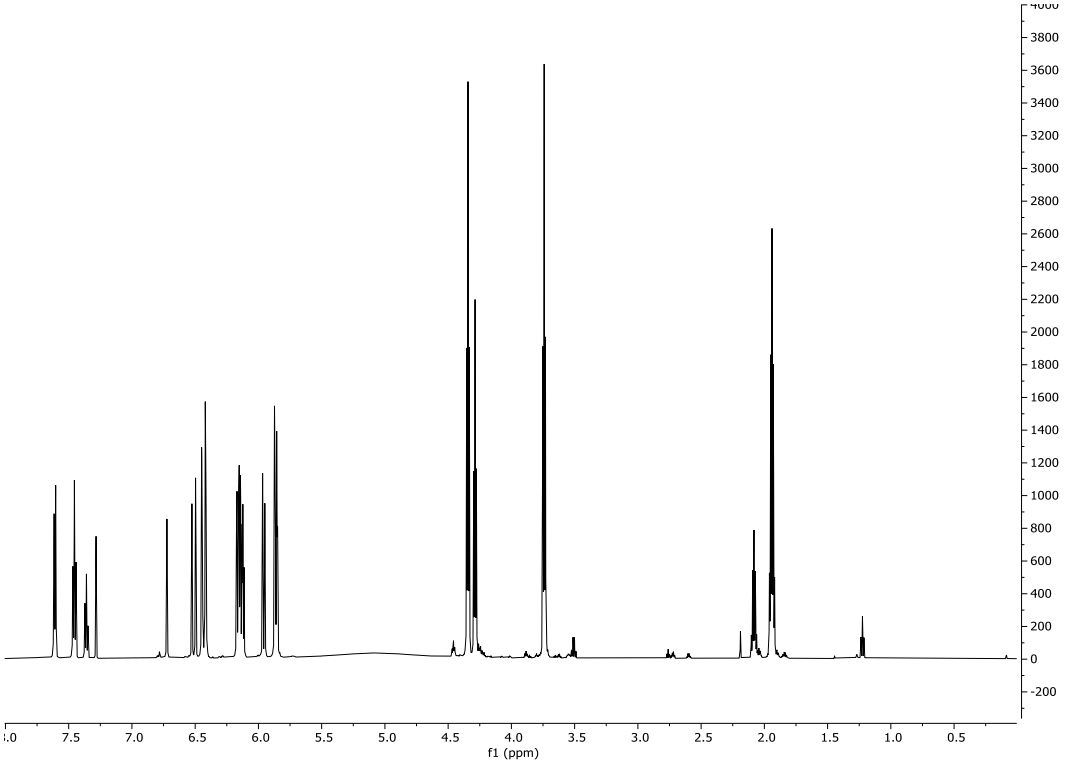

Figure S14: ^{1}H-NMR of **3** & **4** ester product in $CDCl_3$.

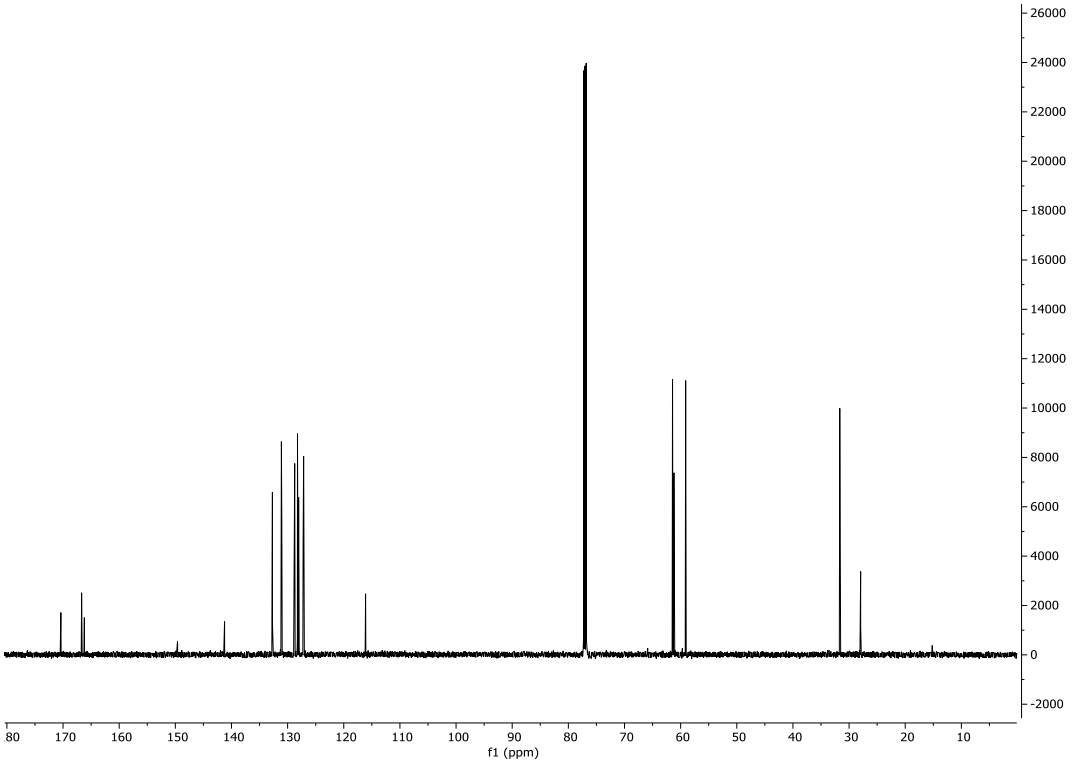

Figure S15: ^{13}C-NMR of **3** & **4** ester product in $CDCl_3$.

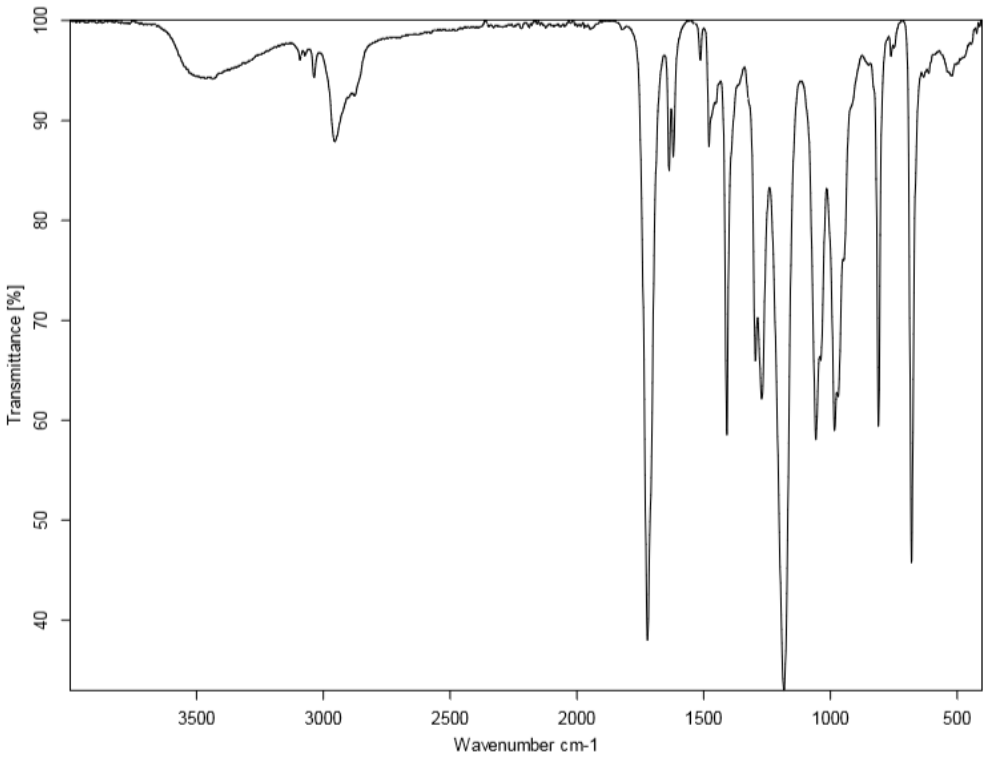

Figure S16: **5** & **6** ester product IR analysis.

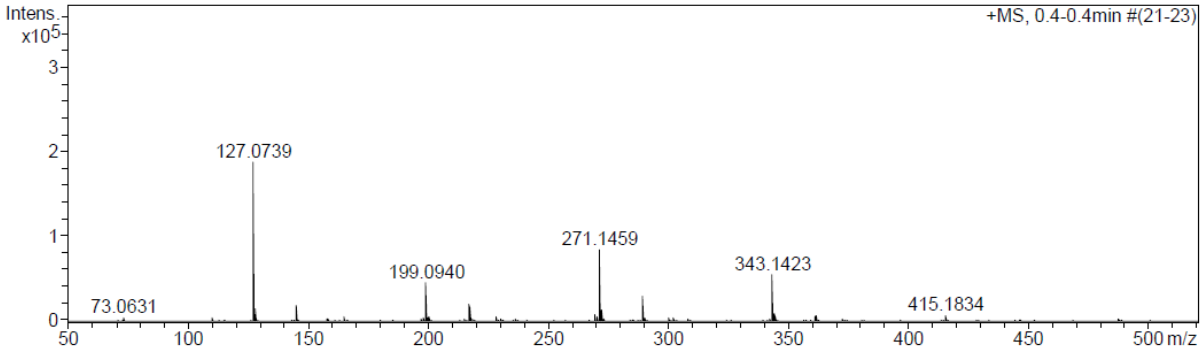

Figure S17 APCI-MS spectrum of **5** & **6** mixture formed from AA and 1,4-butanediol esterification.

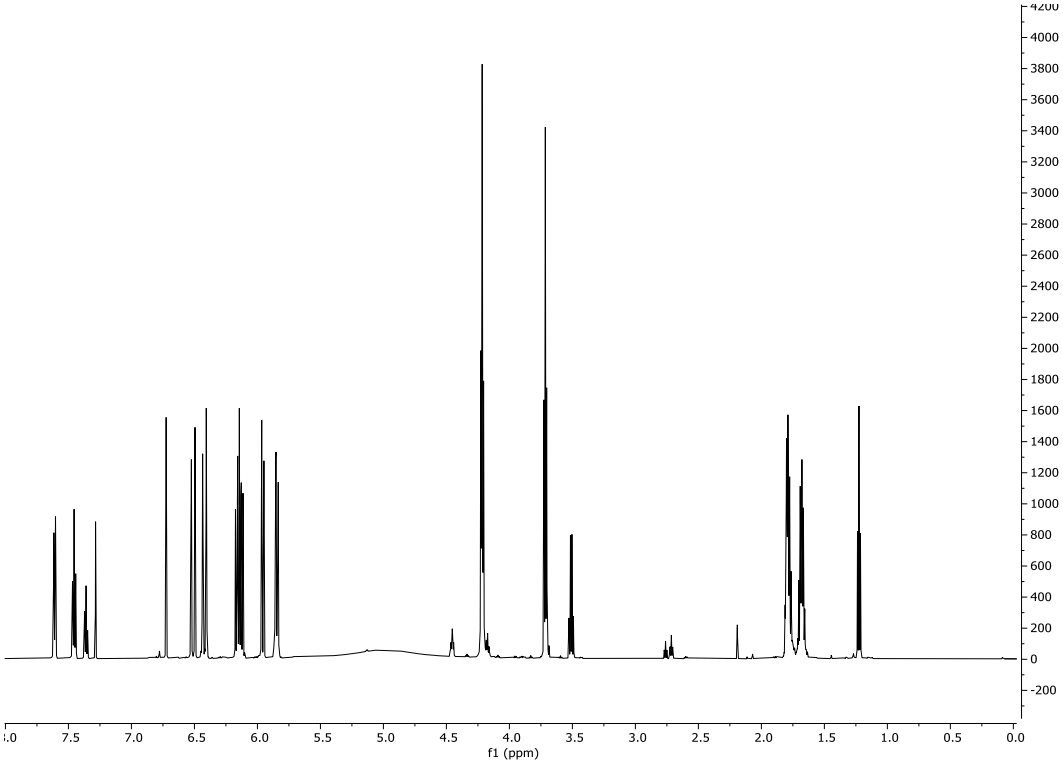

Figure S18: ^{1}H-NMR of **5** & **6** ester product in $CDCl_3$.

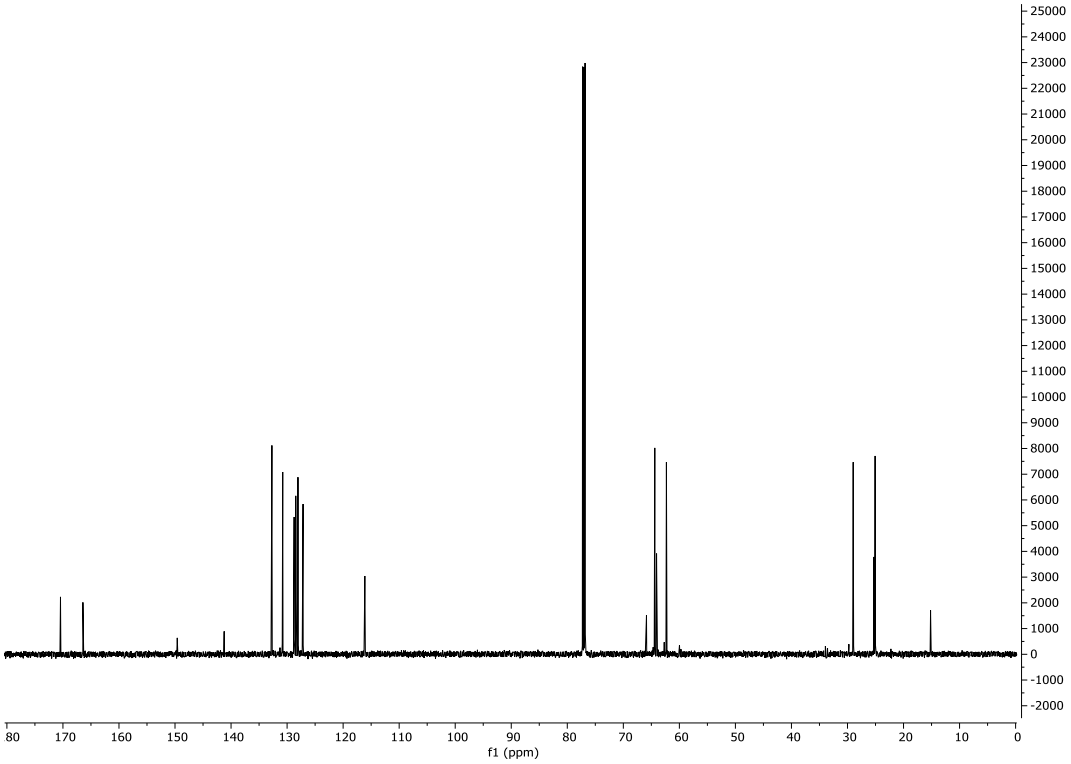

Figure S19: ^{13}C-NMR of **5** & **6** ester product in $CDCl_3$.

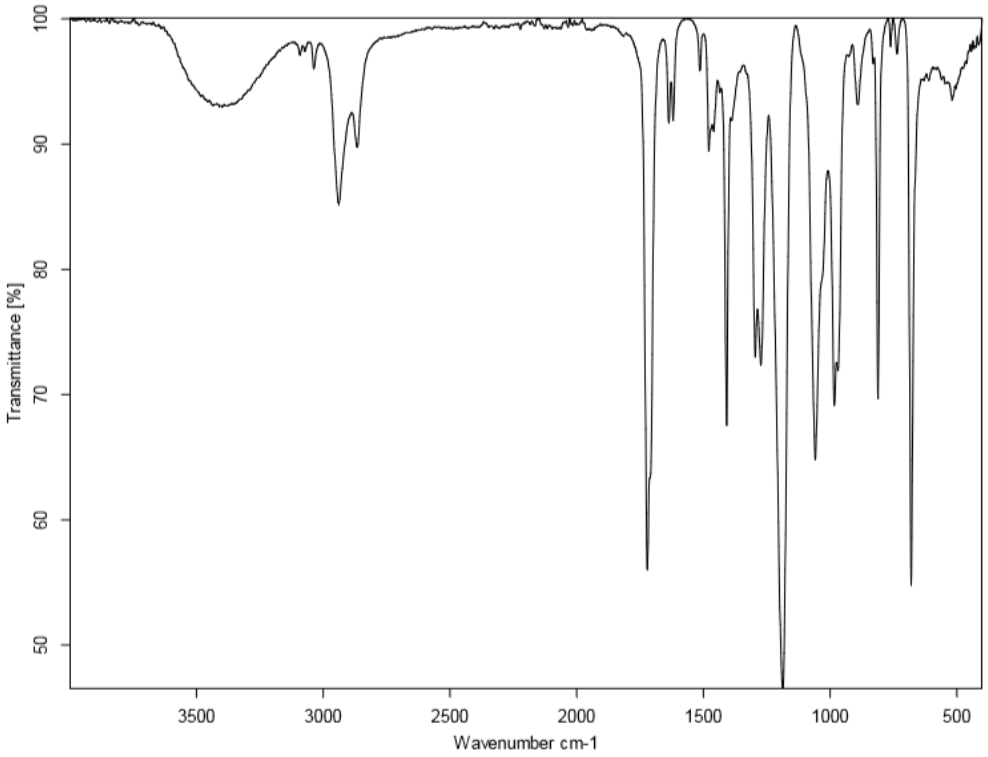

Figure S20: **7** & **8** ester product IR analysis

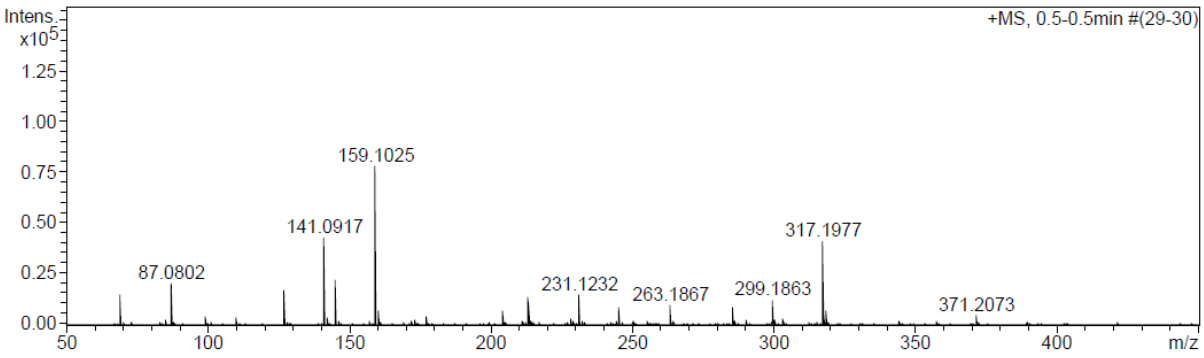

Figure S21 APCI-MS spectrum of **7** & **8** mixture formed from AA and 1,5-pentanediol esterification.

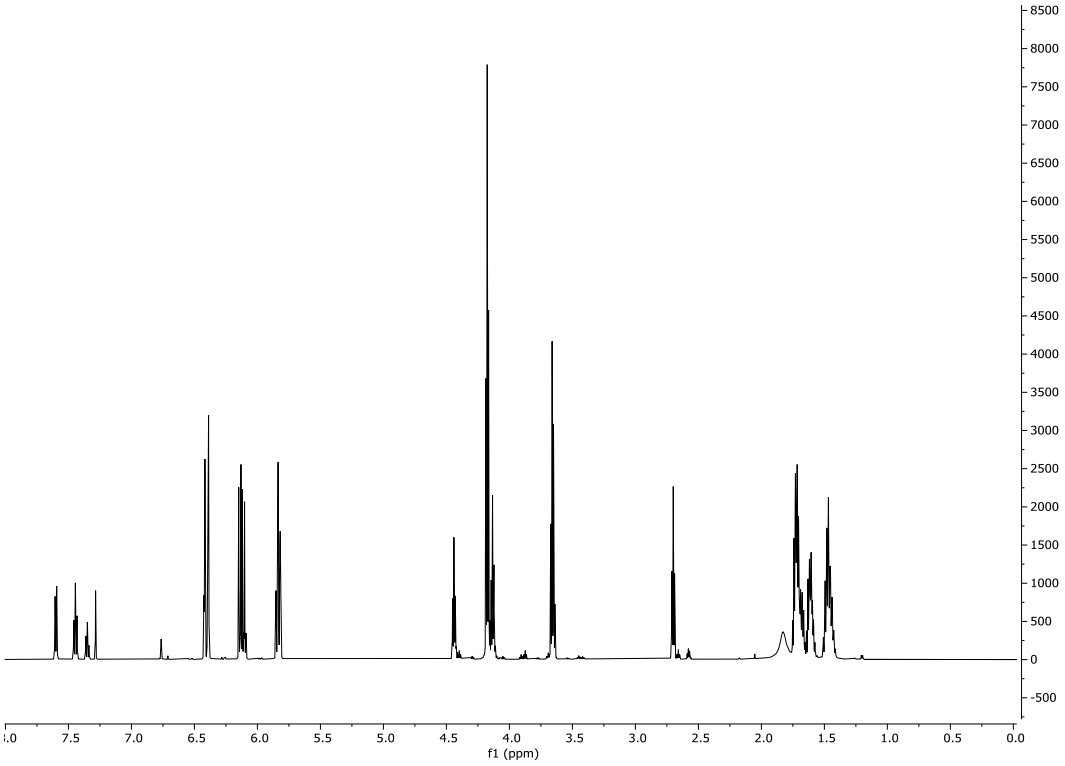

Figure S22: ^{1}H-NMR of **7** & **8** ester product in $CDCl_3$.

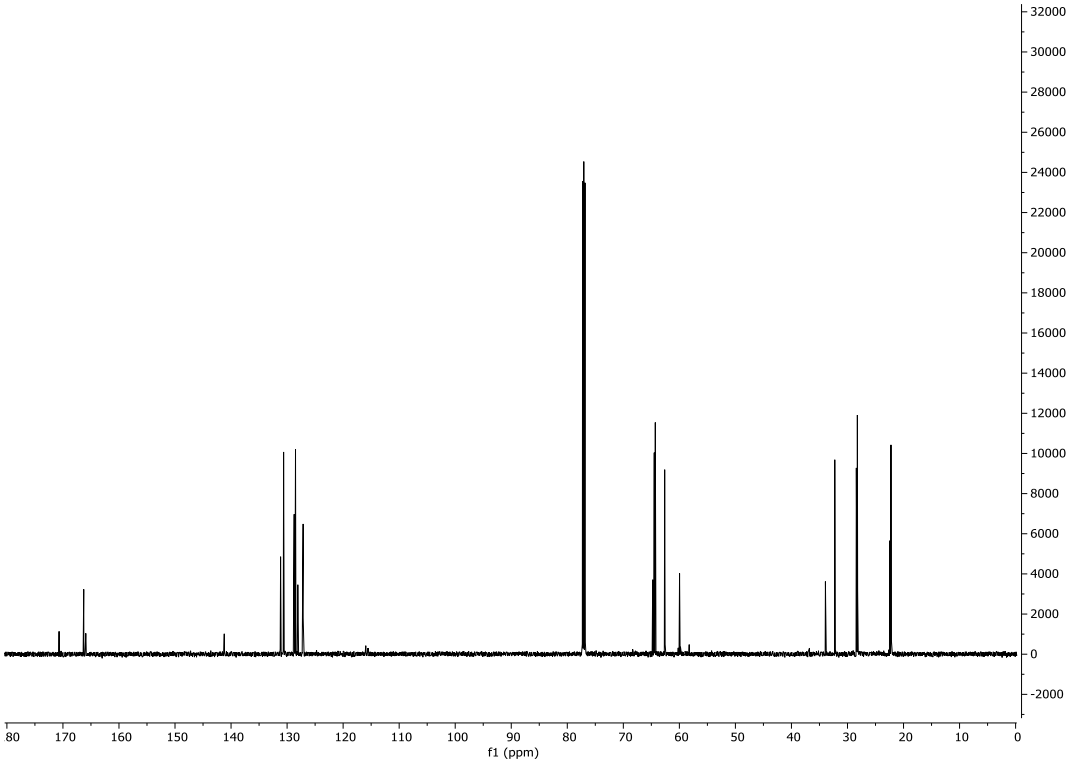

Figure S23: ^{13}C-NMR of **7** & **8** ester product in $CDCl_3$.

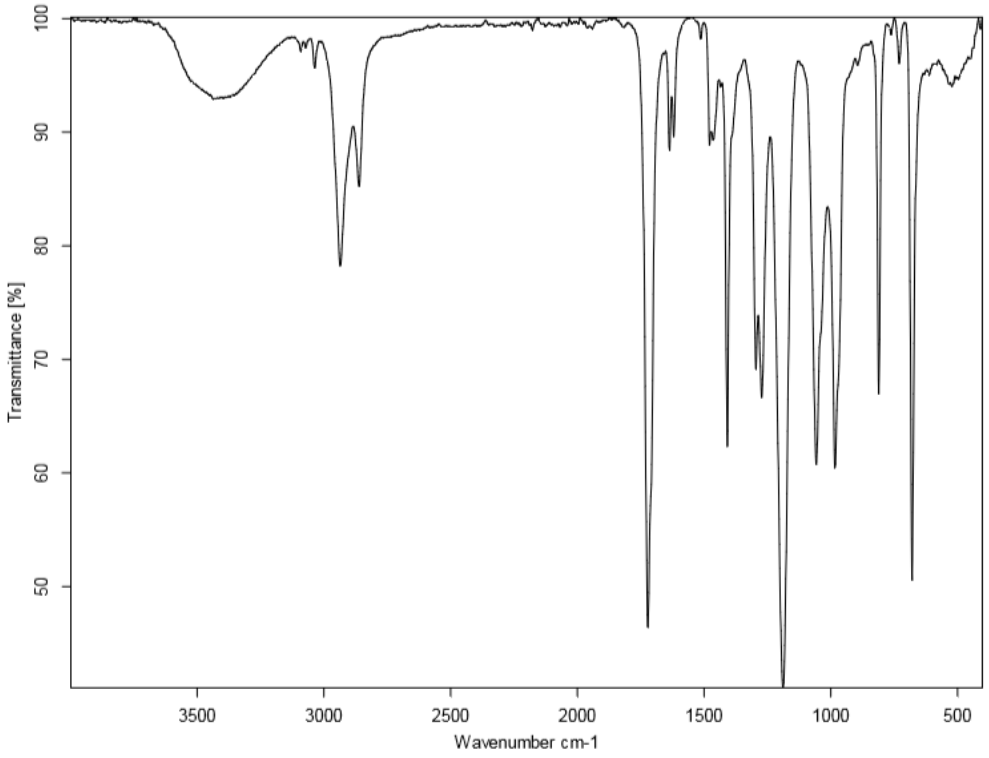

Figure S24: **9** & **10** ester product IR analysis

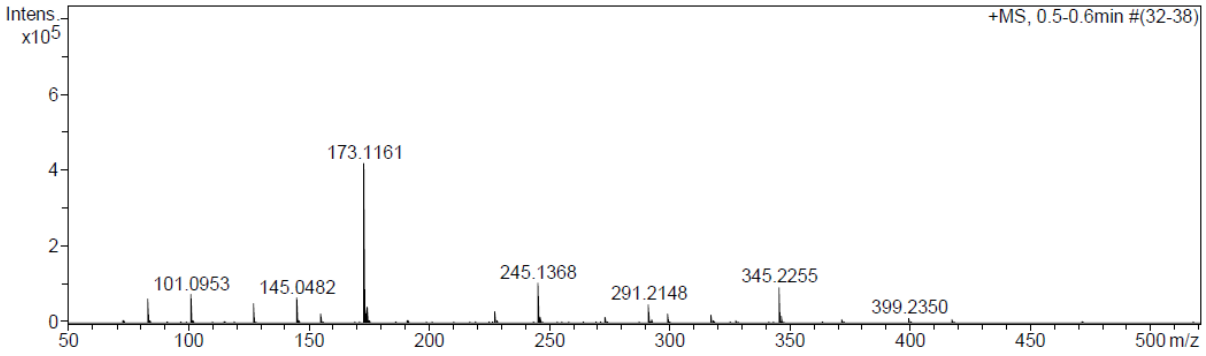

Figure S25 APCI-MS spectrum of **9** & **10** mixture formed from AA and 1,6-hexanediol esterification.

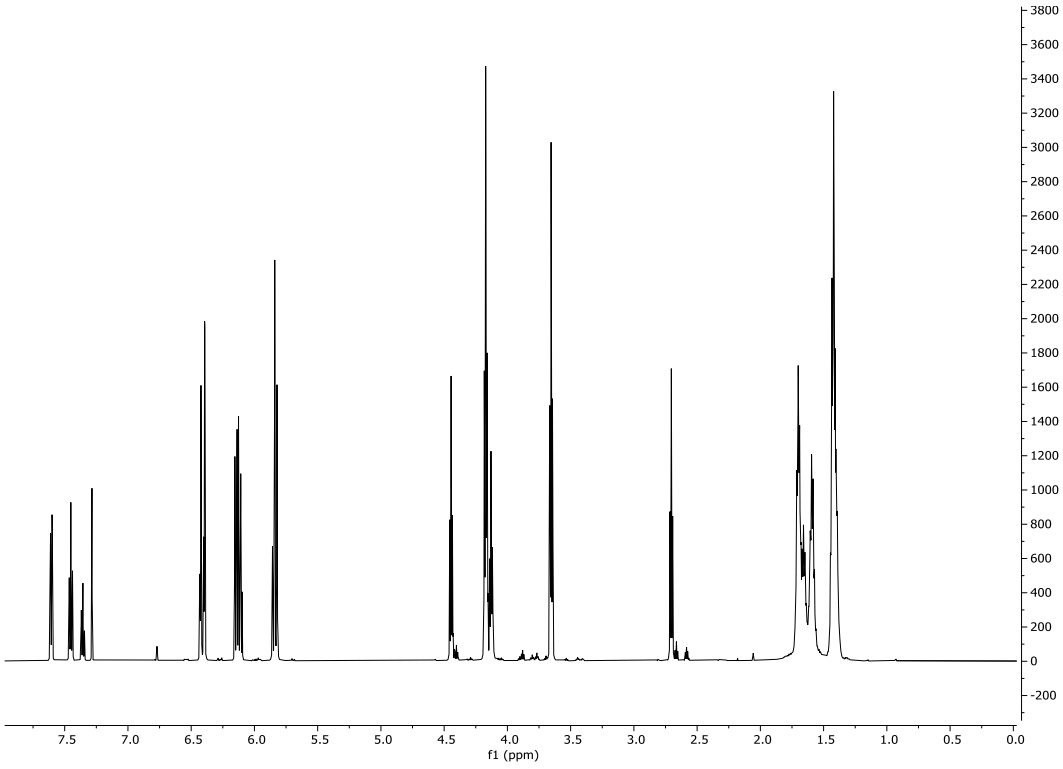

Figure S26: ^{1}H-NMR of **9** & **10** ester product in $CDCl_3$.

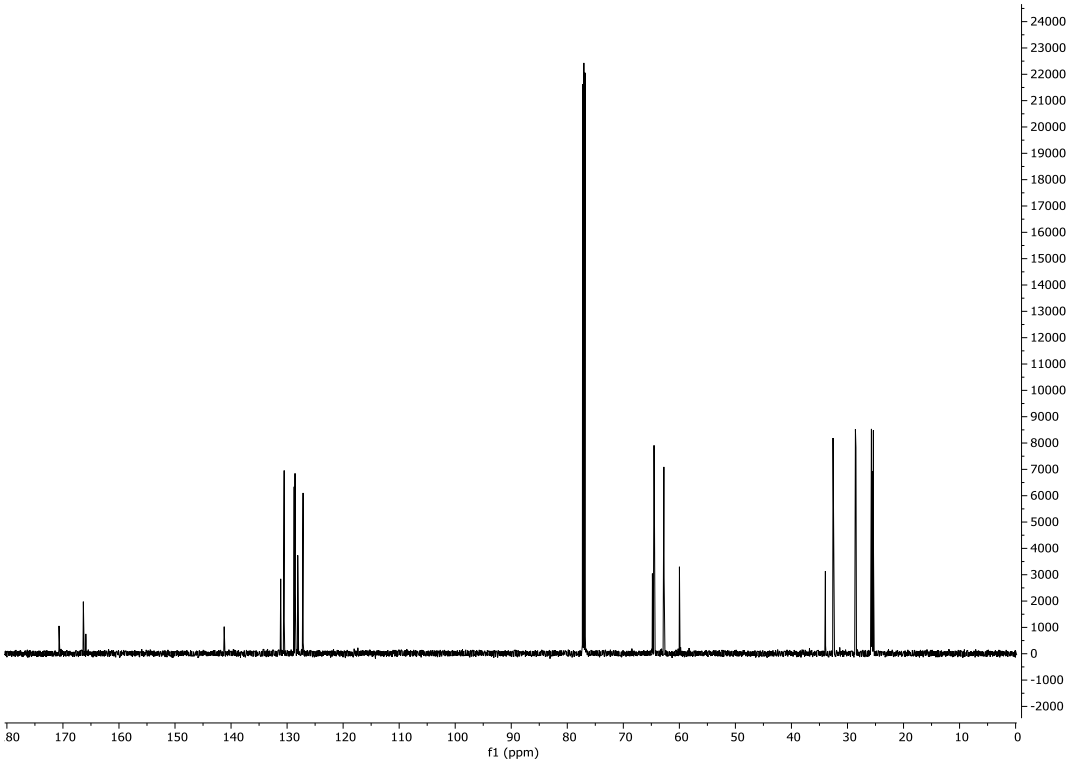

Figure S27: ^{13}C-NMR of **9** & **10** ester product in $CDCl_3$.

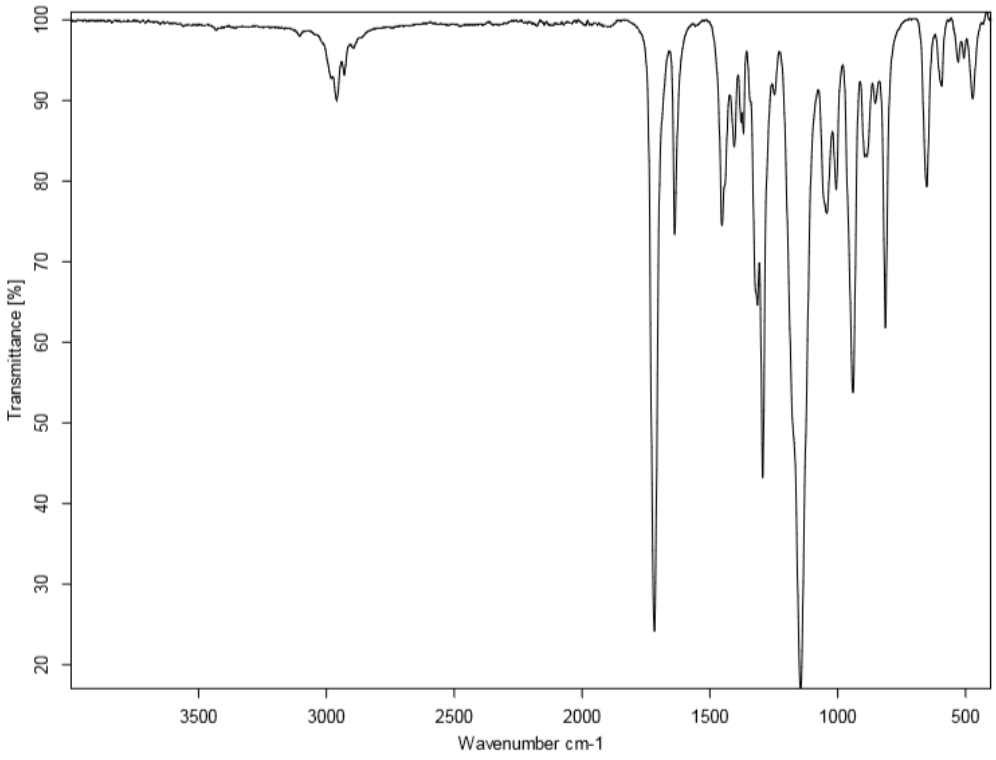

Figure S28: **11** IR analysis

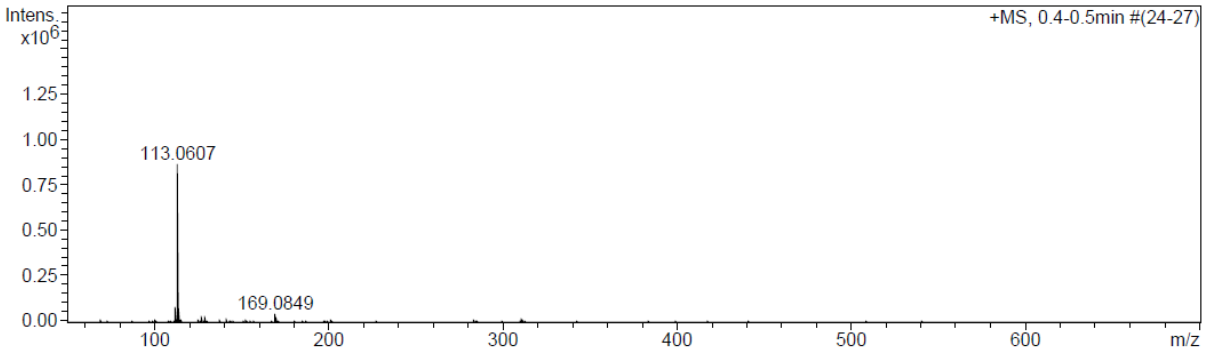

Figure S29 APCI-MS spectrum of **11.**

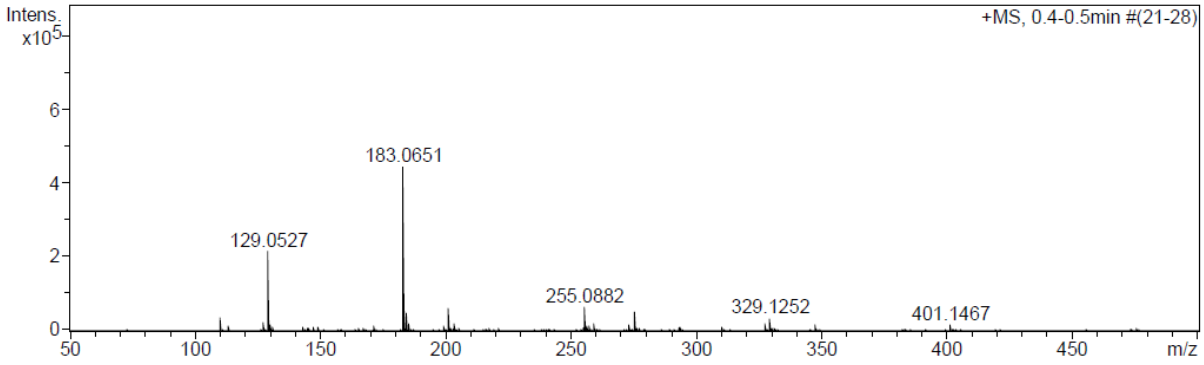

Figure S30 APCI-MS spectrum of **12**, **13** & **14** mixture formed from AA and glycerol esterification.